A Random Field Model for the Prediction of Changes in the Undrained Shear Strength of Petroleum Contaminated Clay Soils

Joseph William Kristof

A Thesis

In the Department

of

Building, Civil and Environmental Engineering

Presented in partial fulfillment of the requirements for the degree of

Doctor of Philosophy

Concordia University

Montreal, Quebec, Canada

December, 2010

CONCORDIA UNIVERSITY

SCHOOL OF GRADUATE STUDIES

This is to certify that the thesis prepared

By: Joseph William Kristof

Entitled: A Random Field Model for the Prediction of Changes in the Undrained
            Shear Strength of Petroleum Contaminated Clay Soils

and submitted in partial fulfillment of the requirements for the degree of

DOCTOR OF PHILOSOPHY (Civil Engineering)

complies with the regulations of the University and meets the accepted standards with
respect to originality and quality.

Signed by the final examining committee:

_____ Chair
Dr. P. Grogono

_____ External Examiner
Dr. P. Mukhopadhyaya

_____ External to Program.
Dr. G. Vatistas

_____ Examiner
Dr. A. Zsaki

_____ Examiner
Dr. M. Elektorowicz

_____ Thesis Co-Supervisor
Dr. P. Fazio

_____ Thesis Co-Supervisor
Dr. A. Foriero

Approved by _____
              Dr. K. Ha-Huy, Graduate Program Director

December 13,201 0   _____
                        Dr. Robin A.L. Drew, Dean
                        Faculty of Engineering & Computer Science

ii

ABSTRACT

A Random Field Model for the Prediction of Changes in the Undrained Shear Strength of Petroleum Contaminated Clay Soils

Joseph William Kristof, Ph.D.
Concordia University, 2010

Quite often grounds in urban areas are subjected to contamination due to leaks from underground storage tanks of gas stations and of heating oil, as well as from spills of trucks and tankers carrying crude oil, heating oil or gasoline. Moreover the ever growing urban population pushes city boundaries to areas where industries had operated and the ground is heavily contaminated by petroleum and/or its derivatives. These contaminants reduce the load carrying capacity of the soil, thus compromising the stability of structures.

A laboratory investigation has been carried out to determine the undrained shear strength of completely saturated contaminated clay. The undrained shear strength, S_u, is the parameter required in the total stress analysis (TSA) of foundations emphasis is placed on the experimental determination of the undrained total stress analyses (short term analysis) parameters. Specifically, the effect of contaminants on the undrained shear strength S_u, must be determined in order to verify the following two requirements:

1. A foundation must not collapse or become unstable under any conceivable loading.

2. Settlement of the structure must be within tolerable serviceability limits.

Indeed experimental tests, as well as a statistical model developed in this study confirm that contaminants deteriorate the undrained shear strength of the soil and have significant effects on the elastic moduli. Consequently the immediate bearing capacity of the soil is affected and the integrity or serviceability of the foundation may be jeopardized.

A statistical random field model, based on the undrained shear strengths obtained in the laboratory, was used to model the contaminated soil. A method was developed to predict the statistical properties of the excursion set of the Gaussian random field above high thresholds. A new heavy tailed random field called the Student Random Field was also introduced, for which the distribution of the size of one cluster of its excursion set was derived. The tail distribution of its supremum was also approximated. Finally, as previously mentioned, this random field theory is applied to real data obtained from a series of triaxial tests with 2, 4 and 6% crude oil, heating oil and gasoline contaminated soil.

ACKNOWLEDGEMENTS

Completion of a Ph.D. dissertation in engineering is an extremely complex and assiduous endeavour. Its success reflects not only the industrious aptitude of the candidate but that of the dedication, talent, cooperation and goodwill of a great number of people.

In my years of study and research I was fortunate to meet and work with exceptional intellects and gentlemen of highest order.

I wish to express my sincere gratitude to my esteemed co-supervisors Professor Dr. Paul Fazio P.Eng., FCSCE, FASCE, FEIC, FCAE, renowned nationally and internationally for his intellect and visionary engineering achievements, and Professor Dr. Adolfo Foriero P.Eng., highly respected academic, civil/geotechnical engineer, expert of special soil conditions of Laval University, Quebec City. These two professors spared neither time nor intellectual resources to guide and help me in my research and in completion of the dissertation.

I am also greatly indebted to the late Dr. A. B. Keviczky and Dr. Qutaibeh Katatbeh. These two professors of mathematics realized the novelty and the significance of my research topic and helped me all the way in developing the

random field model for predicting the effects of petroleum contamination on the bearing capacity of clayey soil.

I would also like to extend my gratitude to Mr. Jacques Payer, technical director at the department of Building, Civil and Environmental Engineering and to his staff Mr. Joseph Herb and Mr. Luc Demers who always cooperated and acted upon my requests without delay.

Professor Dr. Adel Hanna, my former supervisor, recognized the long term importance of my research topic early in my Ph.D. program and I am grateful for it.

My sincere thanks also go to Mr. Javed Khalid, Ph.D. candidate, the most knowledgeable and trusted colleague of mine, who created a rich and fruitful working environment in the lab in the course of my research.

My daughters have always been supportive and patient and I thank them for it.

TABLE OF CONTENTS

Chapter 4

Results and analysis of unconsolidated-undrained (UU) triaxial tests on petroleum contaminated clay soil 27

Chapter 5

Chapter 6

LIST OF FIGURES

LIST OF TABLES

1. INTRODUCTION

1.1 Scope of the research project

When designing geotechnical systems, geotechnical engineers must consider both drained and undrained conditions to determine which of these conditions is critical. Contamination of soils with hydrocarbons complicates this decision.

The rate of loading under the undrained condition is often much faster than the rate of dissipation of the excess porewater pressure and the volume change tendency of the soil is suppressed. The result of this suppression is a change in excess pore water pressure during shearing. A soil with a tendency to compress during drained loading will exhibit an increase in excess porewater pressure under undrained condition resulting in a decrease in effective stress. A soil that expands during drained loading will exhibit a decrease in excess porewater pressure resulting in an increase in effective stress. These changes in excess porewater pressure occur because the void ratio does not change during undrained loading (no volume change). This behaviour is affected to various degrees when a soil is contaminated with hydrocarbons.

During the lifespan of the structure, called the long-term condition, the excess porewater pressure developed as a result of loading is dissipated. This case amounts to the drained condition. Clays generally take many years to dissipate

the excess porewater pressures. During construction and shortly after, called the short term condition, soils of low permeability do not have sufficient time for the excess porewater pressure to dissipate and undrained condition applies. This condition also applies when a soil is contaminated with hydrocarbons.

For permeable coarse grained soils (such as sands) the excess pore water pressure dissipates quickly under static load. Consequently, undrained condition does not apply to clean coarse-grained soils under static loading but only to fine-grained soils and mixtures of coarse and fine-grained soils. In this thesis the study was limited to contaminated fine-grained soils under undrained conditions.

The shear strength of a fine-grained soil under undrained condition is called the undrained shear strength, S_u. Normally Tresca's failure criterion, where the shear stress at failure is one half the principal stress difference, is adopted to interpret the undrained shear strength. For a contaminated soil the shear strength under undrained loading depends not only on the initial void ratio (initial water content) but on the degree of contamination as well. An increase in the confining pressure causes a decrease in initial void ratio and a larger change in excess porewater pressure when a contaminated soil is sheared under undrained conditions. The result is that the Mohr's circle of total stress expands and the undrained shear strength increases for constant degree of contamination.

However under an increase in the degree of contamination, at a constant void ratio, the Mohr's circle of stress decreases and the undrained shear strength decreases for a constant void ratio (Chapter 3 and 4). Consequently S_u is not a fundamental soil shear strength parameter. The value of S_u depends on the magnitude of the initial confining pressure or initial void ratio as well as the initial degree of contamination. Analyses of soil strength using S_u are called total stress analysis (TSA).

The ensuing research considers the undrained shear strength parameter S_u, particularly the contaminated undrained shear strength.

1.2 Problem identification

In the soil, the presence of crude oil and its derivatives, such as heating oil and gasoline, is caused by:

1. Leaking surfaces of underground storage tanks – USTs are widely used to store fuels at sites such as garages, taxi companies, hospitals and on residential properties, etc. The lifespan of USTs is 20-25 years. The majority of these USTs in North America have reached or passed this period. Leakage, due to the underground location, is not easy to detect (Figure 1.1). It migrates vertically towards the water table, and horizontally towards the surrounding area and

buildings. According to Canadian Mortgage and Housing Corporation there are over 20 000 leaking USTs occurring at any moment in Canada;
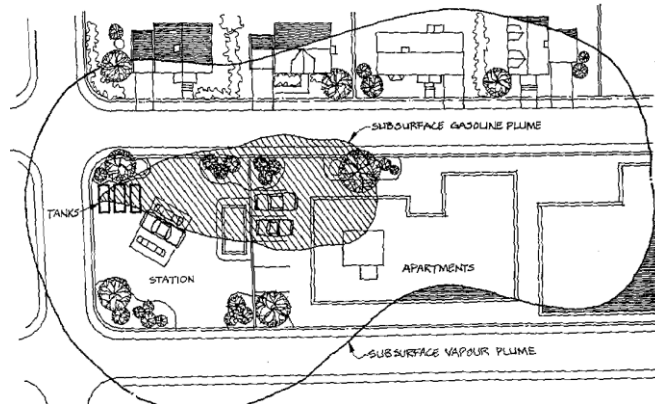
Figure 1.1 Migration of hydrocarbons
(Canadian Mortgage and Housing Corporation, 2003)

2. Leaking heating oil storage tanks, mostly on private properties (Figures 1.2 to 1.5);

3. Oil spills, which are also of great concern. There are thousands of spills in North America on a yearly basis. They happen accidentally, or are caused by human errors;

4. Contaminated sites used or vacated by operations such as refineries or other facilities handling petroleum products, such as garages, hospitals etc.; and

5. Intentional dumping.
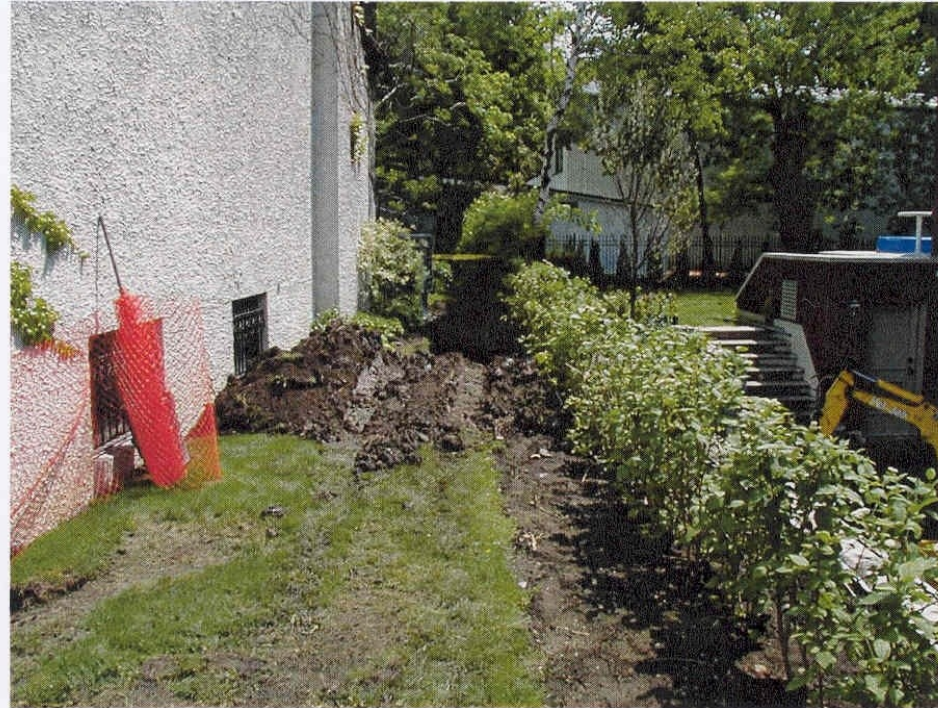
French drain beneath the retaining wall

Figure 1.2 Leaking heating oil tank on private property
(Courtesy of property owner, 2004)

Pumping of free oil and water

Figure 1.3 Leaking heating oil tank and damage
on neighbour's property
(Courtesy of property owner, 2004)

View of driveway excavation before site restoration

Free standing oil in gravels layer against the building footings

Figure 1.4 Soil soaked in heating oil due to neighbour's leaking storage tank

Oil pooling against the building footing adjacent the generator room

Excavation of oil saturated gravel backfill

Figure 1.5 Pool of leaked heating oil at foundation

Once the soil gets contaminated with crude oil, or with its derivatives (the heating oil and the gasoline) the undrained shear strength of the soil, S_u, is considerably reduced. This reduction depends on the degree of contamination. This parameter is necessary for the ensuing total stress (TSA). Moreover contamination will also affect the long term condition (ESA, effective stress analysis), although at this stage we can only assume this fact.

1.3 Objectives of the thesis

The objective of this thesis is to carry out a systematic investigation of the contaminated undrained shear strength, S_u, using a triaxial testing apparatus.

This study also provides a model, backed up by the triaxial experiments on a clay contaminated with sweet brut, heating oil and gasoline, in order to predict the statistical properties of the excursion set of Gaussian Random Field undrained shear strengths above high thresholds :

1. What is the probability that the largest value of the undrained shear strength of a contaminated soil exceeds a given threshold? Answering such a question may give us the reliability of the foundation soil.

2. What is the distribution of the area or the volume of the space where the soil undrained shear strength exceeds a given threshold?

3. If we observe the undrained shear strength of a soil in a given region, then what is the predicted undrained shear strength of the soil in another region?

2. Literature Review

2.1 Literature review of research material dealing with petroleum contaminated soils

Despite all of the efforts to carry out a comprehensive literature review on the subject of the effect of petroleum contamination on the undrained shear strength S_u, ((used in (TSA) for a total stress analysis)) no significant research on this topic could be found.

The author of this thesis, however, came across papers and research material in which mostly the effect of petroleum contamination was studied on Kuwaiti sand (Hassan et al., 1995). Tests in that study were conducted on oil-contaminated sands resulting from exploded oil wells, burning oil fires, destruction of oil storage tanks, and the formation of lakes in Kuwait at the end of the first Gulf War. Testing included basic properties, compaction and permeability tests, and triaxial and consolidation tests on clean and contaminated sand at the same relative density. The authors concluded that oil contamination produces a decreased permeability and strength. As far as strength is concerned, they considered the friction angle. Thus the strength parameter considered is for the long term analysis (effective stress analysis, ESA) of foundations. The reduction in the angle of friction was 2° for specimens prepared at a relative density of 60% and mixed with 6% of heavy crude oil. Oil contamination also resulted in an increased compressibility, which was evidenced from a decreased soil modulus in the triaxial test.

Researchers used different kind of petroleum derivatives in their experiments, such as kerosene, propane, glycerol, motor oil, heavy crude oil and xylean. No research reference was found, however, on the effect of crude oil, heating oil and gasoline - the most frequent contaminants today - contamination on the cohesion (c) of clay soil particles, and ultimately on the bearing capacity of the soil, which is the subject of the present thesis research.

Evgin and Das (1992) experimented with oil contaminated and clean quartz sand. They confirmed that when sand was saturated with motor oil the angle of internal friction φ was notably reduced for both loose and dense sands. Moreover they observed a drastic increase in volumetric strain.

Meegoda and Ratnaweera (1994) examined the compressibility of fine-grained soils via consolidation tests. Their experimental study was performed to investigate factors that control the compression index of contaminated soils and how the addition of chemicals to a soil changes its pore-fluid properties. Also they investigated to what degree contaminants change the mechanical and physicochemical factors and hence its settlement characteristics. In the course of their research they came across a great deal of material that study soil conditions in the vicinity of chemical and petroleum spills and unregulated landfills where numerous industrial solvents have been observed. Although, they state, that modern landfills may not produce contaminated soil, soil contamination may occur due to leakage from underground and aboveground storage tanks and

accidental spills. Therefore, they deem that, it is important to understand the influence of chemicals on settlement characteristics of soil, and moreover, to evaluate the applicability of estimating the compression indices of contaminated soils.

In order to prove their theory that the settlement characteristics of contaminated soils are the net result of both physicochemical and mechanical factors they mixed two chemicals, namely glycerol and propanol with kaolin in various ratios. The experimental results showed a considerable change in the compression index of soils with different degrees of contamination.

The effects of hydrocarbons infiltrating into the soil, and hydrocarbon permeability of soils was also studied by Lorincz, J. (1984). He also studied the effect of soil pollutants such as crude oil, gas oil and petrol on the soil shear strength.

Al-Hattemleh (1995) carried out an experimental evaluation of subsurface contaminations by kerosene mixture on the behaviour of pile foundation and its effect on concrete. The results showed that the effect of kerosene on pile material (concrete) was minor. However it was also shown that kerosene had substantial effect on clayey properties, namely decreasing apparent cohesion.

3. METHODOLOGY OF TRIAXIAL EXPERIMENTS

3.1 Overview

It is known that contaminants, such as petroleum and its derivatives affect the shear strength of soil. However, no systematic investigation has been carried out to determine to what extent the individual constituents of these contaminants affect the undrained shear strength of the clay soil. The present doctoral research was undertaken to determine the extent of the reduction of the undrained shear strength due to petroleum contamination.

In order to achieve this objective, nine batches of soil were prepared with three types of contaminants (namely crude oil/sweet brut, heating oil, and gasoline) at 2%, 4%, 6% of contamination by mass. One batch of clay with zero contamination was added as reference for a total of 10 batches. Three samples from each of the ten batches (total of 30 samples) were placed in latex-stretchers, subjected to a 24-hour static, one dimensional, vertical compaction and tested for their undrained shear strength. The sample with the median undrained shear strength for each batch was selected as the representative value for that batch and used to generate the values included in Tables 4.1 and 4.2.

3.2 Materials used in the research

The clay soil used in the present study originated from Sandersville, Georgia and is known as Rogers kaolin. Rogers kaolin, shipped in powder form, was used in this study because its level of activity is generally inferior to that of illite or montmorillonite. This point is important since factors that affect the undrained shear strength of clays were desired to be limited. Also it is one of the most common minerals and can be widely found in the world. Tables 3.3 to 3.7 give the properties of kaolin used in the present tests. Information on the chemical properties (Tables 3.3 - 3.6) of the Roger kaolin was provided by the supplier of the clay, namely Kaolin Company, Sandersville, GA, USA (please see Appendix). The relative density value (1.8-2.6) of the kaolin (Table 3.7) was obtained from the MSDS (2008) of Mallinckrodt Chemicals, NJ, USA (www.vwrsp.com/msds/).

For the purpose of contaminating the soil specimen, crude oil (sweet brut) known as Hibernia Bland, originating from Whiffen Head, Newfoundland, was utilized. The characteristic properties of the crude oil/sweet brut are given in Table 3.1. Information on the chemical properties of the Hibernia Bland was downloaded from Crude Oil Canada (www.hydro.com/cgi-bin). A copy of this information is attached to the Appendix. Hibernia Bland from Newfoundland was selected for the research since it is the most widely distributed and used crude oil in the eastern part of Canada.

Heating oil and gasoline were the other contaminants used in the course of the tests. These petroleum derivatives were procured from local retailers. Their characteristic properties are given in Table 3.2. and were obtained from Alternative Fuels Data Center, U.S. Department of Energy (www.afdc.energy.gov/afdc/pdfs/fueltable.pdf).

Table 3.1 Crude oil characteristics

API	35.6 deg
Density	0.847 kg/l
Sulphur	0.37 wt%
Pour Point	12.8^o C
Viscosity	5.38 cSt at 20° C
TAN	0.11 mg KOH/g

Source: Hydro-Crude Oil Canada (Appendix)

Table 3.2 Chemical properties of Gasoline and Heating oil/Diesel Fuel

Property	Gasoline	Diesel Fuel/Heating Oil
Molecular Weight	100-105	˜ 200
Composition, Weight		
>Carbon	85-88	87
>Hydrogen	12-15	13
>Oxygen	0	0
Specific gravity, 15.5 ^{o}C	0.72-0.78	0.85
Density, lb/gal@ 15.5 ^{o}C	6.0-6.5	7.07
Boiling temperature ^{o}C	26.6-225	180-340
Reid vapour pressure 37.7 ^{o}C psi	8-15	<0.2
Heating value		
>lower (Btu/gal)	116,090	128,450
>Lower (Btu/lb)	18,676	18,394
>Higher (Btu/gal)	124,340	137,380
>Higher (Btu/lb)	20,004	19,673
>Research octane no.	88-98	-
Freezing point, ^{o}C	-40	40-55
Viscosity, mm^2 /s@15.5 ^{o}C	0.88	2-6
>Water in fuel, volume %	Negligible	Negligible

Source: Alternative Fuels Data Center, U.S. Department of Energy, www.afdc.energy.gov/afdc/pdfs/fueltable.pdf

Table 3.3 Kaolin characteristics - Physical Properties

Physical Properties	Dry M.O.R., psi	950
	M.B.I., meq/100g	10.5
	Surface Area m^2/g	24.0
	pH	4.5

Source: Kaolin Company, Sandersville, GA, USA (Appendix)

Table 3.4 Kaolin characteristics - Particle Size

Particle Size	+325 Mesh, Max. % Retained	1.0
	% Finer than 20µm	99
	10µm	97
	5µm	94
	2µm	85
	1µm	76
	0.5µm	65

Source: Kaolin Company, Sandersville, GA, USA (Appendix)

Table 3.5 Kaolin characteristics - Chemical Analysis

Chemical Analysis (%)			Chemical Analysis (%)	
SiO_2	46.5		K_2O	0.3
Al_2O_3	37.5		Na_2O	0.1
Fe_2O_3	1.0		L.O.I.	13.2
TiO_2	1.3		Carbon	0.1
CaO	0.3		Sulfur	0.13
MgO	0.3			

Source: Kaolin Company, Sandersville, GA, USA (Appendix)

Table 3.6 Kaolin characteristics - Liquid limit, Plastic limit

Liquid limit	49.4
Plastic limit	35.4

Source: Kaolin Company, Sandersville, GA, USA (Appendix)

Table 3.7 Kaolin characteristics - Relative Density

Relative density	1.8 - 2.6

Source: MSDS, 2008, Mallinckrodt Chemicals, NJ, USA
(www.vwrsp.com/msds/10)

It should be noted that the composition range of gasoline varies widely, depending on the origin and on the type of crude oils used, the refinery processes involved, the overall balance of product demand, and product specification. It consists of a mixture of hydrocarbons, additives and blending agents, such as anti-knock agents, anti-oxidants, metal deactivators, lead scavengers, anti-rust agents, anti-icing agents, upper-cylinder lubricants, detergents and dyes (IARC 1989). At the end of the production process of gasoline it typically contains more than150 separate compounds although as many as 1,000 compounds have been identified in some blends (Domask 1984).

3.3 Protocol of experimental process

3.3.1 Specimen preparation

3.3.1.1 Apparatus

Drying Oven - used in the present study was vented, thermostatically-controlled and met the requirements of Specification E145, capable of maintaining a uniform temperature of $110^o \pm 5^o$ C throughout the drying chamber.

Balance GP2 - with 0.1 g readability - used in this study met the ASTM Requirement of Specification D4753.

Miscellaneous: spatulas, knives, wire saw, heavy duty gloves, safety goggles, plastic food-wrapping material, airtight containers.

3.3.1.2 Determining water content of samples obtained from field

Three samples of clay soil were obtained from three different locations in the City area of Montreal, Quebec, Canada. In order to determine the average water content of the three samples procedures described in ASTM Standards (D2216-05) were followed. The three samples were subjected to a 24-hour oven drying process at a temperature of $110^o \pm 5^o$ C. The water content was calculated using the mass of water and the mass of the dry specimen.

The average water content of the three clay soil samples was determined as 23.86%. This determined percentage of water content was used throughout in the present study.

Figure 3.1 Verification of percentage of water content for specimen

3.3.1.3 Wetting powdered kaolin

In order to achieve the desired water content of ω = 23.86%, 143.16 grams of water was added to 600 grams of powdered kaolin and thoroughly mixed.

Adding the calculated amount of water to the powdered kaolin and mixing the specimen were done by hand with a construction spatula. This procedure, protecting the mixture against loss of water, was carried out on a clean steel-top table. Standard practice was followed and the mass was mixed until it was thoroughly blended (ASTM-D1632-07). In order to avoid any evaporation the mixture was placed in plastic food-wrapping material and in airtight plastic container for a 24-hour mellowing period before being subjected to contamination.

Figure 3.2 Preparation of specimens

3.3.1.4 Contamination of specimen

Subsequently calculated amounts of petroleum contaminants - crude oil, heating oil and gasoline - by weight were mixed thoroughly with the specimens to achieve 2%, 4% and 6% respectively, based on the equation of degree of contamination as $\omega_c = m_c/(m_s+m_w)$ where m_c = mass of contaminant, m_s = mass of soil and m_w = mass of water. Mixing was done by hand on a steel-top table using a construction spatula until contaminants were uniformly distributed throughout the batch. The contaminated specimens were placed in airtight plastic containers for a period of two hours.

3.3.1.5 Placement of specimen into membrane stretcher and compaction

Dimensions of each specimen were: 47.5 mm (diameter) x 95.0 mm (height) and are consistent with the dimensions of the top and bottom platens as well as the top and bottom porous stones of the apparatus.

The contaminated specimens were placed in three cylindrical membrane stretchers with vacuum portals. Each specimen was subjected to a 24-hour, static, one dimensional, vertical compaction.

| 3.3 Triplet of stretchers | 3.4 Latex sleeve in stretchers |

3.3.2 Testing procedure

3.3.2.1 Placement of specimen onto the platen of the triaxial cell

Having subjected the specimen to a 24-hour, static, one dimensional, vertical compaction, porous stones were placed on the top and the bottom of the

specimen and placed on the platen of the triaxial cell. Rubber bands were used to prevent water infiltration.
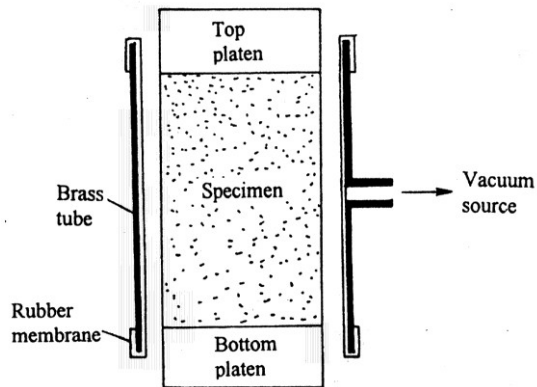
3.5 Airtight specimen in latex sleeve (Graph source: Das, 2005)

3.3.2.2 Actuating the triaxial apparatus

Having the piston gingerly lowered - in order to avoid the destruction of the specimen - on the top platen, the triaxial cell was filled with water. Hydrostatic cell pressure, σ_3, was applied along with increments of axial stresses. Drainage of porewater was not allowed in either the isotropic compression or sheering phases.

3.3.2.3 Triaxial tests conducted on the contaminated specimen

Unconsolidated-undrained tests were conducted on kaolin clay specimens with three different types of contaminants namely crude oil, heating oil and gasoline,

at 2%, 4% and 6% of contamination. These tests were repeated three times in order to obtain median values. A total of 30 unconsolidated undrained shear tests were carried out, including triaxial tests on specimen with 0% contamination.

3.3.2.4 Procedure of Unconsolidated-Undrained Test

In line with standard lab test procedures, the series of laboratory tests in this study followed the procedure discussed by B.M. Das (2005)

In summary, the specimen was placed on the bottom platen of the triaxial cell. Proper adjustments were made so that the piston of the triaxial cell just rests on the top of the platen of the specimen. The chamber of the triaxial cell was filled with water. Hydrostatic cell pressure, σ_3, was applied to the specimen through the chamber fluid. All drainage to and from the specimen were closed. A proper contact between the piston and the top platen was achieved before the apparatus was set to operate.

The triaxial apparatus was connected to an Agilent Vee Pro-Master Data Acquisition Unit and to a home-developed program to record readings.
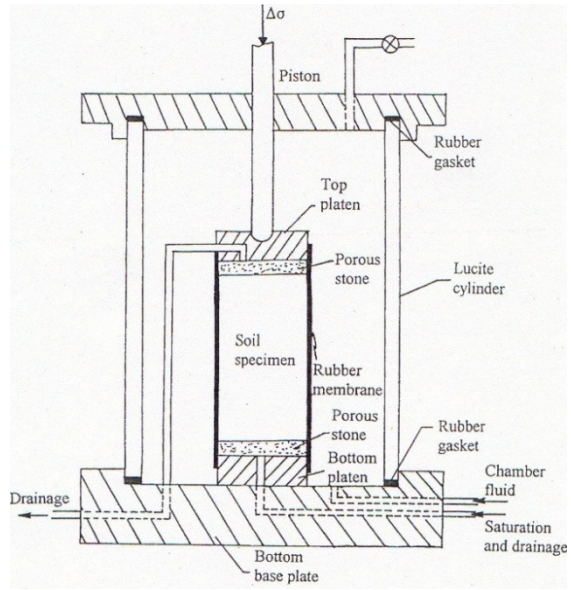
3.6 Diagrammatic representation of the triaxial cell (Das, 2005)

4. RESULTS AND ANALYSIS OF UNCONSOLIDATED, UNDRAINED (UU) TRIAXIAL TESTS ON PETROLEUM CONTAMINATED CLAY SOIL

4.1 Unconsolidated Undrained (UU) Triaxial Test

In the present research the purpose of a UU test is to determine the undrained shear strength of a saturated contaminated soil. The UU test consists of applying a cell pressure to the soil sample without drainage of porewater followed by increments of axial stress. The cell pressure is kept constant and the test is completed very quickly because in neither of the two stages ,consolidation and shearing, is the excess pressure is not allowed to drain. The stresses applied are:

Stage 1: Isotropic compression (not consolidation) phase

$$\Delta\sigma_1 = \Delta\sigma_3, \qquad \Delta u \neq 0 \qquad\qquad \Delta p = \Delta\sigma_1, \qquad \Delta q = 0 \qquad \frac{\Delta q}{\Delta p} = 0$$

Stage 2 : Shearing phase (Fig. 4.1 and 4.2)

$$\Delta\sigma_1 > 0, \qquad \Delta\sigma_3 = 0 \qquad\qquad \Delta p = \frac{\sigma 1}{3}, \qquad \Delta q = \Delta\sigma_1, \quad \frac{\Delta q}{\Delta p} = 3$$

The undrained shear strength, S_u, and the undrained initial and secant elastic moduli, E_u and $(E_u)_s$, are obtained from a UU test. The advantage of the UU test is that the soil sample is stressed in the lateral direction to simulate the field

condition. This test is useful in preliminary (TSA) analysis for design of slopes, foundations, retaining walls, excavations and other earthwork (Budhu, 2007).

In this research thesis three samples of the same soil were tested at the same cell pressure (σ_3 = 100 kPa). Results from these tests (Fig. 4.3) yield Mohr circles of different sizes, due to difference in the percentage of contamination. Mohr's circles, stresses, and stress paths for the UU test are shown in figures below.

$$\sigma_1 = \sigma_3 + \frac{PZ}{A}$$

σ_3
$\Delta u \neq 0$
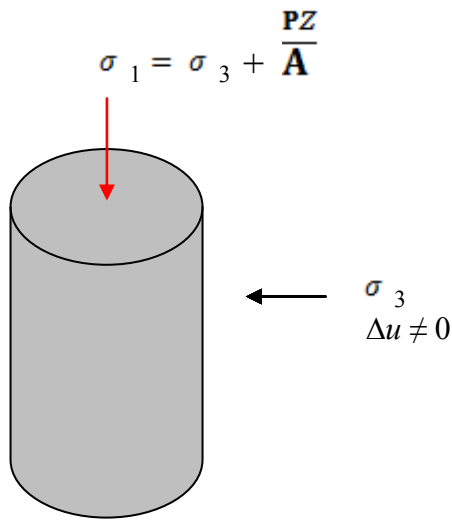
Figure 4.1. Shearing stresses (Budhu, 2007)

q

TPS

P
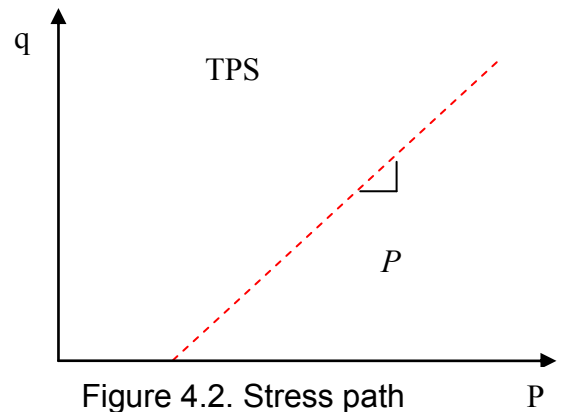
Figure 4.2. Stress path (Budhu, 2007) P

τ

σ
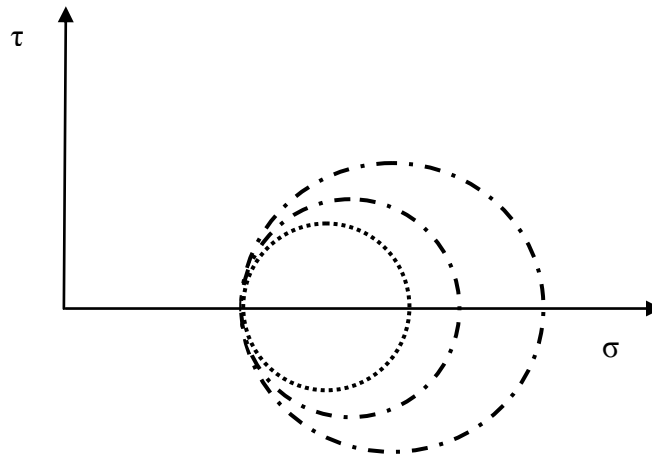
Figure 4.3. Mohr's circles for UU tests

4.1.1 Kaolin with no contamination – Initial Undrained Shear Strength

For kaolin clay with 0% contamination the UU test yields an undrained shear strength S_u = 23.5 kPa (Table 4.1). This represents the initial uncontaminated shear strength of the clay.

From the test results given in the Figure 4.4 below, the undrained shear strength of the clay is calculated as S_u = $(\sigma_1-\sigma_3)/2$ = 23.5 kPa via the Mohr circle of Figure 4.6.
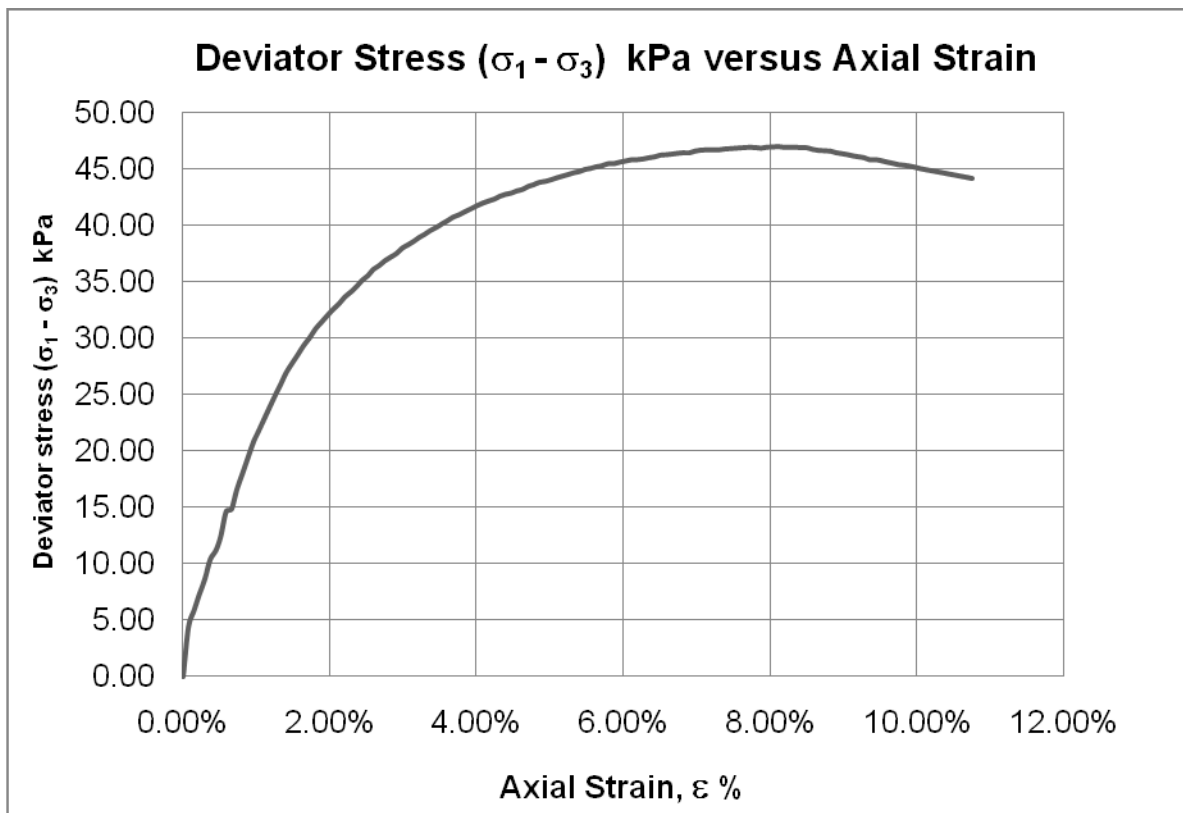
Figure 4.4. Deviator Stress $(\sigma_1 - \sigma_3)$ kPa versus Axial Strain for 0 % contamination

From this figure we can also determine the undrained elastic moduli. Two values are calculated mainly the initial and secant moduli. The figure above (Fig. 4.5) is reproduced below in order to demonstrate the procedure used to calculate the initial and secant moduli.
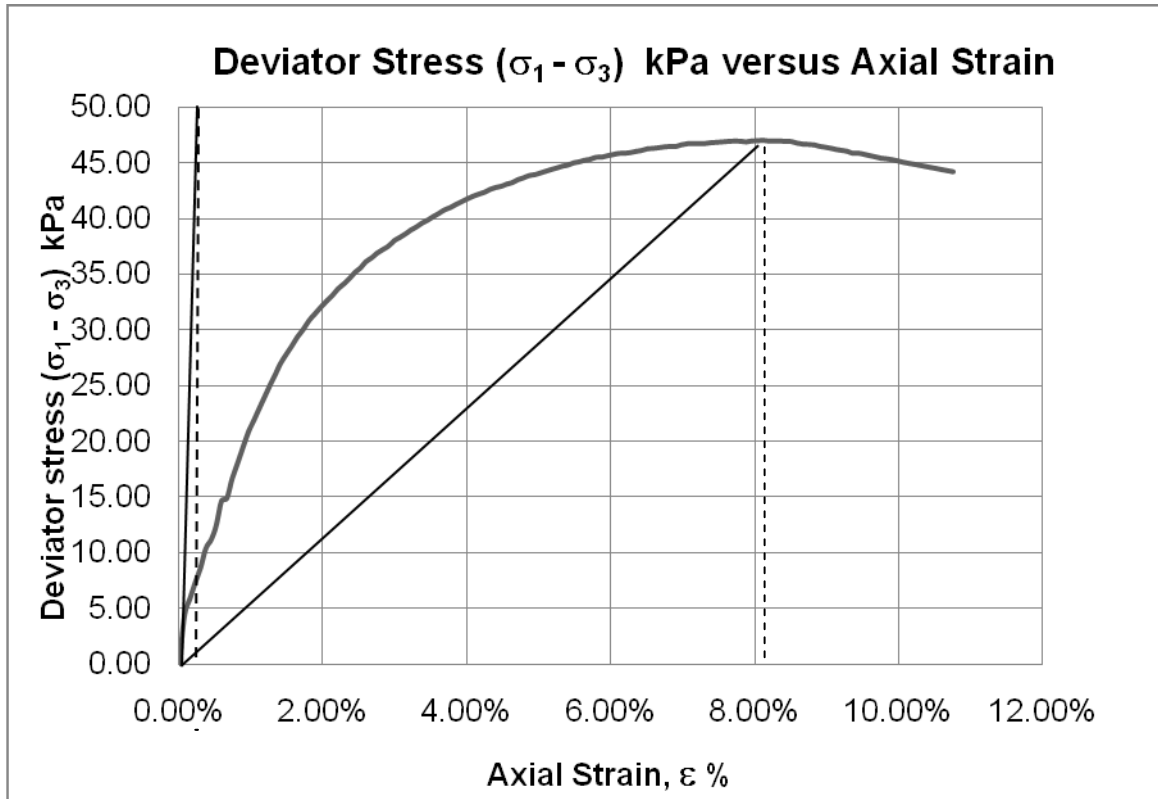
Figure 4.5. E_u and $(E_u)_s$ moduli for clay with 0% contamination.

The values obtained for the tangent and secant modulus are respectively

E_u = 50 kPa / 0.003 = 16,666.66 kPa   and $(E_u)_s$ =   47.00538607 / 0.0812 = 578.88 kPa

The tangent as well as secant modulus is used in elastic analysis to calculate immediate settlements of foundations. If the foundation soil is highly nonlinear then the secant modulus is preferred over the tangent modulus. Results show that the initial modulus is much greater than the secant modulus as confirmed by the tests and in foundation practice.

Figure 4.7 below gives a visual summary of the tests just described.
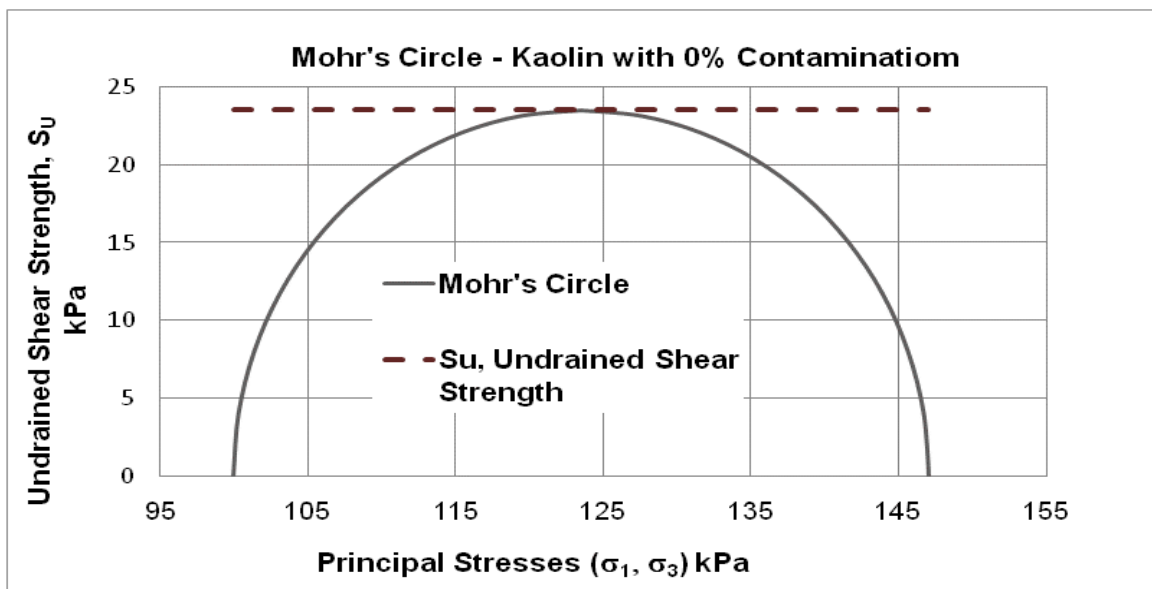
Figure 4.6. Mohr's Circle – Kaolin with 0% Contamination
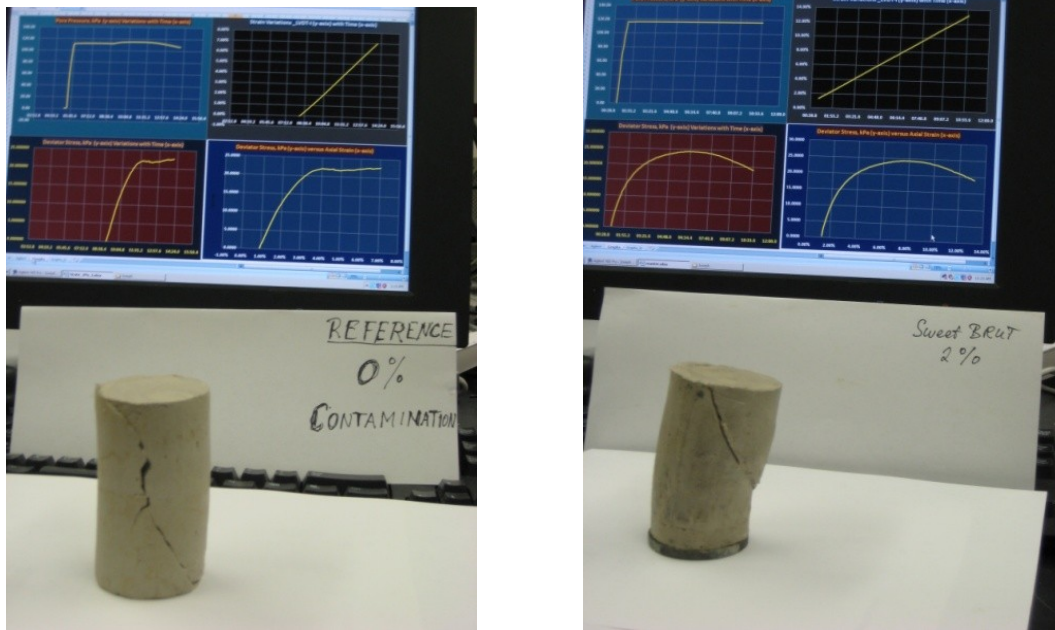
Figure 4.7. Specimen with 0% and 2% sweet brut contamination

4.2 Contamination of kaolin clay with sweet brut

4.2.1 Kaolin clay contaminated with 2% sweet brut

For kaolin clay with 2% contamination the UU test yields an undrained shear strength, S_u = 17.5 kPa (Table 4.1). Like the previous calculation for the undrained shear strength, the contaminated undrained shear strength of the clay is calculated as

$S_u = (\sigma_1-\sigma_3)/2 = 17.5$ kPa   (Figure 4.10).

This result confirms a significant drop in the undrained shear strength of 6 kPa (Table 4.2), when compared with the previous result for the uncontaminated specimen. This represents a decrease of 25.53% (Table 4.2) in the undrained shear strength.
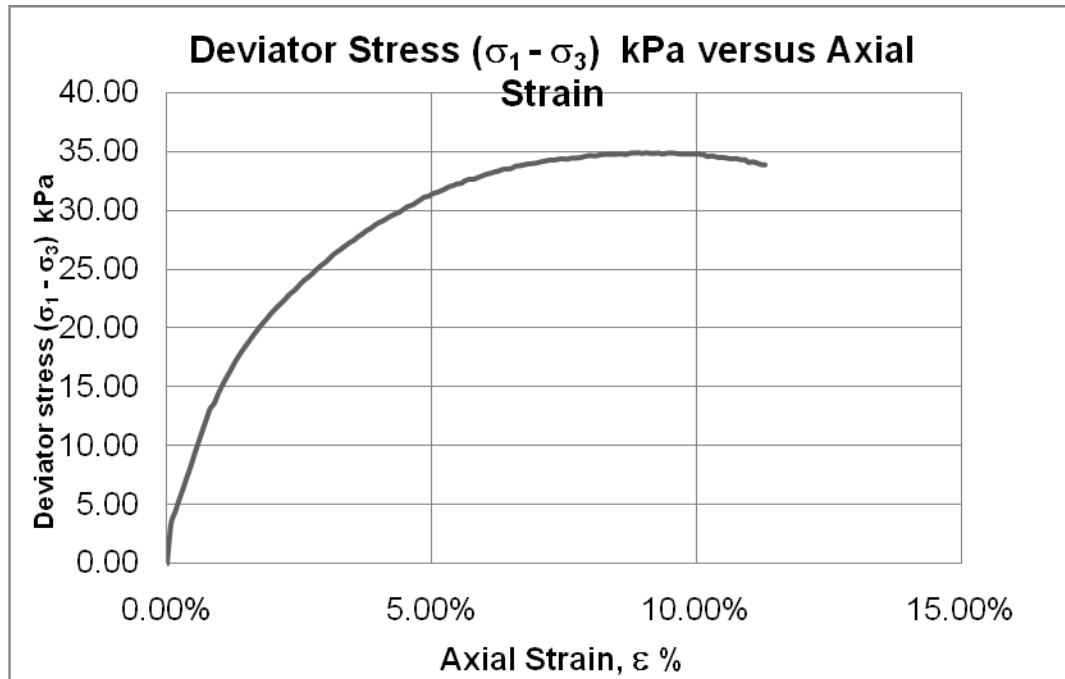
Figure 4.8. Deviator Stress (σ_1- σ_3) kPa versus Axial Strain for 2% contamination with sweet brut

Again from this figure the undrained elastic moduli can be determined. As previously two values are calculated mainly the initial and secant moduli. The Figure 4.8 above is reproduced below (Figure 4.9) in order to demonstrate the procedure used to calculate the initial and secant moduli.
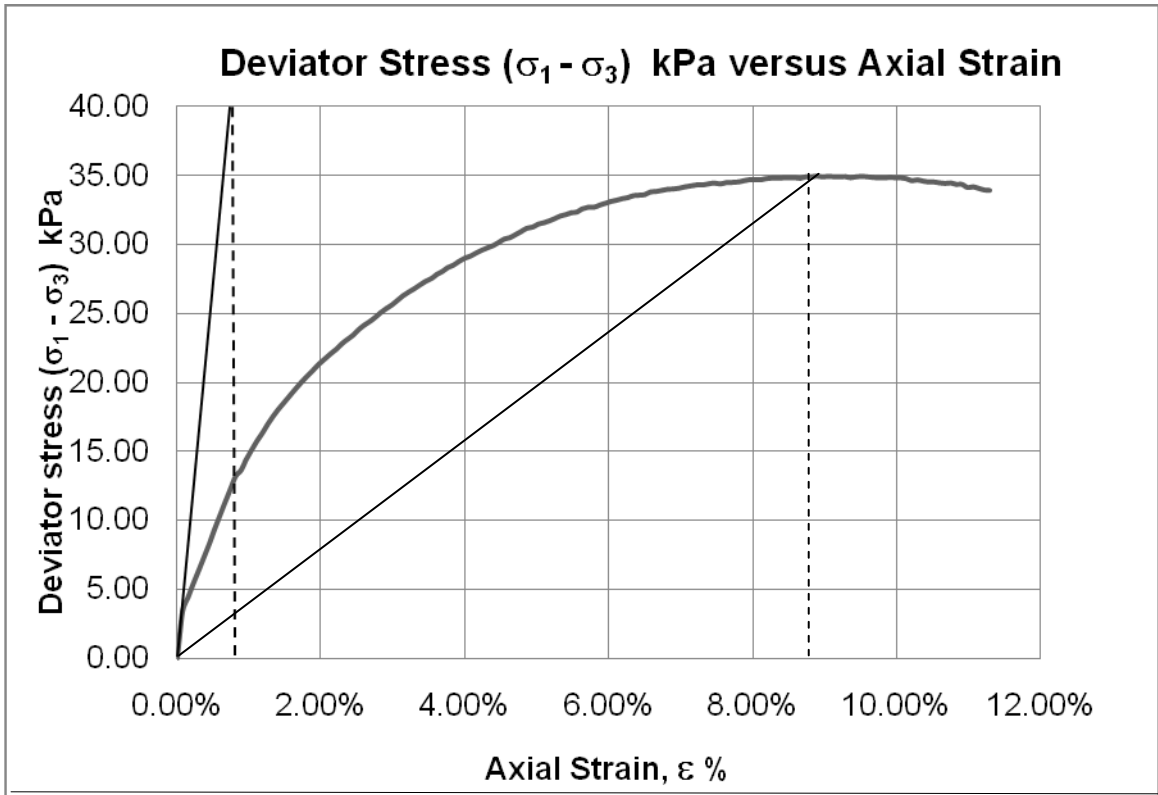
Figure 4.9. E_u and $(E_u)_s$ moduli for clay with 2% sweet brut contamination.

In this instance results for the initial and secant modulus are respectively

E_u = 40 kPa / 0.008 = 5,000 kPa   and

$(E_u)_s$ = 34.95527994 / 0.0089 = 392.75 kPa

These values confirm that contamination seriously affects the compressibility of the underlying soil. The calculated elastic settlements would be much greater because of the loss in stiffness when compared to the previous uncontaminated case. Results still show that the initial modulus is much greater than the secant modulus when the soil is contaminated.
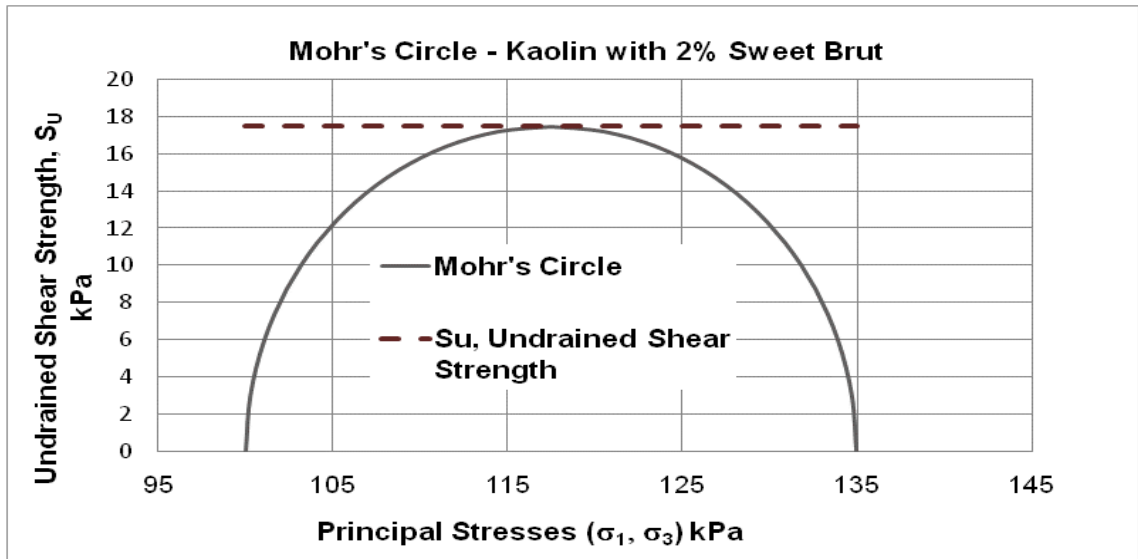
Figure 4.10. Mohr's Circle – Kaolin with 2% sweet brut contamination

A similar analysis of all the tests results conducted in the present research is given below.

4.2.2 Kaolin clay contaminated with 4% sweet brut

For kaolin clay with 4% contamination the UU test yields 15.0 kPa (Table 4.1). From the figure below the undrained shear strength of the clay is calculated as

$S_u = (\sigma_1 - \sigma_3)/2 = 15.0$ kPa   (Figure 4.13).

Contaminated by 4% of sweet brut the shear strength of the clay soil in examination dropped by 8.5 kPa (Table 4.2), due to contamination, to 15.0 kPa from the initial shear strength (with 0% of contamination) of 23.5 kPa.

This represents a decrease of 36.17% (Table 4.2) in shear strength compared to the initial shear strength.
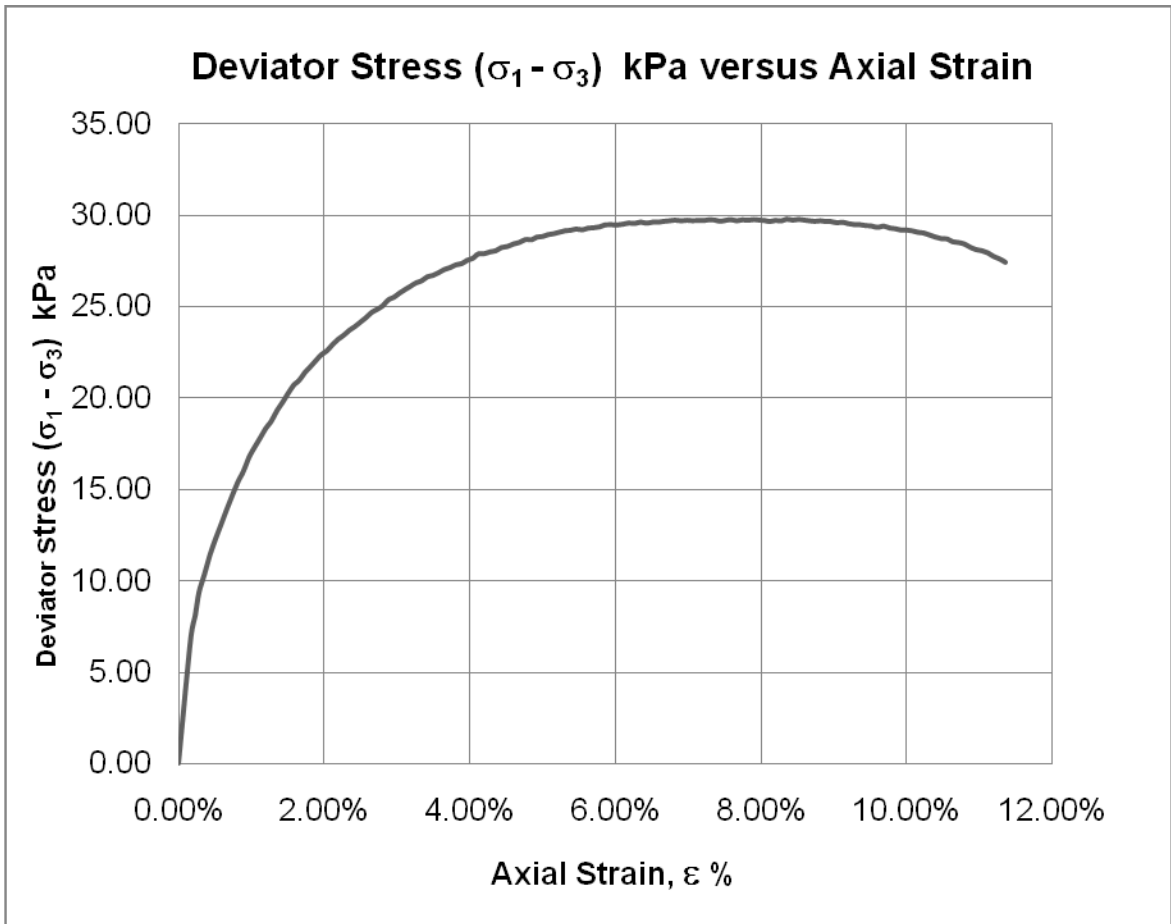
Figure 4.11. Deviator Stress (σ_1 - σ_3) kPa versus Axial Strain for 4% contamination with sweet brut

The undrained elastic moduli can also be determined from this figure. Two values, the initial and secant moduli, are calculated. The figure above is reproduced below in order to demonstrate the procedure used to calculate the initial and secant moduli.
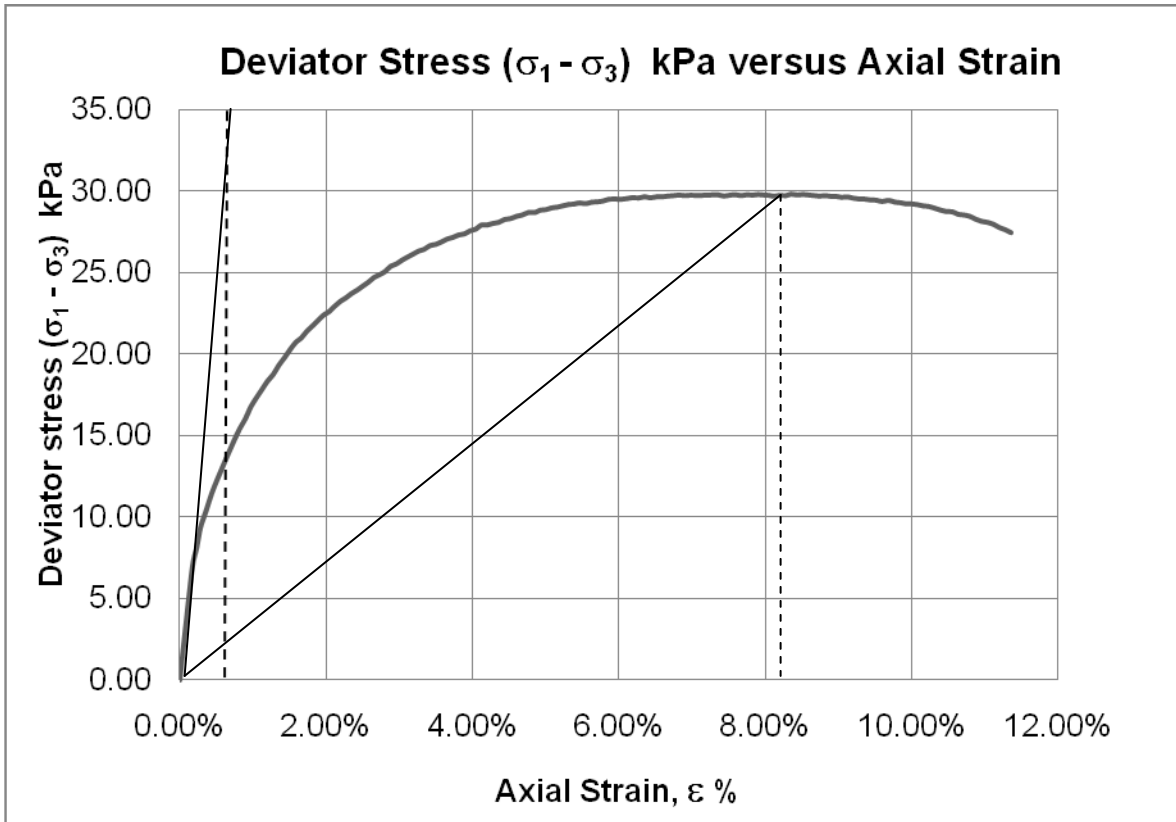
Figure 4.12. E_u and $(E_u)_s$ moduli for clay with 4% sweet brut contamination.

E_u = 35 kPa / 0.002 = 17,500 kPa and

$(E_u)_s$ = 29.801464 / 0.0835 kPa = 356.90 kPa

where E_u, the tangent modulus, is used to calculate the incremental movement due to an incremental load as in the case of the movement due to a high-rise building.

$(E_u)_s$, the secant modulus is used to predict the movement due to the first application of a load, as in the case of a spread footing. (Briaud, 2001)

37

Results confirm once again that the initial modulus is much greater than the secant modulus.
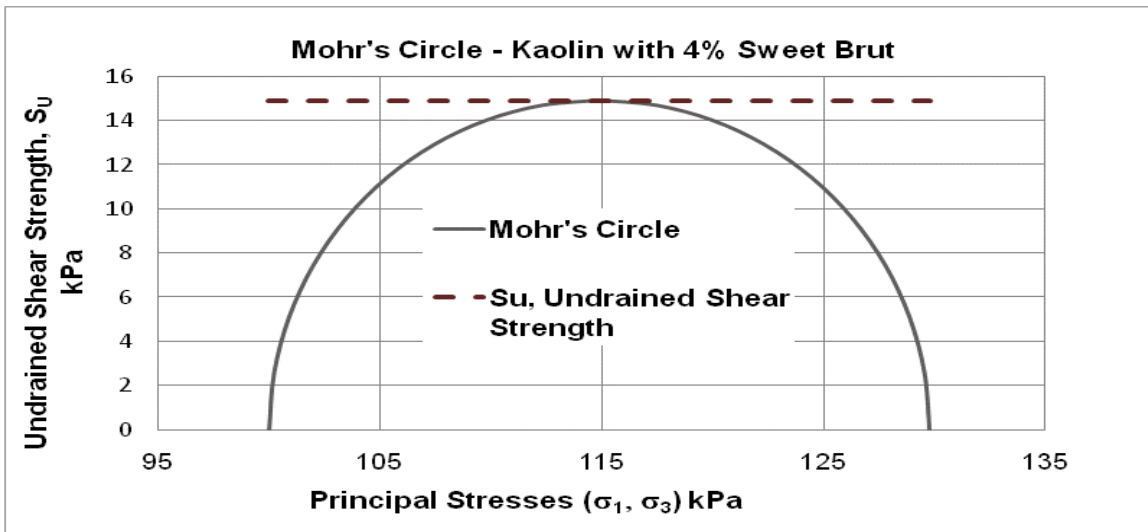
Figure 4.13. Mohr's Circle – Kaolin with 4% sweet brut contamination

4.2.3 Kaolin clay contaminated with 6% sweet brut

For kaolin clay with 6% contamination the UU test yields 11.5 kPa (Table 4.1). From the figure below (Figure 4.14) the undrained shear strength of the clay is calculated as

$S_u = (\sigma_1 - \sigma_3)/2 = 11.5$ kPa (Figure 4.16).

Contaminated by 6% of sweet brut the shear strength of the clay soil in examination dropped by 12 kPa (Table 4.2), due to contamination, to 11.5 kPa from the initial shear strength (with 0% of contamination) of 23.5 kPa.

This represents a decrease of 51.60% (Table 4.2) in shear strength compared to the initial shear strength.
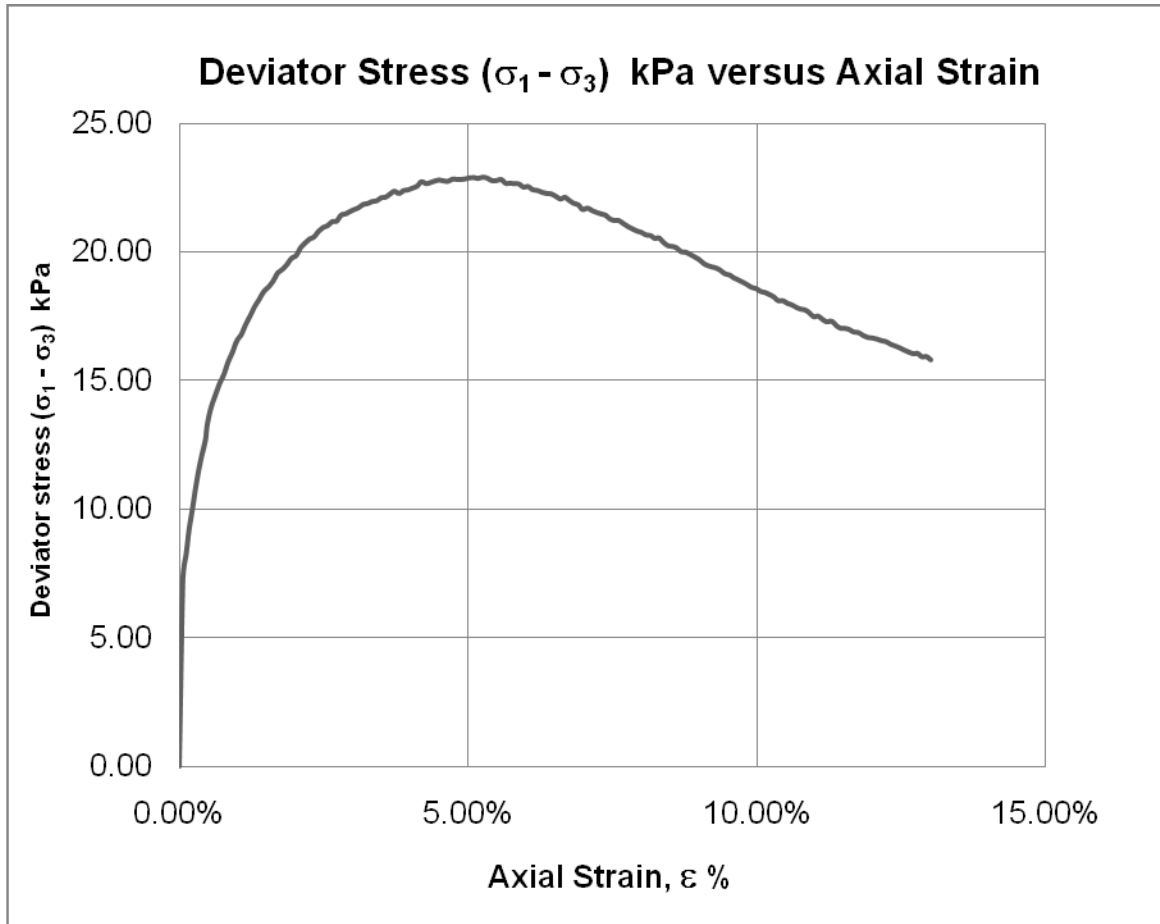
Figure 4.14. Deviator Stress (σ_1- σ_3) kPa versus Axial Strain for 6% contamination with sweet brut

As in the previous discussions the undrained elastic moduli can be determined. Two values are calculated, mainly the initial and secant moduli. The figure above is reproduced below in order to demonstrate the procedure used to calculate the initial and secant moduli.
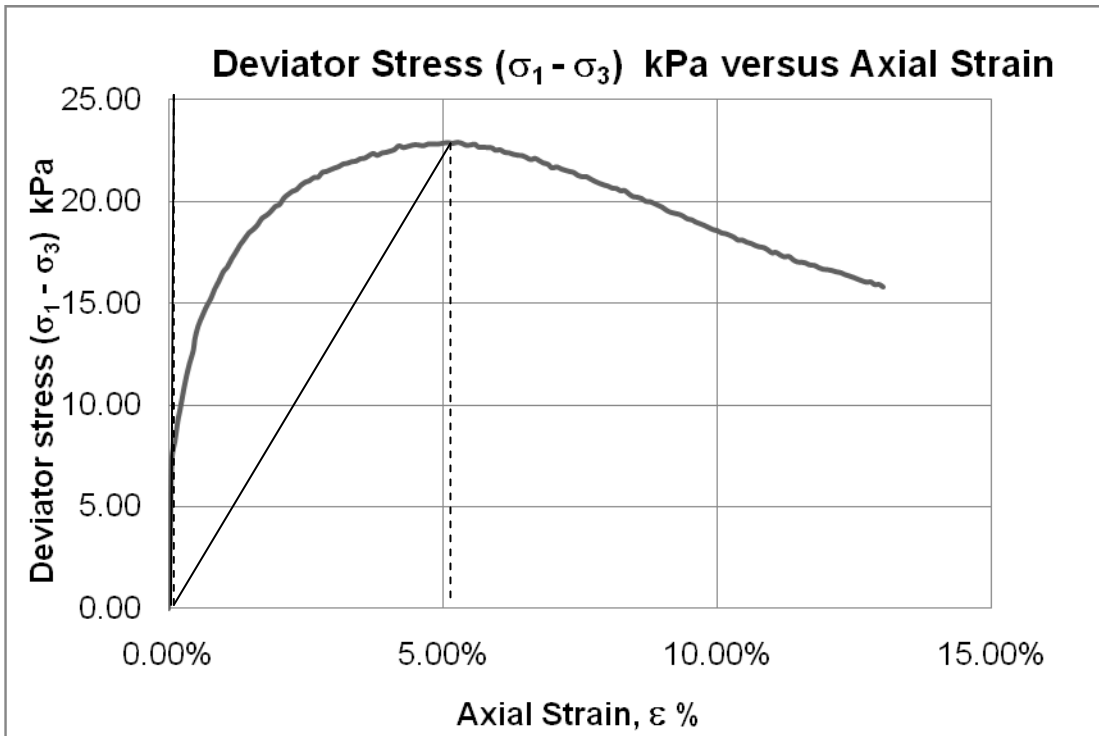
Figure 4.15. E_u and $(E_u)_s$ moduli for clay with 6% sweet brut contamination.

E_u = 25 kPa / 0.0028 = 8,928.57 and

$(E_u)_s$ = 22.8995381 / 0.0526 kPa = 435.35 kPa

Again results show that the initial modulus is much greater than the secant modulus as confirmed in practice.
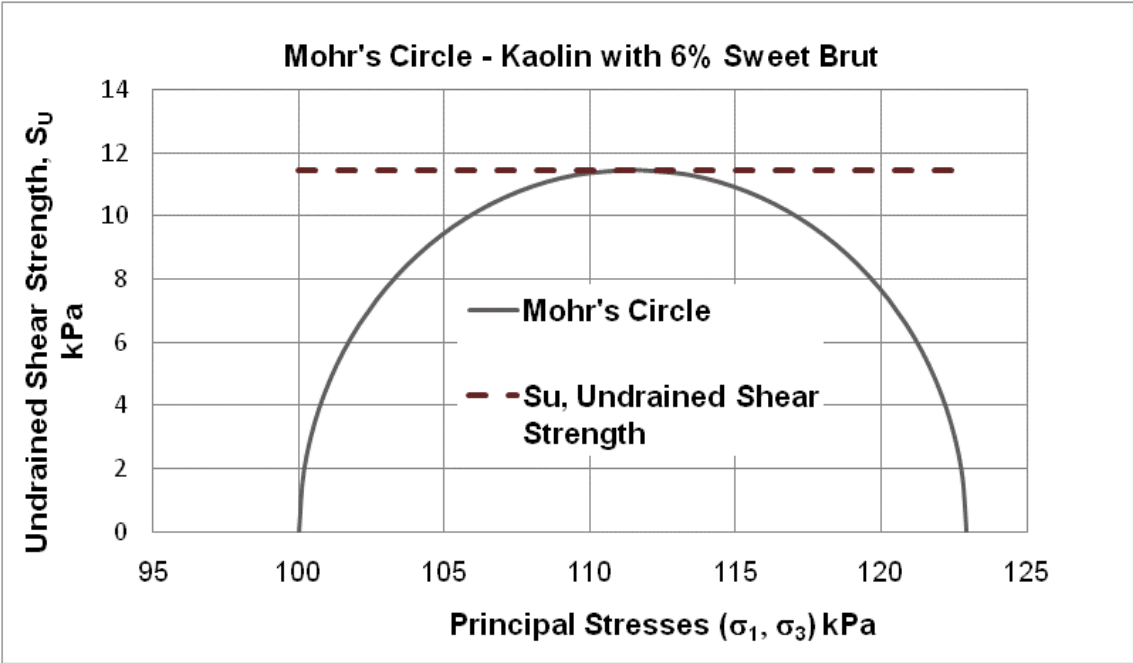
Figure 4.16. Mohr's Circle – Kaolin with 6% sweet brut contamination
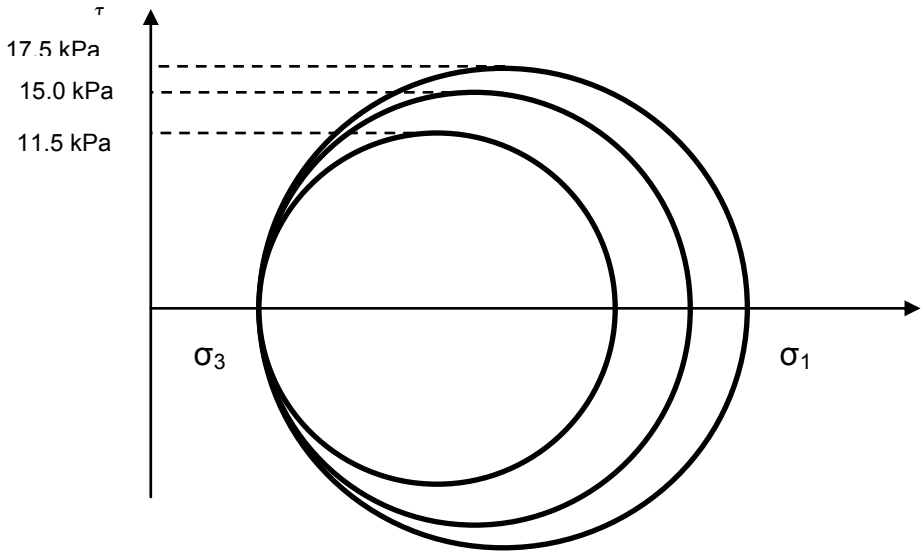
Figure 4.17. Combined Mohr's circles for 2%, 4% and 6% sweet brut
contamination
S_u = 17.5 k Pa, 15.0 kPa, 11.5 kPa; σ_3 = 100

41

4.3 Contamination by heating oil

4.3.1 Kaolin clay contaminated with 2% heating oil

From the Figure 4.18 below the undrained shear strength of the clay is calculated as

S_u = $(\sigma_1-\sigma_3)/2$ = 14.5 kPa (Figure 4.20).

Contaminated by 2% of heating oil the shear strength of the clay soil in examination dropped by 9 kPa (Table 4.2), due to contamination, to 14.50 kPa (Table 4.1) from the initial shear strength (with 0% of contamination) of 23.5 kPa (Table 4.2).

This represents a decrease of 38.30% in shear strength compared to the initial shear strength.
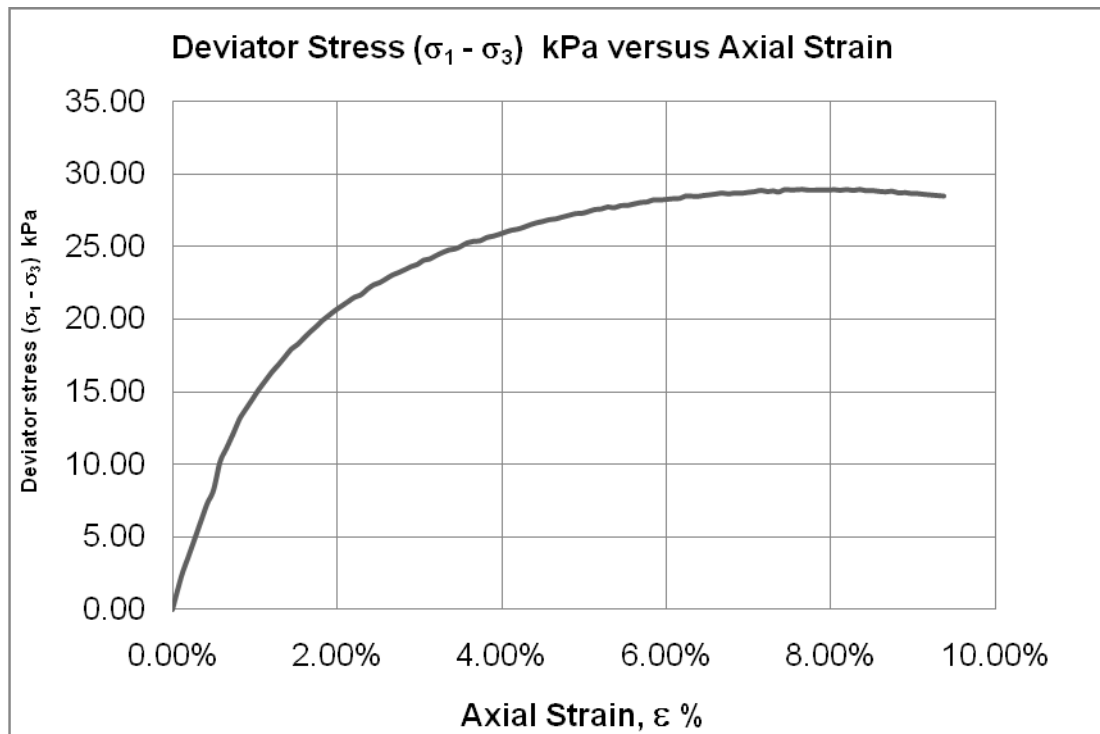
Figure 4.18. Deviator Stress (σ_1- σ_3) kPa versus Axial Strain for 2% contamination with heating oil

From Figure 4.18 the undrained elastic moduli can be also determined. Two values are calculated, mainly the initial and secant moduli. The same figure above is reproduced below in order to demonstrate the procedure used to calculate the initial and secant moduli.
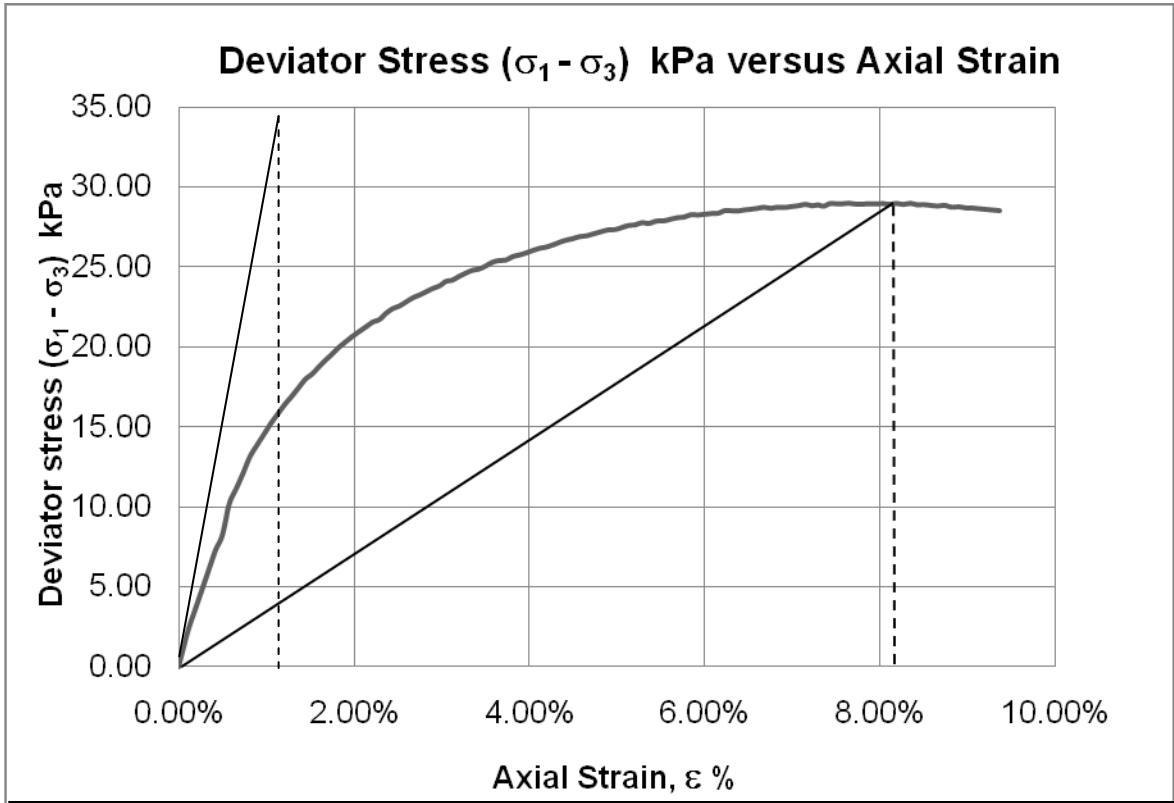
Figure 4.19. E_u and $(E_u)_s$ moduli for clay with 2% heating oil contamination.

E_u = 35 kPa / 0.0149 = 2,348.99 kPa   and

$(E_u)_s$ = 28.9835088 / 0.0835 = 347.10 kPa

Results show that the initial modulus is much greater than the secant modulus as confirmed by the previous tests.
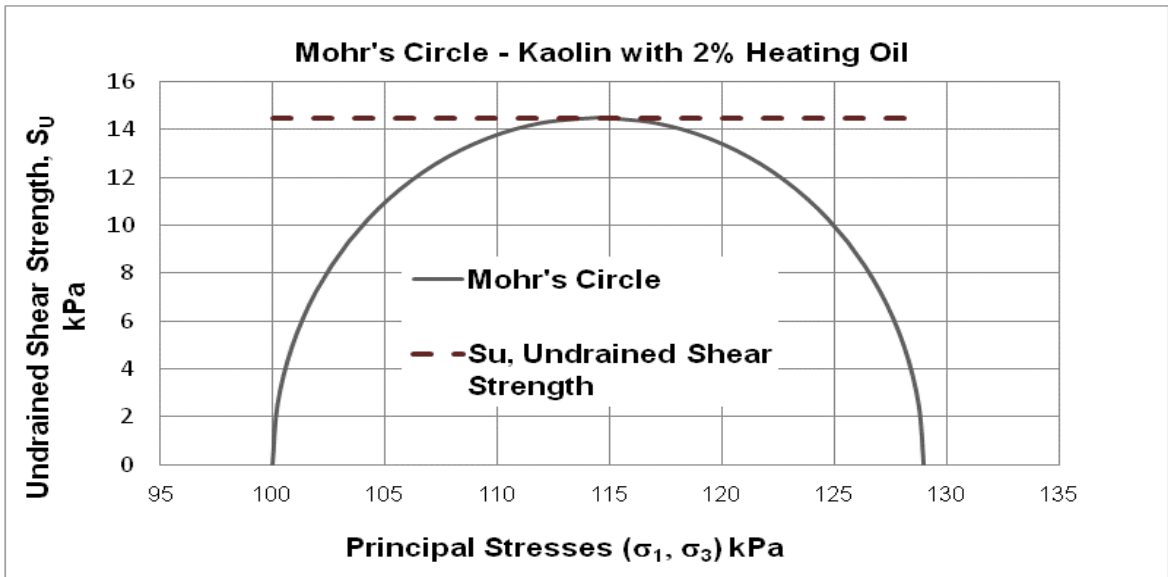
Figure 4.20. Mohr's Circle – Kaolin with 2% heating oil contamination

4.3.2 Kaolin clay contaminated with 4% of heating oil.

From the Figure 4.21 the undrained shear strength of the contaminated clay is calculated as (Figure 4.23)

S_u = $(\sigma_1-\sigma_3)/2$ = 13.0 kPa

This shear strength experienced a drop of 10.5 kPa when compared with the initial shear strength   (0% of contamination) of   23.5 kPa. This represents a decrease of 44.68% when compared to the initial shear strength.
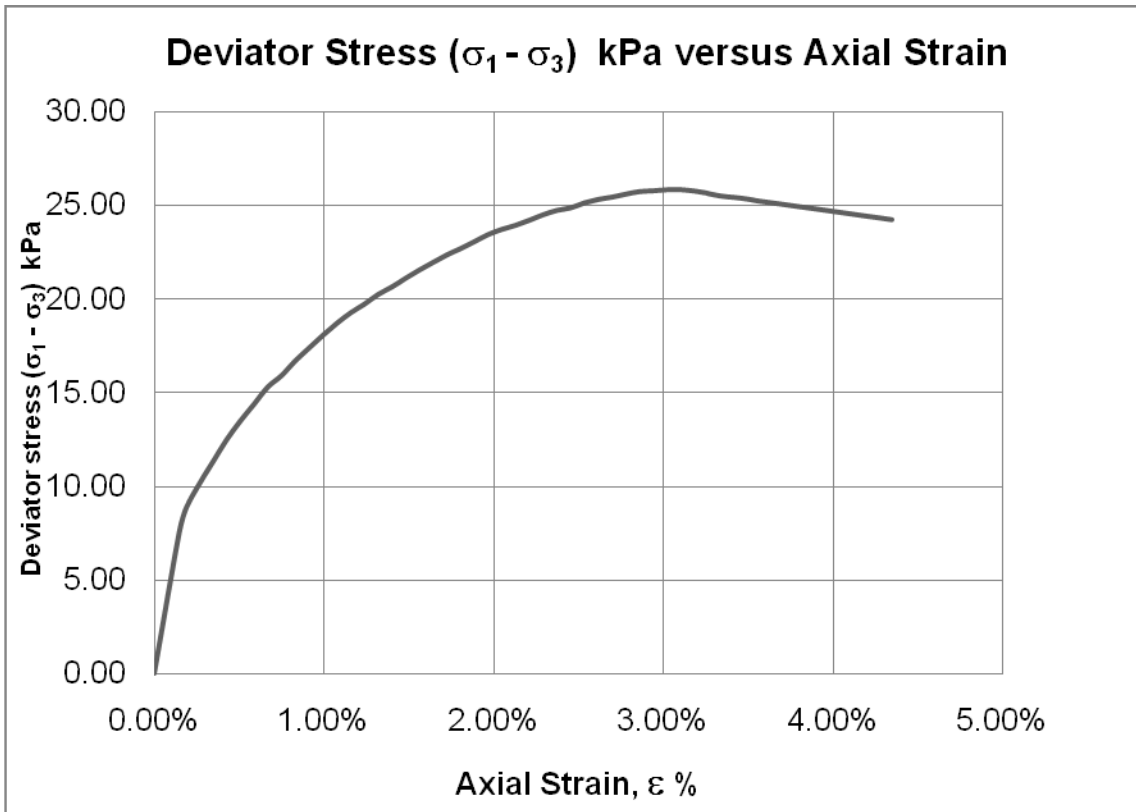
Figure 4.21 Deviator Stress (σ_1- σ_3) kPa versus Axial Strain for 4% contamination with heating oil

From Figure 4.21 the undrained elastic moduli can also be determined. Two values are calculated, mainly the initial and secant moduli. The figure above is reproduced below in order to demonstrate the procedure used to calculate the initial and secant moduli.
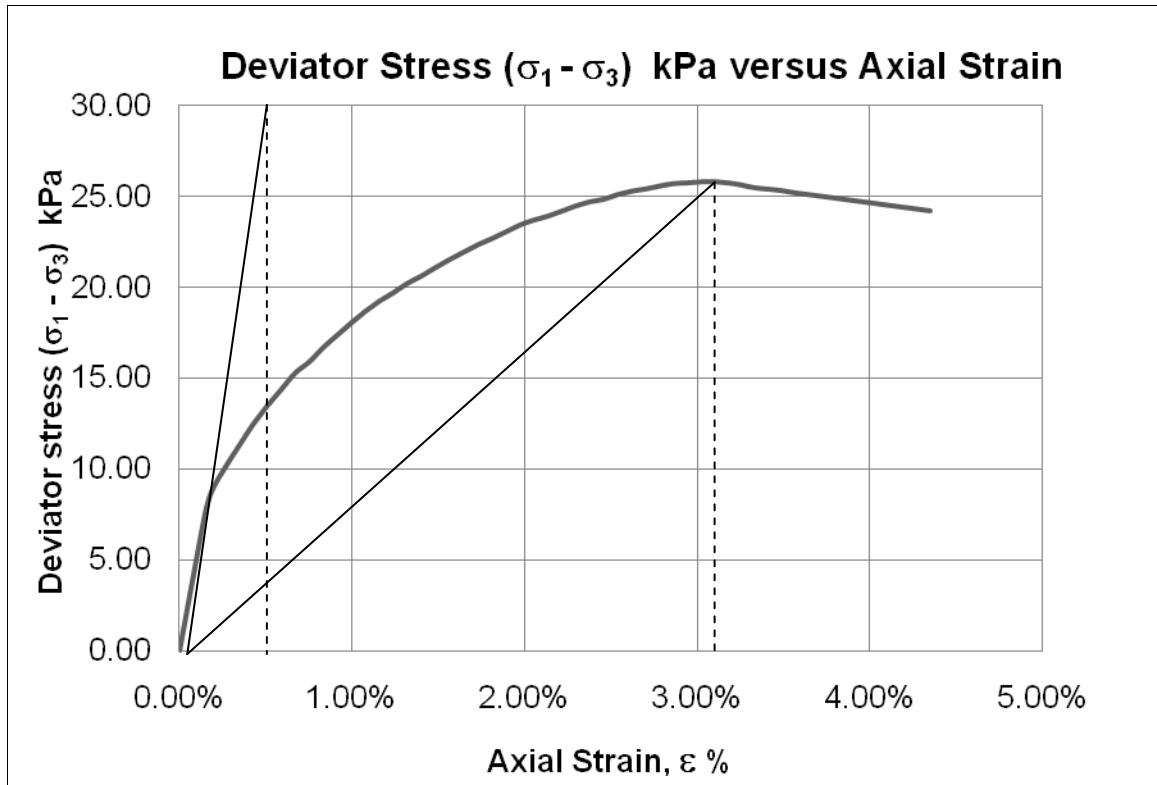
Figure 4.22. E_u and $(E_u)_s$ moduli for clay with 4% heating oil contamination.

E_u = 30 kPa / 0.005 = 6,000 kPa   and

$(E_u)_s$ = 25,853464494 / 0.0302 = 856.07 kPa

These results show that the initial modulus is significantly higher than the secant

modulus. This fact is in agreement with tests and foundation practices.
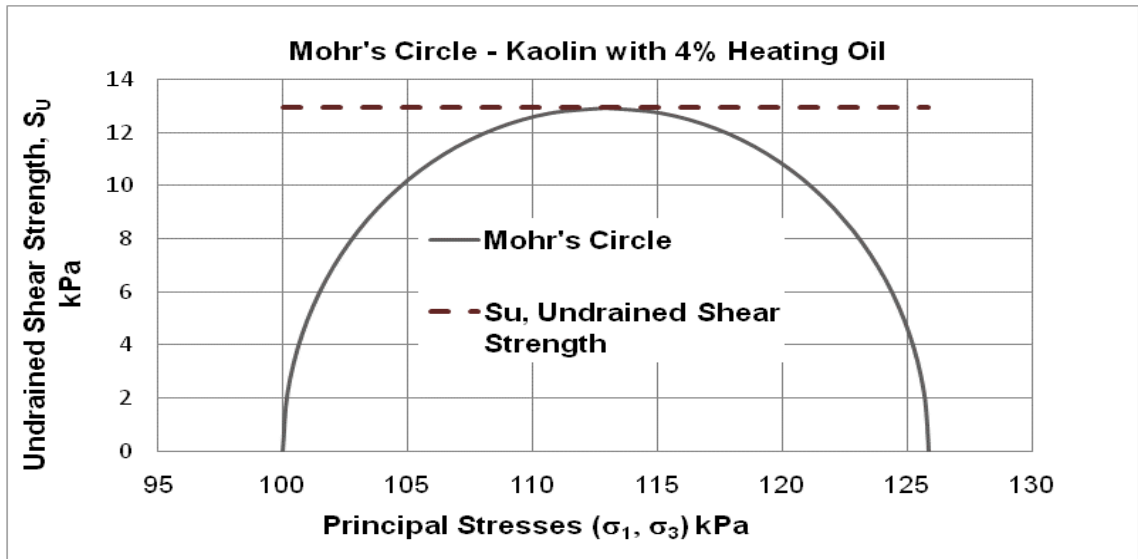
Figure 4.23. Mohr's Circle – Kaolin with 4% heating oil contamination

4.3.3 Kaolin clay contaminated with 6% heating oil

For kaolin clay with 6% heating oil contamination the UU test yields 10.5kPa (Table 4.1.).

From Figure 4.24 the undrained shear strength of the clay is calculated as

S_u = (σ_1-σ_3) / 2 = 10.5 kPa (Figure 4.26)

For Kaolin clay, contaminated with 6% of heating oil, the shear strength of the clay soil dropped from 23.0 kPa (Table 4.2) to 13.0 kPa. This represents a decrease of 55.32% (Table 4.2) in shear strength compared to the initial shear strength.
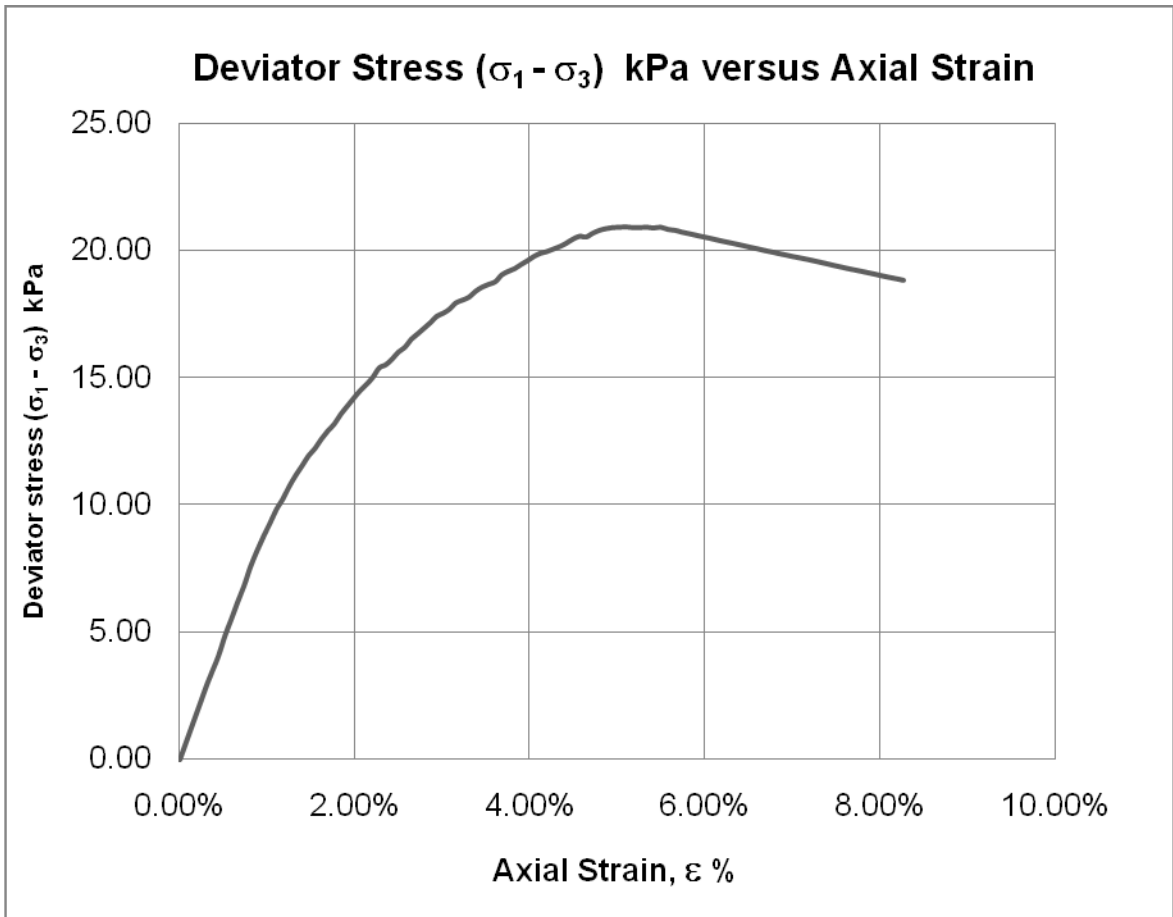
Figure 4.24. Deviator Stress (σ_1- σ_3) kPa versus Axial Strain for 6% contamination with heating oil

From this figure we can also determine the undrained elastic moduli. Two values are calculated mainly the initial and secant moduli. The figure above is reproduced below in order to demonstrate the procedure used to calculate the initial and secant moduli.
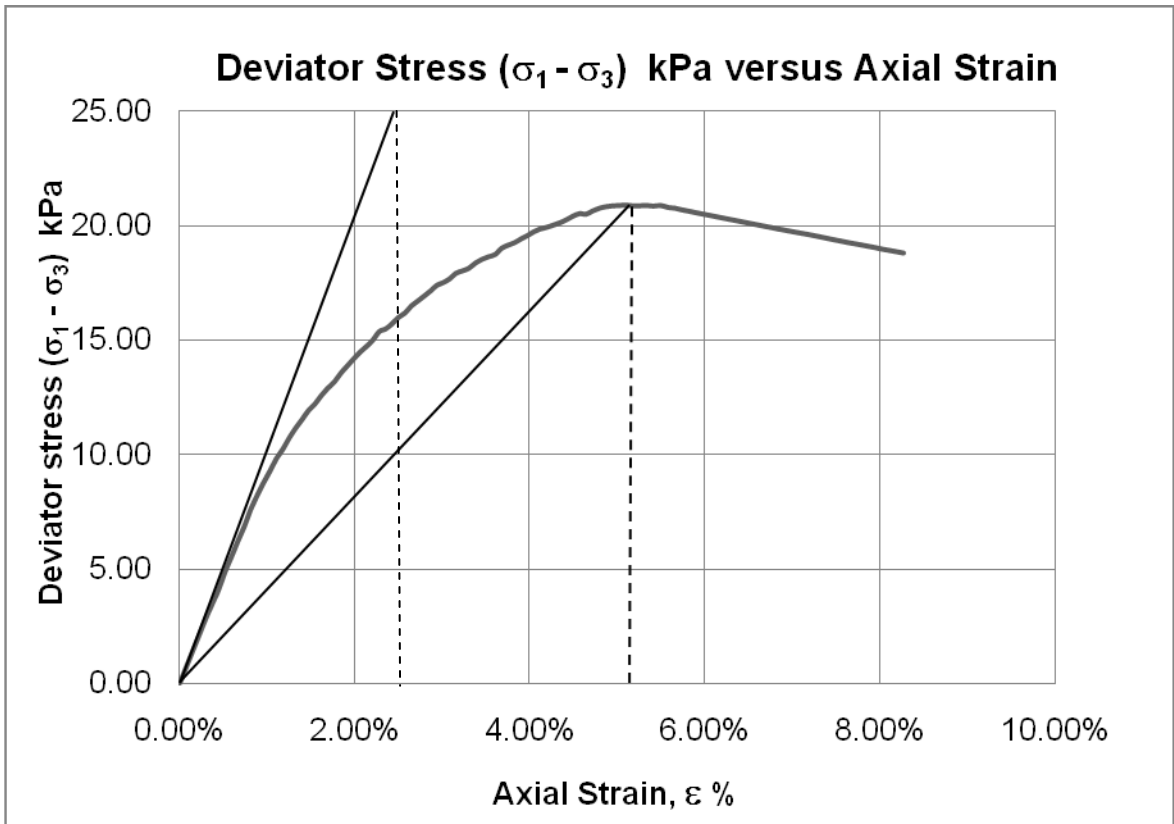
Figure 4.25 E_u and $(E_u)_s$ moduli for clay with 6% heating oil contamination.

E_u = 25 kPa / 0.025 = 1,000 kPa and

$(E_u)_s$ = 20.92385643 / 0.051 = 410.27 kPa

Figure 4.28 gives a visual summary of the tests just described.
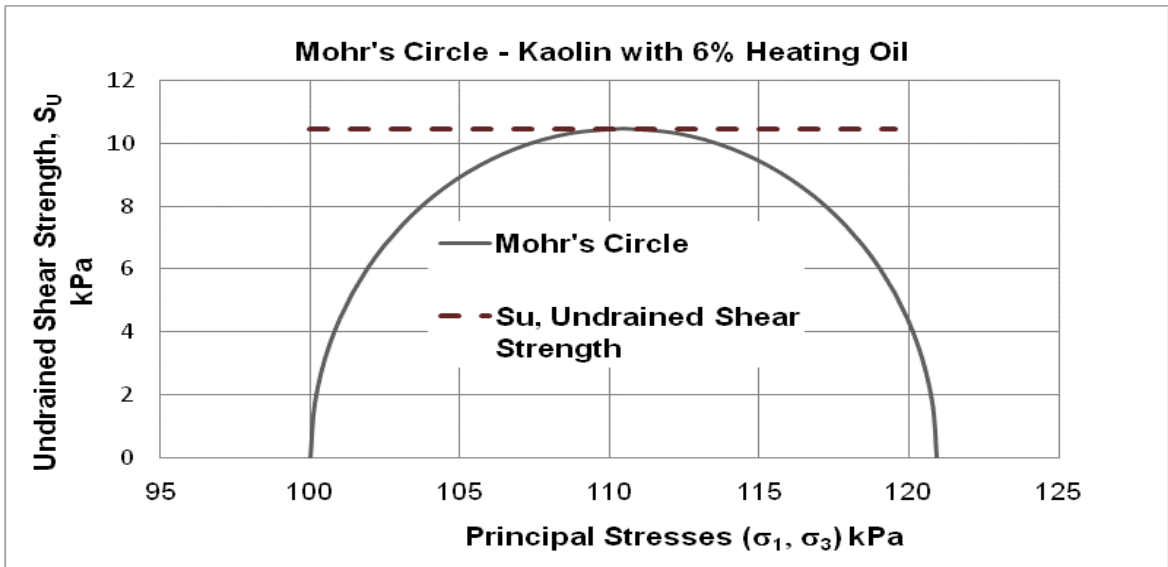
Figure 4.26. Mohr's Circle – Kaolin with 6% heating oil contamination
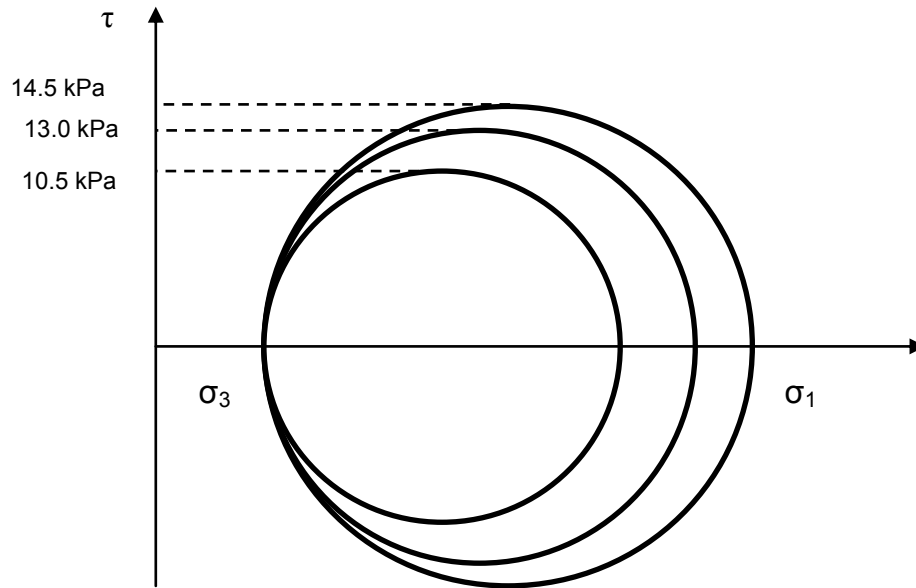
Figure 4.27. Combined Mohr's circles for 2%,4% and 6% heating oil
contamination
S_u = 14.5 k Pa, 13.0 kPa, 10.5 kPa; σ_3 = 100
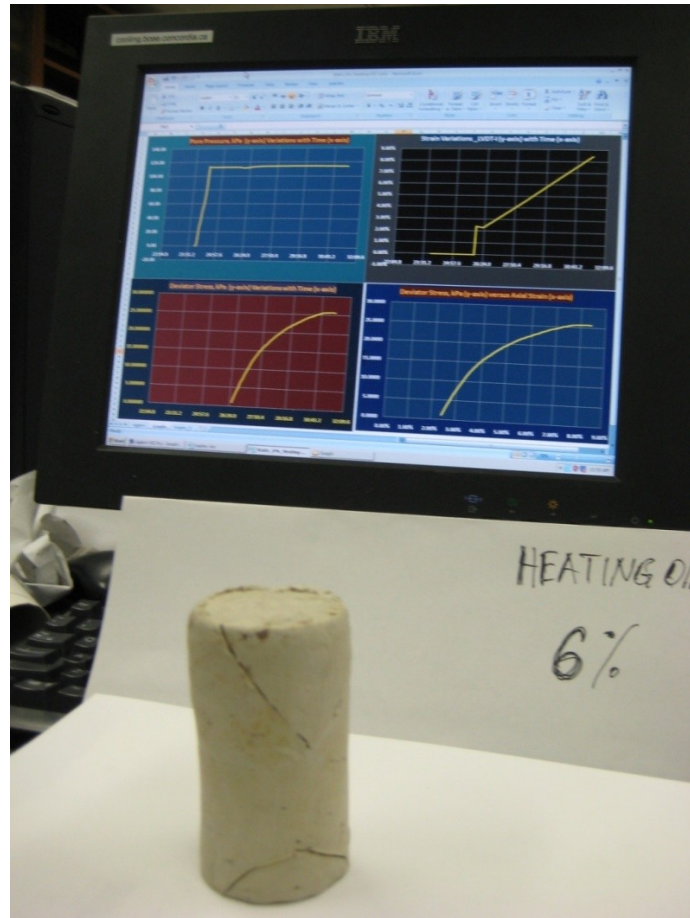
Figure 4.28. Specimen with 6% heating oil contamination

4.4 Contamination by Gasoline

4.4.1 Kaolin clay contaminated with 2% gasoline

From Figure 4.29 the undrained shear strength of the clay is calculated as

$S_u = (\sigma_1 - \sigma_3)/2 = 12.0$ kPa   (Figure 4.31)

Contaminated with 2% of gasoline the shear strength of the clay soil in examination dropped by 11.5 kPa (Table 4.2), due to contamination, to 12.0 kPa (Table 4.1) from the initial shear strength (with 0% of contamination) of 23.5 kPa (Table 4.1).

This represents a decrease of 46.80% (Table 4.2) in shear strength compared to the initial shear strength.
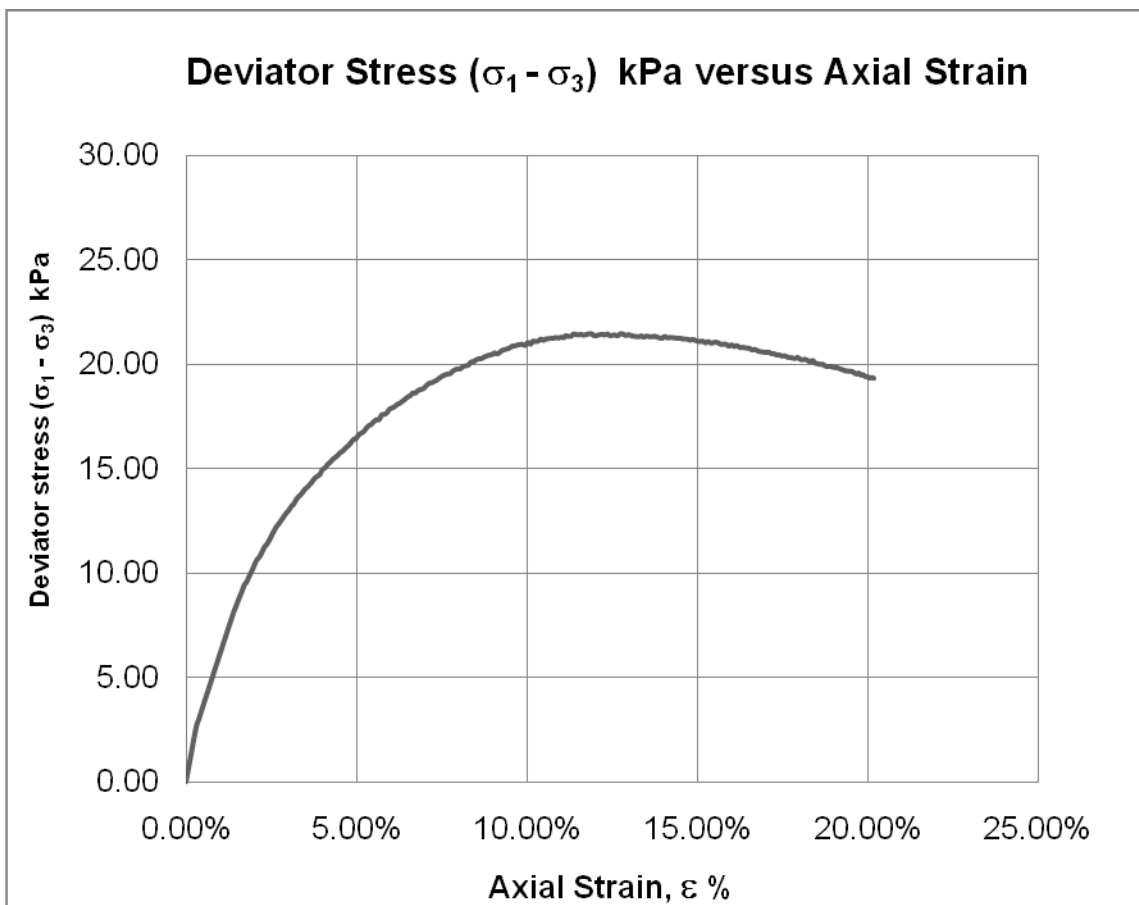
Figure 4.29. Deviator Stress (σ_1- σ_3) kPa versus Axial Strain for 2% contamination with gasoline

From Figure 4.29 the undrained elastic moduli can also be determined. Two values calculated in Figure 4.30 are the initial and secant moduli.
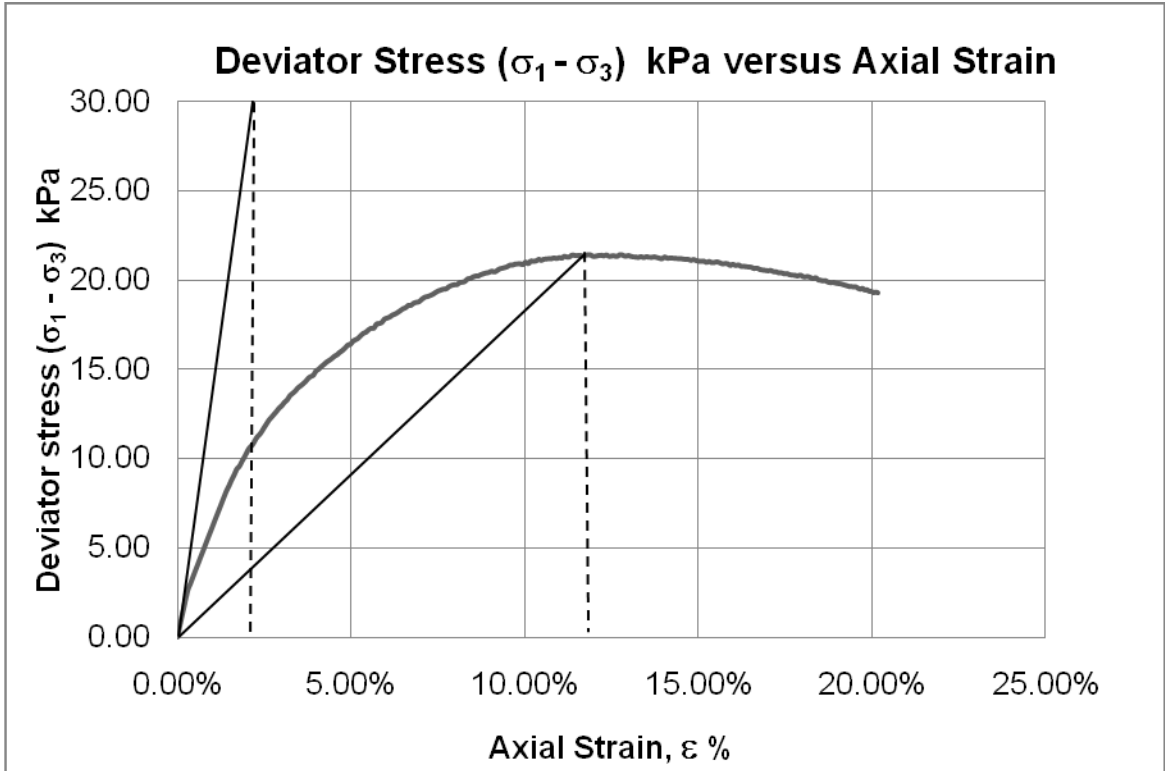
Figure 4.30. E_u and $(E_u)_s$ moduli for clay with 2% gasoline contamination.

E_u = 30 kPa / 0.002 = 15,000 kPa   and

$(E_u)_s$ = 21.45942713 / 0.1274 = 168.44 kPa

Results above show that the initial modulus is much greater than the secant modulus and are in conformity with foundation science.
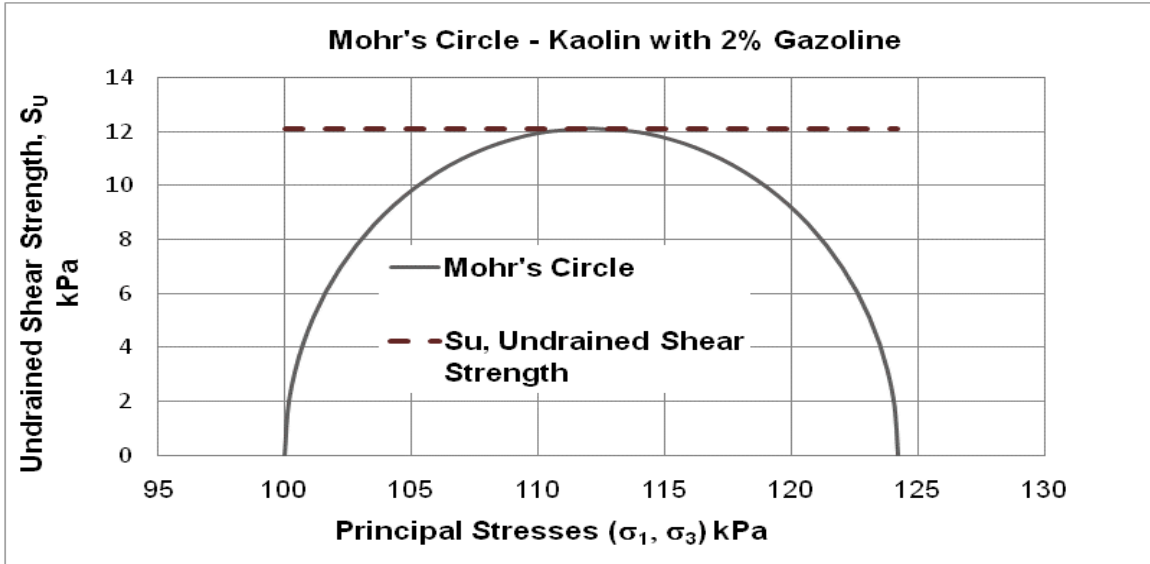
4.31. Mohr's Circle – Kaolin with 2% gasoline contamination

4.4.2 Kaolin clay contaminated with 4% of gasoline

For kaolin clay with 4% contamination the UU test yields 10.5 kPa (Table 4.1).

This undrained shear strength of the clay is calculated from Figure 4.32   as

S_u = $(\sigma_1-\sigma_3)/2$ = 10.5 kPa   (Figure 4.34)

 The shear strength of the clay soil in examination dropped by 13.0 kPa (Table 4.2), due to contamination, to 10.5 kPa (Table 4.1) from the initial shear strength (with 0% of contamination) of 23.5 kPa (Table 4.2) .

This represents a decrease of 55.32% (Table 4.2) in shear strength compared to the initial shear strength.
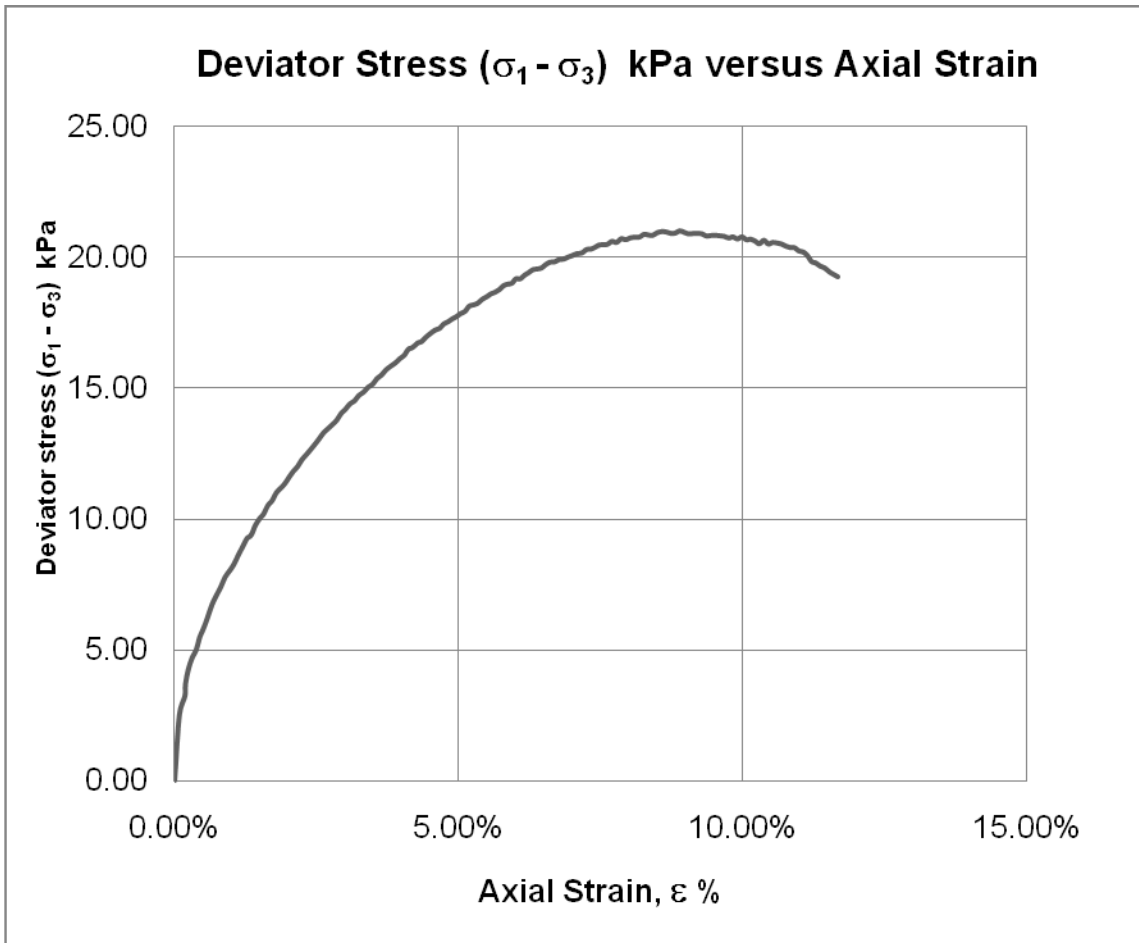
Figure 4.32. Deviator Stress (σ_1- σ_3) kPa versus Axial Strain for 4% contamination with gasoline

From this figure above (Figure 4.32) two values of the undrained elastic moduli can also be determined, the initial and secant modulus. The figure above is reproduced below in order to demonstrate the procedure used to calculate the initial and secant moduli.
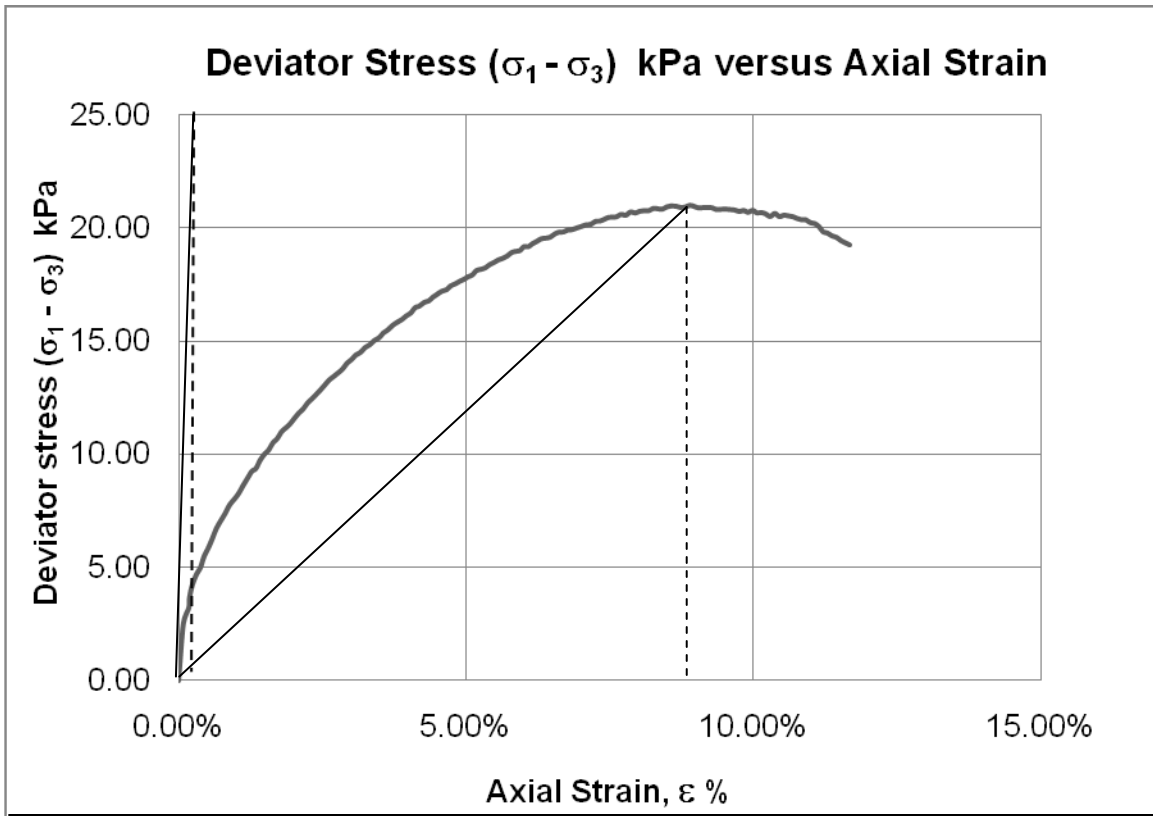
Figure 4.33. E_u and $(E_u)_s$ moduli for clay with 4% gasoline contamination.

E_u = 25 kPa / 0.002 = 12,500 kPa   and

$(E_u)_s$ = 21.0048423 / 0.0888 = 236.54 kPa

The fact that the initial modulus is much greater than the secant is in agreement with the previous results.
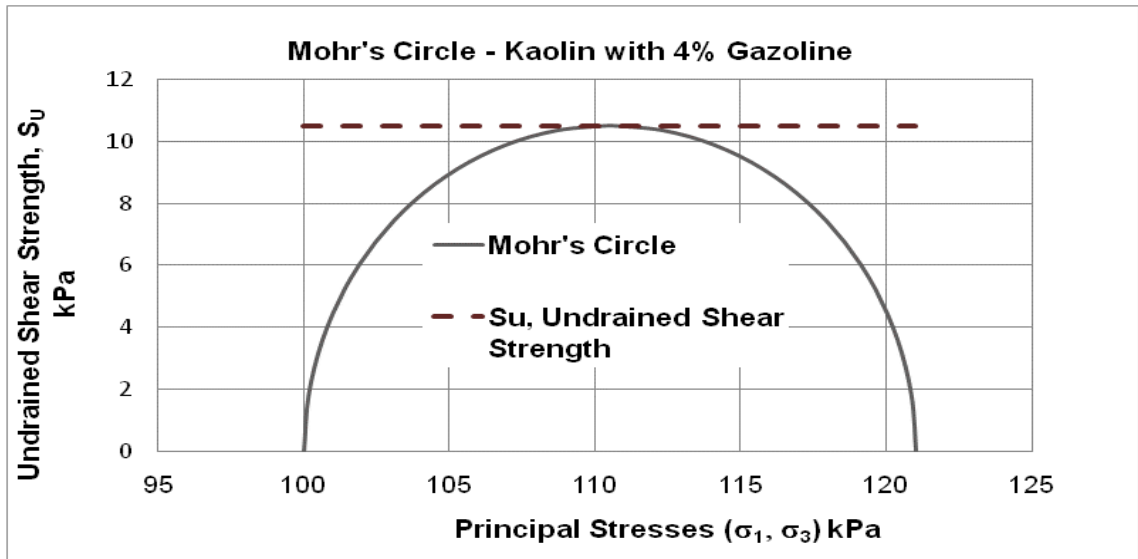
Figure 4.34. Mohr's Circle – Kaolin with 4% gasoline contamination

Figures below depics the clay sample after being removed from the triaxial cell.
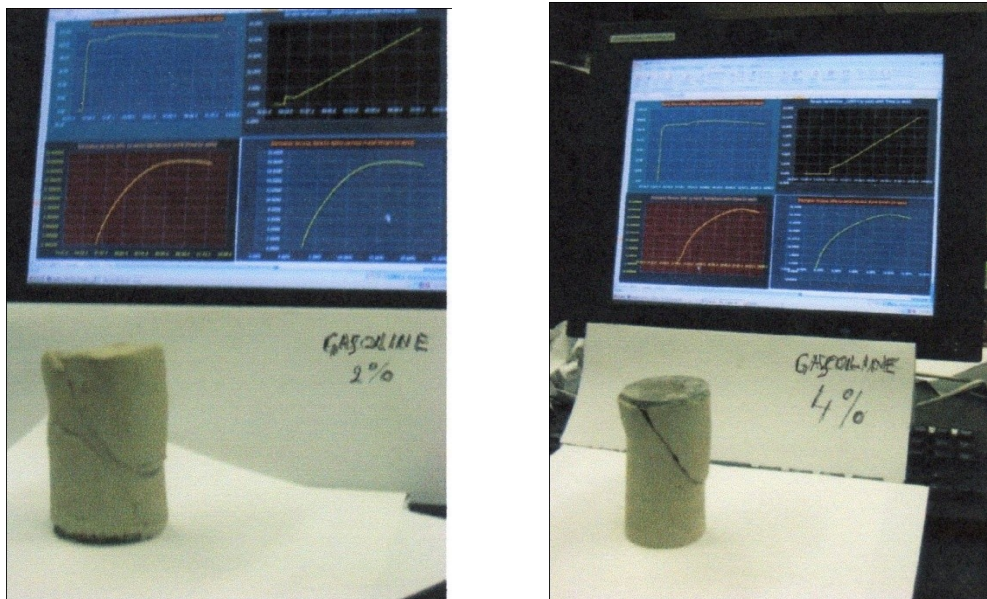
Figure 4.35. Specimens with 2% and 4% gasoline contamination
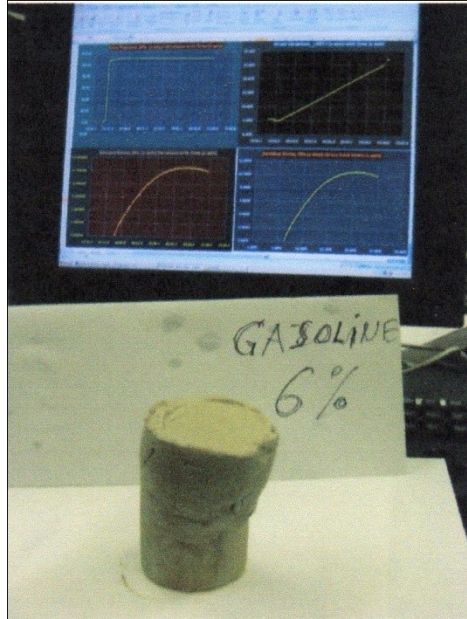
Figure 4.36. Specimen with 6% gasoline contamination

4.4.3 Kaolin clay contaminated with 6% of gasoline

For kaolin clay with 6% gasoline contamination the UU test yields 7.5 kPa (Table 4.1).

From the figure below (Figure 4.37) the undrained shear strength of the clay is calculated as

$S_u = (\sigma_1 - \sigma_3)/2 = 7.5$ kPa   (Figure 4.39)

The shear strength of the kaolin clay soil in examination dropped by 16.0 kPa (Table 4.2), due to contamination, to 7.5 kPa (Table 4.1) from the initial shear strength (with 0% of contamination) of 23.5 kPa (Table 4.1).

This represents a decrease of 68.08% (Table 4.2) in shear strength compared to the initial shear strength.
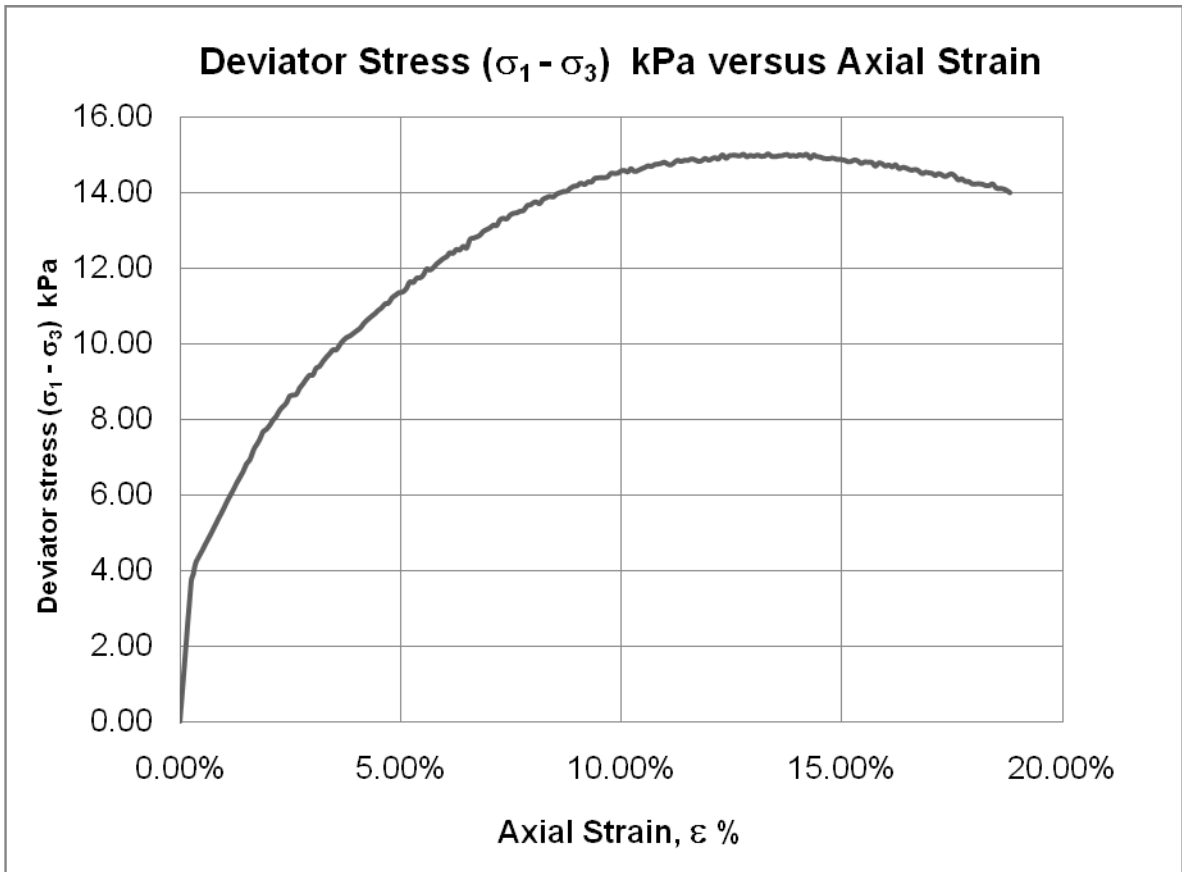
Figure 4.37. Deviator Stress (σ_1 - σ_3) kPa versus Axial Strain for 6% contamination with gasoline

From the figure above (Figure 4.37) two values of the initial and secant modulus of the undrained elastic moduli can also be determined. The figure above is reproduced below in order to demonstrate the procedure used to calculate the initial and secant moduli.
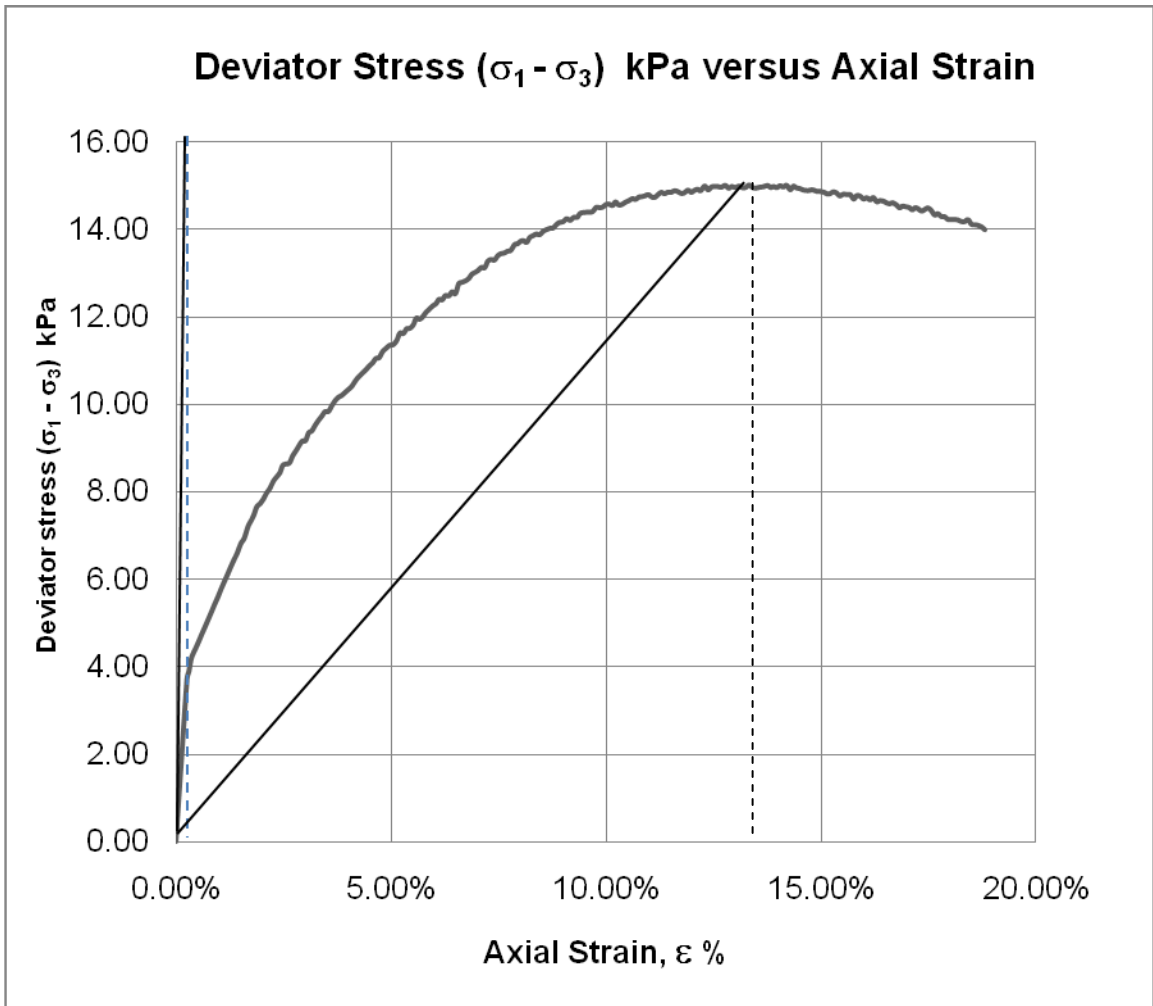
Figure 4.38. E_u and $(E_u)_s$ moduli for clay with 6% gasoline contamination.

E_u = 16 kPa / 0.004 = 4,000 kPa   and

$(E_u)_s$ = 15.00750189 / 0.1375 = 109.14 kPa

Again we observe the important difference between the initial and secant modulus.
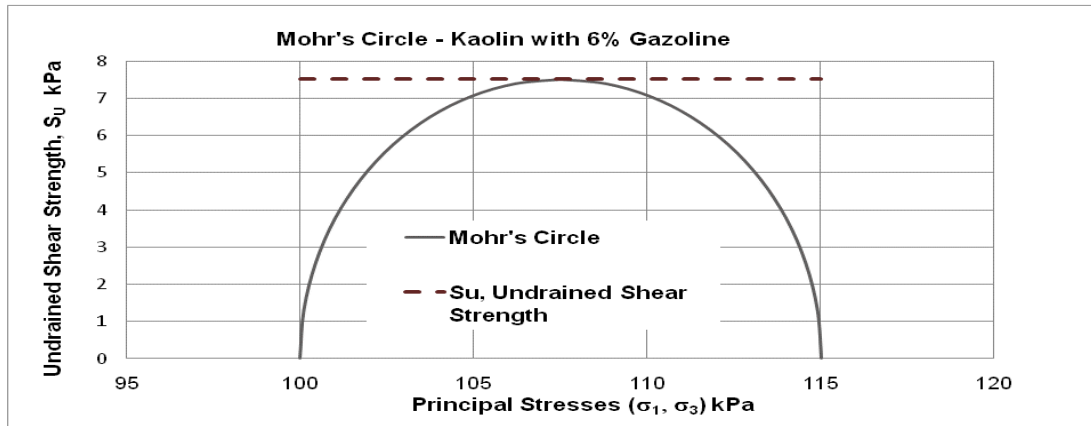
Figure 4.39. Mohr's Circle – Kaolin with 6% Gasoline Contamination
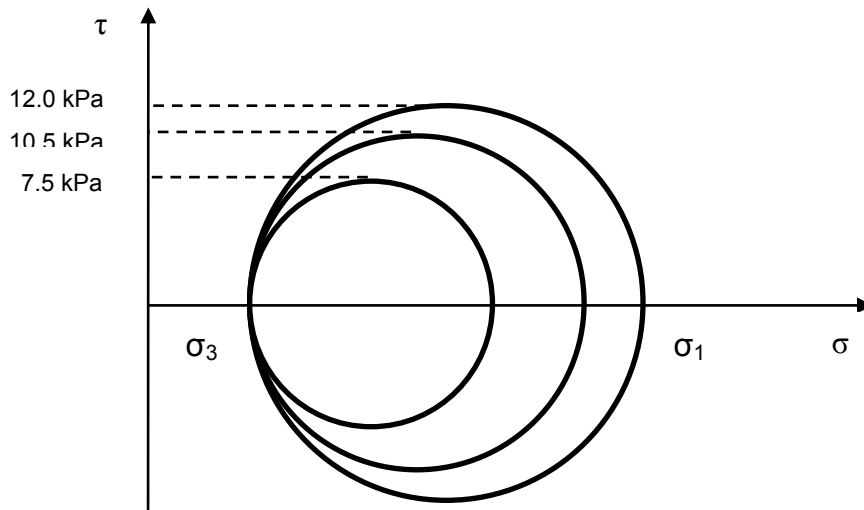
Figure 4.40. Combined Mohr's circles for 2%,4% and 6% gasoline contamination
S_u = 12.0 k Pa, 10.5 kPa, 7.5 kPa; σ_3 = 100

61
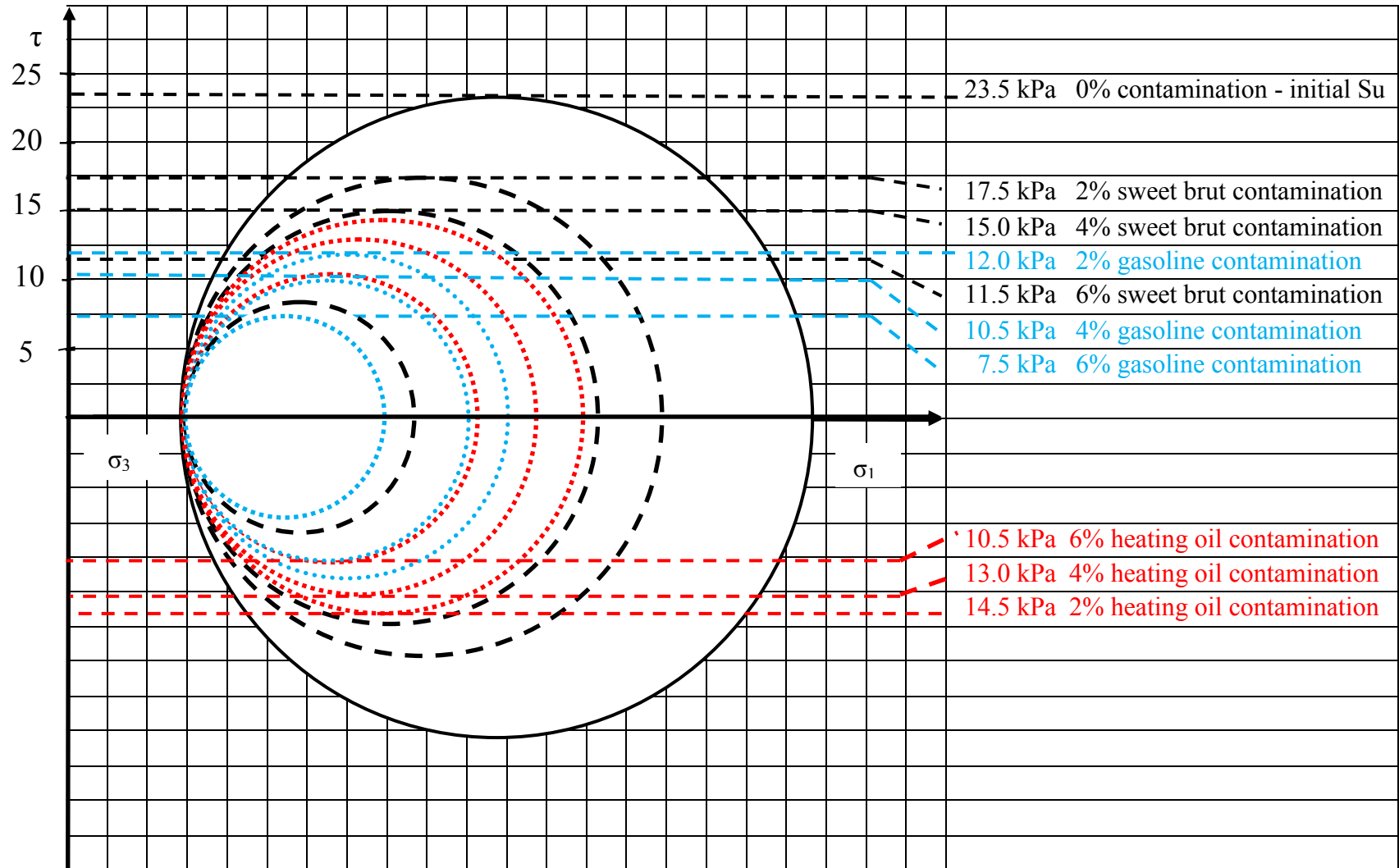
Figure 4.41: Combined Mohr's circles for 2%,4% and 6% sweet brute, heating oil and gasoline contamination; $\sigma_3 = 100$

The following labels appear on the figure:

- 23.5 kPa 0% contamination - initial Su
- 17.5 kPa 2% sweet brut contamination
- 15.0 kPa 4% sweet brut contamination
- 12.0 kPa 2% gasoline contamination
- 11.5 kPa 6% sweet brut contamination
- 10.5 kPa 4% gasoline contamination
- 7.5 kPa 6% gasoline contamination
- 10.5 kPa 6% heating oil contamination
- 13.0 kPa 4% heating oil contamination
- 14.5 kPa 2% heating oil contamination

4.5.1 Contaminated Soil versus Decrease of Shear Strength (UU test at a cell pressure σ_3=100kPa)

Table 4.1 Contaminated soil versus decrease of shear strength

	Sweet brut	**Heating Oil**	**Gasoline**
Shear Strength with 23,86 % water content and with 0% contamination	23.5 kPa	23.5 kPa	23.5 kPa
Shear Strength with 23,86 % water content and with 2% contamination	17.5 kPa	14.5 kPa	12.0 kPa
Shear Strength with 23,86 % water content and with 4% contamination	15.0 kPa	13.0 kPa	10.5 kPa
Shear Strength with 23,86 % water content and with 6% contamination	11.5 kPa	10.5 kPa	7.5 kPa

Nine batches of soil were prepared with three types of contaminants (crude oil/sweet brut, heating oil, gasoline) at three levels of contamination percentage by mass (2%, 4%, 6%). One batch of clay with zero contamination was added as reference for a total of 10 batches. Three samples from each of the ten batches (total of 30 samples) were placed in latex-stretchers, subjected to a 24-hour static, one dimensional, vertical compaction and tested for their undrained shear strength. The sample with the median undrained shear strength for each batch was selected as the representative value for that batch and used to generate the values included in Table 4.1. The data sets corresponding to the representative samples have been included in the Appendix.

4.5.2 Contaminated soil versus decrease of shear strength in kPa and

percentage   (UU test at a cell pressure σ_3 = 100kPa)

Table 4.2 Contaminated soil versus decrease of shear strength in kPa and
percentage

	Sweet brut	Heating Oil	Gasoline
Shear Strength with 23,86 % water content and with 0% contamination (Reference)	**23.5 kPa 100% (Reference)**	**23.5 kPa 100% (Reference)**	**23.5 kPa 100% (Reference)**
Shear Strength with 23,86 % water content and with 2% contamination	**-6 kPa -25.53%**	**-9 kPa -38.30%**	**-11.5 kPa -46.80%**
Shear Strength with 23,86 % water content and with 4% contamination	**-8.5 kPa -36.17%**	**-10.5 kPa -44.68%**	**-13 kPa -55.32%**
Shear Strength with 23,86 % water content and with 6% contamination	**-12 kPa -51.60%**	**-13 kPa -55.32%**	**-16 kPa -68.08%**

4.5.3 Sensibility - S_u (UU test at a cell pressure σ_3 = 100kPa)

Table 4.3 Sensibility - S_u

	Sweet brut	Heating Oil	Gasoline
Shear Strength with 23,86 % water content and with 0% contamination (Reference)	100% (Reference)	100% (Reference)	100% (Reference)
Shear Strength with 23,86 % water content and with 2% contamination	134.28%	162.06%	195.83%
Shear Strength with 23,86 % water content and with 4% contamination	156.66%	180.76%	223.81%
Shear Strength with 23,86 % water content and with 6% contamination	204.34%	223.81%	313.33%

4.5.4 E_u and $(E_u)_s$ moduli values (kPa)

Table 4.4. E_u and $(E_u)_s$ moduli values (kPa)

Contaminants	Percentage of contamination	E_u	$(E_u)_s$
Contaminants	0 %	16,666.66	578.88
Sweet brut	2%	5,000.00	392.75
Sweet brut	4%	17.500.00	356.90
Sweet brut	6%	8,928.57	435.35
Heating oil	2%	2,348.99	347.10
Heating oil	4%	6,000.00	856.07
Heating oil	6%	1,000.00	410.27
Gasoline	2%	15,000.00	168.44
Gasoline	4 %	12,500.00	236.54
Gasoline	6%	4,000.00	109.14

5. RANDOM FIELDS AND SOIL PROPERTIES

5.1 Theoretical Approach

As mentioned before, petroleum pollution affects the engineering properties of the soil namely the undrained shear strength. These effects of the petroleum contamination on the undrained shear strength, S_u, are viewed as random field variables distributed on a region of space. Soils are seldom homogeneous and more likely to be anisotropic in nature which renders the undrained shear strength intractable. Consequently this random distribution necessitates the development of a suitable statistical model which is undertaken in the following development.

The extreme values of a soil property are very important here, since they refer to high changes in the soil quantities. Since the soil properties vary in the space, we need a set of correlated random variables to represent this soil property across the space.

In this section of the thesis statistical methods are developed based on random fields' theory to analyze experimental data sets.

As an application the model, developed in the course of the present research, is very useful to decision makers since it can be employed to predict the shear strength of the clay at a given level of contamination. Such information helps the decision maker to decide whether to proceed with the construction or not, or what

kind of soil remediation should take place. As an example of such information is the probability that the size of one connected component of the excursion set exceeds a given threshold. This threshold may be called the risk threshold. This probability is very important since is represents the probability of a risk.

Random fields are highly used in the literature to model similar random quantities. A random field can be thought of as a random function $X(t)$ (a function which takes its values according to the chance), where t varies in some set C. If $X(t)$ represents the soil property at t, then the statistical distribution of the quantity $\sup_{t \in C} X(t)$, the extreme value of $X(t)$ in C, is of central interest in this thesis.

The set of all points t in C for which $X(t)$ exceeds a high threshold u, i.e., the set of all points t in C for which $X(t) \geq u$ is called the excursion set of $X(t)$ in C above u. For high values of u, the excursion set is related to the extreme values of $X(t)$. In this research, the excursion set of the soil property represents the part of the region C where the soil property is extreme.

A random field $X(t)$, $t \in C$, is said to be Gaussian Random field if for every $t_1, t_2, \cdots, t_n \in C$, the set of random variables $X(t_1), \cdots, X(t_n)$ follow the multivariate Gaussian distribution, i.e, has a density of the form

$$f(x) = \frac{1}{(2\pi)^{n/2} \, |\Sigma|^{1/2}} e^{-\frac{1}{2}(x-m)^T \Sigma^{-1}(x-m)}, \qquad -\infty < x_i < \infty, \quad i = 1, 2, \cdots, n,$$

where $x = (x_1, \cdots, x_n)$, m and Σ are the mean vector and the covariance matrix of

$X(t_1), \cdots, X(t_n)$, respectively. Gaussian random fields are very good tolls for

analyzing changed soil properties since they are analytically tractable, so they

are widely used in the literature as models for many random responses.

The excursion set of a smooth Gaussian random field has been studied

extensively in Adler (1981). It is shown that the excursion set has simple topology

above high threshold, i.e., it is a union of disjoint clusters or clumps where each

clump is ellipsoid in shape. Moreover, the number of such clusters follows the

Poisson distribution, i.e., the number of cluster N has the distribution

$$P\{N = n\} = \frac{e^{-\lambda} \lambda^n}{n!}, \quad n = 0, 1, 2, \cdots,$$

where λ is a parameter. Adler's results are valid only for large thresholds, i.e., for

large values of u. This means his theory cannot be used to predict the

excursions set characteristics above low thresholds.

Neither the prediction of the excursion set characteristics above any level *u,* nor

finding prediction intervals for these characteristics has been studied by any

author yet. Earlier methods for predicting these characteristics were proposed,

and the validity of the method using simulation will be tested.

In some random responses, the distribution is not Gaussian since it has heavier

tails than the Gaussian ones. Hence, another random field is needed with

heavier tail probability distributions.

A new non-Gaussian random field called the Student random field was introduced. The Student random field has heavier tail distribution than the Gaussian ones.

It is also shown that the Student random field is a generalization to the Gaussian random field. The characteristics of its excursion set above high thresholds are also shown. Simulation is used to check the validity of our findings.5.2 Predicting the Excursion Set of Gaussian Random Field

5.2 Predicting the Excursion Set of a Gaussian Random Field

5.2.1 Conceptual Approach

Understanding various engineering properties of the soil is the goal of many geotechnical problems. This includes the intrinsic soil properties, the shear strength, the soil type and the level of contamination in the soil. Crude oil contamination in the soil is one of the factors that affects the shear strength and therefore it is important to determine the statistical measures for this soil property in a given region. If soil property in a given region is C, then soil property in another region D may be predicted.

These properties are unknown and may be modeled by a set of random variables. Since these quantities vary spatially, they may be modeled by a random function or random field.

A random field is simply a collection of random variables indexed by a spatial set. The focus of this section is to determine the probability distribution of the undrained shear strength in a region of interest subjected to petroleum contamination. For example, it may be needed to determine the probability that a soil property exceeds some given threshold u in a region of interest, or the proportion of the space where the soil property exceeds u.

These statistical properties are used as measures of reliability for the soil used for the structures. The objective of this thesis is to predict the excursion set and some of its characteristics of a smooth and stationary Gaussian random field in a given region of interest based on a realization of the field on a region.

To setup the notation, assume that the region of interest is $C \subset R^d$, the d-dimensional Euclidean space. A family of random variables $\{X(t), t \in C \subset R^d\}$, $d > 1$, is called a d-dimensional random field. If d = 1, the family is called a random process. For every random field $X(t)$, two functions can be defined, the mean function $\mu(t) = E\{X(t)\}$, and the covariance function $K(t,s) = \text{cov}\{X(t), X(s)\}$, $t, s \in C$. A d-dimensional random field is called a Gaussian random field if $(X(t_1), ..., X(t_n))$ is a multivariate normal distribution for every choice $\{t_1, ..., t_n\} \in C$. The mean and the covariance matrix of $(X(t_1), ..., X(t_n))$ are given by $\mu = (\mu(t_1), ..., \mu(t_n))$ and $M = \left(K(t_i, t_j)\right)^n_{i,j=1}$. Every random field $X(t)$ can be described by its set of finite-dimensional distributions, i.e., the set of all joint probability distributions of the form

$$F_{X(t_1), X(t_2), ..., X(t_k)}(y_1, y_2, ..., y_k) = P\{X(t_1) \leq y_1, X(t_2) \leq y_2, ..., X(t_k) \leq y_k\},$$

where k = 1, 2, …, $y_i \in R$ and $t_i \in C$,

The random field *X(t)* is said to be homogeneous or stationary if $(X(t_1),...,X(t_n))$ and $(X(t_1 + h),...,X(t_n + h))$ have the same distribution for any $h \in R^d$ and is said to be isotropic random field if $(X(t_1),...,X(t_n))$ and $(X(qt_1),...,X(qt_n))$ have the same distribution for any rotation *q* in R^d. For a stationary random field the mean function is constant, i.e., $\mu(t) = \mu$ for every $t \in R^d$.

In this thesis, it is assumed that $X(t)$ is smooth and stationary Gaussian random field with mean $\mu(t) = \mu$ and variance $var\{X(t)\} = \sigma^2$. Let $X_i(t)$ be the first derivative of *X(t)* with respect to the ith coordinate of t and $X_{ij}(t)$ be the second partial derivative of *X(t)* with respect to i^{th} and j^{th} coordinates. It is also assumed that the following condition is fulfilled

$$\underset{i,j}{max}\, E\left\{\left|X_{ij}(t) - X_{ij}(0)\right|^2\right\} \le c\|t\|^2,$$

for c > 0 and t in some neighbourhood of 0. Here ||.|| denotes the Euclidean norm in R^D.

The excursion set of a random field *X(t)* in *C* above a level *u* is defined as the set of points $t \in C$ for which $X(t) \ge u$ (Adler, 1981) . Denote the excursion set of *X(t)* in *C* above *u* by $A(X,u,C)$. Then

$$A(X,u,C) = \{t \in C : X(t) \ge u\}. \qquad (1)$$

The excursion set is very important and has been studied extensively in [1]. With probability tending to one as $u \to \infty$, the excursion set of smooth Gaussian random field $X(t)$ has simpler topology, i.e., it is a union of disjoint convex components where each convex component contains one local maximum of $X(t)$. Moreover, N, the number of convex components of $A(X,u,C)$, follows approximately the Poisson distribution (see [1]). The mean of this Poisson distribution is given by

$$E\{N\} = vol(C)\,det(\Lambda)^{\frac{1}{2}}\,\sigma^{-(2d-1)}u^{d-1}(2\pi)^{-(d+1)/2}\,exp\left(-\frac{u^2}{2\sigma^2}\right) \quad (1)$$

where vol(C) is the volume of C and Λ is the covariance matrix of $(X_1(t),...,X_d(t))$. Then $E\{N\}$ can be used to find the following accurate approximation for $P\{sup_{t \in C}\,X(t) \geq u\}$:

$$P\left\{\sup_{t \in C} X(t) \geq u\right\} \approx E\{N\}.$$

So the problem of approximating $P\left\{\sup_{t \in C} X(t) \geq u\right\}$ is reduced to the problem of approximating $E\{N\}$.

5.2.2 PROBLEM Identification

Let t be a location in a region of interest C and $X(t)$ be the soil property at t. Let $X(t)$ be a smooth and stationary Gaussian random field. Let $X_1 = (X(t_1),...,X(t_n))$ be the observed values of $X(t)$ at the locations $t_1,...,t_n \in C \backslash D = \{t \in C : t \notin D\}$,

where $D \subset C$. The goal is to predict the excursion set of *X(t)* and its characteristics in the domain *D*, i.e., to predict $\mathbf{X}_2 = (X(s_1),..., X(s_m))$ where $s_1,...,s_m \in D$. If denoting an n-dimensional vector of ones by 1_n, then from the multivariate normal theory, the stacked vector $\mathbf{X}^T = (\mathbf{X}_1, \mathbf{X}_2)$ has (n+m)-dimensional multivariate normal distribution with mean $\mu = \mu 1_{n+m}$, where 1_{n+m} is (n+m)-dimensional vector of ones, and covariance matrix

$$\Sigma = \begin{pmatrix} \Sigma_{11} & \Sigma_{12} \\ \Sigma_{12}^T & \Sigma_{22} \end{pmatrix},$$

where $\Sigma_{11} = \left(K(t_i,t_j)\right)_{i,j=1}^n, \Sigma_{22} = \left(K(s_i,s_j)\right)_{i,j=1}^m$ and $\Sigma_{12} = \left(K(t_i,s_j)\right)_{i=1,j=1}^{n,m}$.

The conditional distribution of X_2 given $X_1 = x_1$ is also *m*-dimensional multivariate normal with mean

$$\mu_{2.1} = \mu_2 + \Sigma_{21}\Sigma_{11}^{-1}(x_1 - \mu_1)$$

and covariance matrix

$$\Sigma_{2.1} = \Sigma_{22} - \Sigma_{21}\Sigma_{11}^{-1}\Sigma_{12}^T,$$

where $\mu_1 = \mu 1_n$ and $\mu_2 = \mu 1_m$. The mean $\mu_{2.1}$ is a function in x_1 which can be used to predict X_2. Various covariance functions for $X(t)$ are available in the literature [4]. A common choice is the following one

$$K(t,s) = \exp\left(-\frac{1}{2\tau^2}\|t-s\|^r\right), \quad r \in (0,2], \quad \tau > 0. \qquad (2)$$

5.2.3 Prediction

Denote the predictive distribution of X_2 given $X_1 = x_1$ by $f(x_2|x_1)$. The

predictive distribution of X_2 given $X_1 = x_1$ depends on the parameters σ^2, μ

and τ^2. So they are estimated using the data X_2 and then the estimates are

plugged in the density $f(x_2|x_1)$. To predict the characteristic of the excursion set

A(X, u, D) in D, a large sample from the distribution of X_2 given $X_1 = x_1$ is

simulated.

These realizations can then be used to predict the size of the excursion set, the

cluster size, the number of components above u and $sup_{t \in D} X(t)$. The general

form of the predictor is $E\{H(X_2)|X_1 = x_1\}$, where $H(X_2)$ denotes a

characteristic of the excursion set of X(t) in D. Since it is not possible to simulate

a random field on a compact set D, $\tilde{D}$ is used instead, a grid of D. Let X_{2j},

$j = 1,...,M$ be M realizations from $f(x_2|x_1)$. Then the following characteristics of

the excursion set can be predicted

1. Size of A(X, u, D): The size of A(X, u, D) can be predicted as

$$E\left\{A(X, u, \tilde{D}) \mid X_1 = x_1\right\} = \frac{1}{M}\sum_{j=1}^{M}\left|A(X_{2j}, u, \tilde{D})\right|.$$

2. Cluster size of *A(X, u, D)*: For large u, let $S(X_{2j}, \tilde{D})$ be the cluster size of

$$X_{2j} \text{ on } \tilde{D}, \quad j = 1,...,M,$$

then the cluster size can be predicted as follows

$$E\{S(X,\tilde{D}) \mid X_1 = x_1\} = \frac{1}{M}\sum_{j=1}^{M} S(X_{2j}, \tilde{D}).$$

3. Number of clusters *N*: Let $\tilde{N}_j$ be the number of components of $X_{2j}(t)$ on

$\tilde{D}$. Then N can be predicted by

$$E\{N \mid X_1 = x_1\} = \frac{1}{M}\sum_{j=1}^{M} \tilde{N}_{j}..$$

4. $sup_{t \in \tilde{D}} X(t)$: The supremum of *X(t)* on *D* can be predicted by

$$E\left\{\sup_{t \in \tilde{D}} X(t) \mid X_1 = x_1\right\} = \frac{1}{M}\sum_{j=1}^{M} \max\{X_{2j}\}..$$

5.2.4 Prediction intervals

Based on a large number of realizations from $f(x_2 | x_1)$, a 95% prediction

intervals can be found for *A(X, u, D)*, *N*, *S(X,u)* and $\sup_{t \in D} X(t)$. The following

algorithm is designed to find these prediction intervals.

1. Simulate $X_{2j}(t)$, $j = 1,...,M$, realizations from $f(x_2 | x_1)$.

2. For each *j*, find $A(X_{2j}, u, \tilde{D})$, the excursion set of X_{2j} on $\tilde{D}$.

3. For each excursion set in 2, find the clusters size, the number of clusters

and the $\max\{X_{2j}\}$.

4. For each characteristic you find in 3, the prediction interval is [*L, U*], where *L* and *U* are the 2.5% and the 97.5 percentiles of the empirical distribution.

5.2.5 ESTIMATION OF μ, σ^2 AND τ^2

Since the parameters μ, σ^2 and τ^2 are unknown and the predictive density $f(x_2|x_1)$ depends on these parameters, their estimates are plugged in $f(x_2|x_1)$.

The Maximum Likelihood Estimates (MLE's) of μ, σ^2 and τ^2 are the values $\hat{\mu}$, $\hat{\sigma}^2$ and $\hat{\tau}^2$ which maximize the likelihood function

$$L(\mu,\sigma^2,\tau^2) = (2\pi)^{-\frac{n}{2}} \det(\Sigma_{11})^{-\frac{1}{2}} \exp\left(-\frac{1}{2\sigma^2}(x_1-\mu 1_n)^T \Sigma_{11}^{-1}(x_1-\mu 1_n)\right)$$

5.2.6 Simulation

Simulation is restricted to the case *d* = 1. Simulation of a Gaussian process in *D* = [0, *A*] is equivalent to the simulation of a Gaussian vector on a grid of *D*. So, to simulate a stationary Gaussian process $X(t)$, $t \in D = [0,A]$ with covariance function *K(t,s)*, the following steps are followed:

1. Consider the grid $\tilde{D} = \{0 = t_1, ..., t_B = A\}$

2. Find the covariance matrix $\Sigma = \left(K(t_i, t_j)\right)_{i,j=1}^{B}$ and the mean vector $\mu = \mu 1_B$

3. Simulate a random vector of length *B* from $N_B(\mu, \Sigma)$

Considering the covariance function (2) and the value $\mu = 0$, $\sigma = 1$, and $\tau = 1$ to simulate a sample path of $X(t)$ on the interval C=[0, 256], then the data is divided into two vectors $X = (X_1, X_2)$ where X_1 represents the first 128 entries of X and X_2 the remaining 128 entries. So X_1 is considered as the observed data and X_2 as the reference data for our prediction.

The theory developed in this thesis is used to predict the characteristics of the excursion of *X(t)* in *D* = [129, 256]. The excursion set of the reference data X_2 has the observed characteristics: $A(X_{2j}, 2, \widetilde{D}) = 4$, $S(X_{2j}, \widetilde{D}) = 1$, N = 4 and max X_2 = 2.5544. A large sample of $M = 5000$ realizations from $f(x_2|x_1)$ is simulated and 95% prediction intervals for these excursion set characteristics are obtained (Katatbeh et al., 2007)

Results are summarized in Table 5.1.

Table 5.1 Prediction interval for excursion set characteristics

Characteristics	$A(X, 2, \widetilde{D})$	$S(X, \widetilde{D})$	N	$\sup_{t \in \widetilde{D}} X(t)$
Prediction interval	[0, 8]	[0, 3]	[0,6]	[1.735, 3.462]

5.3 Random Field Model for Analyzing the Shear Strength of the Soil

5.3.1 Overview

In this section, a random field model was developed to analyze the experimental data obtained from an environmental field.

Let C be the region under study. Representative samples are selected from different locations in region C, and are tested for strength and contamination. Let X(t) denote the shear strength of the sample at the location t.

If $t_{(n+1)}$ denotes the location of a new unobserved specimen in the experiment, the model developed in this research can be applied to predict the value of the undrained shear strength of this new specimen.

If it is assumed that the initial shear strength, i.e., the shear strength in the absence of pollution, at t is S_0, then $Y(t) = S_0 - X(t)$ represents the change, i.e., the loss, in the shear strength due to contamination. Since t varies in space, then the random quantity $Y(t)$ defines a random function or random field.

A random field is simply a collection of random variable indexed by a spatial index. The excursion set of a random field represents those spatial points in the space that show high changes in the value of the random field. Since the pollution varies spatially in the soil, it is reasonable to use a random field model to describe the change in the shear strength.

The statistical distributions of sizes and number of components of a future excursion set of a random field are very important. Katatbeh et al. (2007) gave predictors to some characteristics such as mean and number of components of a intervals for these characteristics.

5.3.2 Excursion Sets of Random Fields

The probability $P\{\sup_{t \in C} X(t) \geq u\}$, for large u, is very important in many applications of random fields and processes. In general, it is not possible to find its exact value. Other good approximations for this probability can be derived based on the geometry of the excursion set of the random filed X(t) above a threshold u.

The following notation will be used. R^j is the j-dimensional Euclidean space. For normal random variable, Z, with mean μ and variance σ^2 we use $Z \sim N(\mu, \sigma^2)$, while $Z \sim \chi_v^2$ for a chi square random variable with v degrees of freedom. $\Phi(.)$ is the distribution function of the standard normal random variable and $\Gamma(.)$ is the Gamma function.

If $a = (a_1, a_2, ..., a_n)$ and $A = (a_{kl})_{k,l=1}^n$, then $a_{|j} = (a_1, a_2, ..., a_j)$ and $A_{|j} = (a_{kl})_{k,l=1}^n$. Then Lebesque measure in R^D is denoted by $\mu_D(.)$ for a random vector Z, cov(Z) is denoted for its covariance matrix. The following result will be used in this paper. If $S \sim \chi_v^2$, then

$$E\left\{ S^k \exp\left(-\frac{a}{2} S \right) \right\} = \frac{\Gamma\left(k + \frac{v}{2} \right) 2^k}{\Gamma\left(\frac{v}{2} \right)} (1-a)^{-(k+v/2)},\qquad (2)$$

for any non-negative integer k and positive real a.

For wide class of smooth random fields and processes, the excursion set is finite union of convex sets such that each convex set contains a local maximum for X(t) as $u \to \infty$. Let $\chi(A(X,u,C))$ be the Euler characteristic of $\chi(A(X,u,C)$, which counts (the number of connected components) − (the number of holes) + (the number of hallows) in $\chi(A(X,u,C)$, (Adler, 1981). Therefore, for large u, $\chi(A(X,u,C))$ counts the number of connected components in $\chi(A(X,u,C)$. So Hasofer (1978) gives the following accurate approximation

$$P\left\{\sup_{t \in C} X(t) \geq u\right\} \approx E\{\chi(A(X,u,C))\}, \text{ as } u \to \infty.$$

The excursion set of the field above the threshold u = 3.5 is also given. The total area of the clusters in the excursion set represents the part of the space which shows extreme change in the shear strength.
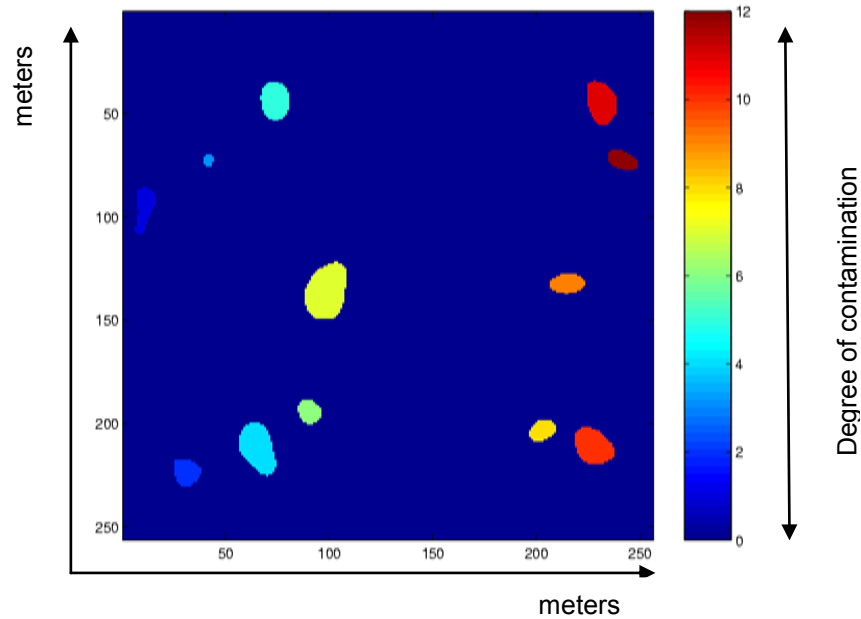
Figure 5.1 Excursion set of a student random field with $v = 5$ above the threshold $u = 3.5$. A, det(A) and A^{-1} are used for the determinant and the inverse of A, respectively.

Figure 5.1 represents a realization, using computer simulation, of the excursion set of a student random field with v=5 degrees of freedom above a threshold u=3.5. It appears that the excursion set (which is the set of all points of extremes values of the field) decomposes into finite ellipses. The excursion set and the areas or volumes of its components (ellipses) are very important since they represent the portion (set of points) in the space (of construction) where the random field which represents high contamination. The value of the threshold u is determined by data from the field. But in this present simulation it was chosen so that 5% of the student field values are above u, i.e., u was selected so that the probability that the field T exceeds u is 5%. In this case values above u are considered as extreme values. The value of v (degrees of freedom) allows the student field to fit experimental data which have heavier tail distribution. As v

goes to infinity the field becomes identical to the Gaussian one. The value v=5 is chosen small to differ from the Gaussian one.

Aldous (1989) introduced the *Poisson clumping heuristic* (PCH), which means throwing random sets (clumps) at random according to a Poisson point process, i.e., the centers of the sets are generated by Poisson random variable. Cao (1999) used the PCH to model the excursion set $\chi(A(X,u,C))$, where each cluster is considered as a clump and the local maximum is considered to be the center of the cluster.

Let N be the number of connected components of $\chi(A(X,u,C))$ and $C_1,...,C_N$ be the sizes of these clusters. So

$$E\{\mu_D(A(X,u,C))\} = E\{NE(C_1)\},$$

$$= E\{N\}E\{C_1\}. \qquad (3)$$

The average of the total area may be calculated by the following formula

$$E\{\mu_D(A(X,u,C))\} = \mu_D(C)P\{X(0) > u\}.$$

The average proportion volume of the space that shows high change in shear strength can be calculated as follows:

$$\hat{p} = \frac{E\{\mu_D(A(X,u,C))\}}{\mu_D(C)}$$

If E{N} by $E\{\chi(A(X,u,C))\}$ is approximated, then

$$E\{C_1\} \approx \frac{\mu_3(C)P\{X(0) > u\}}{E\{\chi(A(X,u,C))\}} \qquad (4)$$

5.3.3 Student Random Field

Further on, a non-Gaussian random field extending the Gaussian random field is introduced.

The new field is called the *student random field*.

The expected value of the Euler characteristic of its excursion set is calculated and an algorithm to simulate the student random field is also proposed.

From here on, it will be assumed that all random variables and vectors used have densities.

<u>Definition 1</u>

A random vector Z is said to be m-dimensional Multivariate Gaussian with mean vector μ and covariance matrix Σ, denoted by Z~Nm(μ,Σ), if its pdf is on the form

$$f_Z(z) = \frac{1}{(2\pi)^{D/2} \det(|\Sigma|)^{1/2}} \exp\left(-\frac{1}{2}(z-\mu)'\Sigma^{-1}(z-\mu)\right), \ z \in R^m \qquad (5)$$

<u>Definition 2</u>

A random vector W is said to be m-dimensional multivariate student with parameters v, μ and Σ if its pdf is of the form

$$f_W(w) = \frac{\Gamma((v+m)/2)}{\Gamma(v/2)(v\pi)^{m/2}} \det(\Sigma)^{-1/2} \left[1 + \frac{1}{v}(w-\mu)'\Sigma^{-1}(w-\mu) \right]^{-(v+m)/2}, w \in R^m .$$

The parameters μ, Σ and *v* are called location, scale and degrees of freedom parameters, respectively. The notation $t \sim t_m(\mu, \Sigma, v)$ will be used to denote an m-dimensional multivariate student distribution with parameters μ, Σ and *v*.

Definition 3

A random field X(t) is said to be Gaussian random field if every finite-dimensional distribution is a multivariate Gaussian.

Definition 4

A random field T(t) is said to be a student random field with v degrees of freedom if every finite-dimensional distribution is a multivariate student with v degrees of *freedom.*

Every student random field can be characterized by the following theorem:

<u>Theorem</u>

Let T(t), $t \in C \subset R^D$ be a homogeneous student random field with zero-mean, v(v>2) degrees of freedom and covariance function $R_T(t)$. Then T(t) admits the following stochastic representation

$$T(t) = \sqrt{\frac{v}{S}} X(t),$$

where X(t) is a homogeneous Gaussian random field with zero mean, unit variance, covariance function $R_x(t) = (v-2)R_T(t)/v$ and S is a chi-square random variable with v degrees of freedom independent of X(t).

Proof: Let $t = t_1, t_2, ..., t_n \in C$. Then $W = (T(t_1), ..., T(t_n))$ has a multivariate student with v degrees of freedom. From multivariate theory, a random vector $Z \sim t_n(\mu, \Sigma, v)$ if and only if $Z \stackrel{d}{=} \mu + \sqrt{\frac{v}{S}} H$, where $H \sim N_n(0, \Sigma)$. So the vector W admits the representation $W \stackrel{d}{=} \sqrt{\frac{v}{S}} (X(t_1), ..., X(t_n))$, where $(X(t_1), ..., X(t_n)) \sim N_n(0, \Sigma^*)$, and Σ^* is the $n \times n$ matrix $(cov(T(t_i), T(t_j)), i,j = 1, ..., n$.

This implies that $T(t) \stackrel{d}{=} \sqrt{\frac{v}{S}} X(t)$ and the covariance function of X(t) is (v-2)R_T(t)/v. This establishes the theorem.

It is known that the student distribution is similar in shape to the Gaussian distribution, but with heavier tail. Therefore, the student random field defined above has more variability than the Gaussian random field. Since (6) converges to (5) as $v \to \infty$, the student random field is an extension to the Gaussian

random field. One more advantage of the student field is that it is easy to simulate and its covariance function is proportional to the Gaussian one. Since the random variable S does not depend on t, it can be shown that

$$P\left\{\sup_{t\in C} T(t) \ge u\right\} = \int_0^\infty P\left\{\sup_{t\in C} X(t) \ge u\sqrt{s/v}\right\} f_S(s)ds, \quad (7)$$

where $f_S(s)$ is the pdf of S. In Piterbarg (1996), several good approximations are available for $P\left\{\sup_{t\in C} X(t) \ge u\sqrt{s/v}\right\}$, but they cannot be plugged in (7) since they are valid for large levels. So the left hand side of (7) will be approximated based on the Euler characteristic of $\chi(A(T,u,C))$.

To study the geometric properties of the excursion set of a random field, the random field has to satisfy regularity conditions given in Adler (1981). It will be assumed that X(t), $x\in C \subset R^D$ satisfies these conditions. Moreover, X(t), is a zero-mean, unit variance, homogeneous and twice differentiable in the mean-square sense Gaussian random field. Let $\dot{X}(t)$, and $\ddot{X}(t)$ be the gradient and the matrix of the second partial derivatives of X(t), respectively. The covariance function of T(t) is

$$R_T(t_1,t_2) = \frac{v}{v-2} R_x(t_1,t_2) \quad \text{for } v > 2,$$

where $R_X(t_1, t_2)$ is the covariance function of X(t). Therefore, mean-square differentiability of X(t) implies the means-square differentiability of T(t) and $\dot{T}(t) = \sqrt{\frac{v}{S}}\dot{X}(t)$ and $\ddot{T}(t) = \sqrt{\frac{v}{S}}\ddot{X}(t)$. It is easy to see that the field T(t) satisfies the regularity conditions.

5.3.4 Expected Euler characteristic of T(t)

Let X(t), $t \in C \subset R^3$ be an isotropic random field. Cao and Worsley (1999) define the jth Euler characteristic intensity of the field X(t) in R^j by $\rho_0^X(u) = P\{X(0) \geq u\}$ for j = 0, and for j ≥ 1,

$$\rho_j^X(u) = E\{\dot{X}_j^+ \det(-\ddot{X}_{|j-1}) | \dot{X}_{|j-1} = \mathbf{0}, X = u\} f_{|j-1}^X(\mathbf{0}, u),$$

(8)

where $f_{|j-1}^X(\mathbf{0}, u)$ is the density of $\dot{X}_{|j}$. Let $w_j = 2\pi^{j/2}/\Gamma(j/2)$ be the surface area of a that (j-1)-sphere in R^j.

For smooth isotropic Gaussian random field (S(t), with smoothing parameter $\lambda = |cov(\dot{X}(0))|^{\frac{1}{2}}$, the values of $\rho_j^X(u)$ for j = 0, 1, 2, 3 are given in Worsley and Friston (2000) as follows

$$\rho_0^X(u) = 1 - \Phi(u) \ ,$$

$$\rho_1^X(u) = \frac{\sqrt{\lambda}}{2\pi}e^{-u^2/2} \ ,$$

$$\rho_2^X(u) = \frac{\sqrt{\lambda}}{(2\pi)^{3/2}} e^{-u^2/2},$$

$$\rho_3^X(u) = \frac{\lambda^{3/2}(u^2-1)}{(2\pi)^2} e^{-u^2/2}.$$

According to Worsley and Friston (2000), if X(t) is an isotropic random field then,

$$P\left\{\sup_{t\in C} T(t) \geq u\right\} \approx \sum_{j=0}^{3} \rho_i^X(u)\mu_j(C),$$

where $\mu_j(C)$, j = 0, 1, ..., 3 are the intrinsic volumes of C. Adler (2000) gives the

following expression for $E\{\chi(A(X,u,C)\}$

$$E\{\chi(A(X,u,C)\} = \mu_D(C)\rho_D^X(u) = \mu_D(C)\frac{\exp\left(-\frac{u^2}{2}\right)(\det(\Lambda))^{\frac{1}{2}}}{(2\pi)^{(D+1)/2}} H_{D-1}(u),$$

where

$$H_n(x) = n! \sum_{j=0}^{[n/2]} \frac{(-1)^j x^{n-2j}}{j!(n-2)!2^j},$$

is the n-th Hermite polynomial and Λ = Var(X(0)). Since T(t) is a mixture of

Gaussian random fields, then using (8) and the total probability law, we can write

$E\{\chi(A(T,u,C))\}$ as

$$E\{\chi(A(T,u,C))\} = E\{E\{\chi(A(T,_{u\sqrt{S/v}},C))\}\}. \text{ So}$$

$$E\{\chi(A(T,u,C))\} = \frac{\mu_D(C)\det(\lambda)^{1/2}\Gamma(D)}{(2\pi)^{\frac{D+1}{2}}} E\left\{\exp\left(-\frac{u^2 S}{2v}\right)H_{D-1}\left(u\sqrt{\frac{S}{v}}\right)\right\},$$

$$= \frac{\mu_D(C)\det(\lambda)^{1/2}\Gamma(D)}{(2\pi)^{\frac{D+1}{2}}} \sum_{j=0}^{\left[\frac{D-1}{2}\right]} \frac{(-1)^j u^{D-1-2j} E\{S^{\frac{D-1-2j}{2}} \exp(-\frac{u^2 S}{2v})\}}{j!(D-1-2j)!2^j v^{\frac{D-1-2j}{2}}},$$

$$= \frac{\mu_D(C)\det(\lambda)^{1/2}\Gamma(D)}{(2\pi)^{\frac{D+1}{2}}} \times$$

$$\sum_{j=0}^{\left[\frac{D-1}{2}\right]} \frac{(-1)^j u^{D-1-2j} 2^{\frac{D-1}{2}-2j}\Gamma(\frac{D+v-1}{2}-j)(1+\frac{u^2}{v})^{-(\frac{D+v-1}{2}-j)}}{j!(D-1-2j)!\Gamma(\frac{v}{2})v^{\frac{D-1}{2}-j}} \ .$$

Similarly, it can be shown that $\rho_j^{T(u)} = E\{\rho_j^X(u\sqrt{S/v})\}$. Because they are

important in application we will find $\rho_1^{T(u)}$, $\rho_2^{T(u)}$ and $\rho_3^{T(u)}$ for the case D = 3.

Using (2) we obtain

$$\rho_0^{T(u)} = 1 - P\{T(0) > u\} \ ,$$

$$\rho_1^{T(u)} = \frac{\sqrt{\lambda}}{2\pi} E\{\exp(-\frac{u^2 S}{2v})\} = \frac{\sqrt{\lambda}}{2\pi}(1+\frac{u^2}{v})^{-v/2} \ ,$$

$$\rho_2^{T(u)} = \frac{\kappa\lambda\Gamma(\frac{v+1}{2})u}{2\pi^{3/2}\sqrt{v}\Gamma(v/2)}(1+\frac{u^2}{v})^{-(\frac{v}{2}+1)} \ ,$$

$$\rho_3^{T(u)} = \frac{\lambda^{3/2}}{(2\pi)^2}\left(\left(1-\frac{1}{v}\right)u^2 - 1\right)(1+\frac{u^2}{v})^{-(\frac{v}{2}+1)}$$

It is easy to check that $\lim_{v\to\infty} \rho_i^X(u)$ for I = 1, 2, 3.   The following can be

written

$$P\left\{\sup_{t\in C} T(t) > u\right\} \approx \sum_{j=0}^{D} \rho_j^T(u)\mu_j(C) \ .$$

For large u the first and the last term can be used (Hasofer, 1987).

5.3.5 Distribution of one cluster

Following the same argument as in Alodat (2006), the volume of each cluster by a D-dimensional ellipsoid may be approximated. So

$$V \approx w_D 2^{\frac{D}{2}} \det(\Lambda)^{-\frac{1}{2}} \left(\frac{W}{u}\right)^{\frac{D}{2}} , \qquad (12)$$

x = cluster size
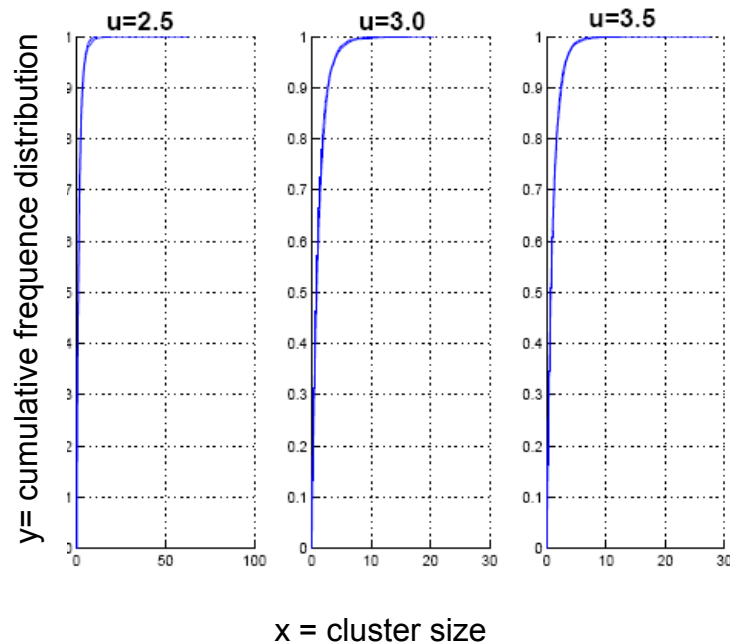
Figure 5.2 Exact and approximate CDF's of C_1 different thresholds

Where W is an exponential random variable with mean 1/u. A simulation study can be conducted to compare the empirical distributions of V with the exact one. The results are presented in Figure 5.2. The x-axis = cluster size and y-axis = cumulative frequence distribution. Lines in the figures represent the cumulative distribution functions of both exact (obtained via simulation) and the

approximation. Each figure contains two lines one is smooth, representing approximation, and the other is dotted, representing the exact. Since the two curves close to each other it can be noted that the approximation is very accurate.

5.3.6 Simulation of $T(\tau)$

A student random field can be simulated by simulating a multivariate student distribution on a grid or a lattice of C. Here it is proposed the following algorithm to simulate a student random field:

1. Simulate a S from χ_v^2 ;

2. Simulate a Gaussian random field X(t) independent of S.

5.4 Application to real experimental data

In this section, the theory developed is applied to analyze the experimental data obtained from an experiment designed by the author in the lab.

5.4.1 Field investigation and tests

In today's world tens of thousands of trucks, tankers carry crude oil, heating oil as well as gasoline across countries, cities and other residential areas with an ever increasing number of accidents.

Leaking underground storage tanks are becoming more and more of a threat for not only for the environment but it also has serious effects on the engineering properties of the soil. There are over 20,000 leaking USTs in Canada at any time (Canadian Mortgage and Housing Corporation, 2003), and there were over 400,000 leaking underground storage tank (LUST) sites identified up to 1999 in the United States of America (Connor, 2000).

Due to these contaminations the soil and the site conditions may quickly change resulting in weakening its shear strength and its bearing capacity.

In order to develop a random field model and apply it to real experimental data a series of triaxial experiment was carried out with petroleum contaminated soil, as it is detailed in Chapter 3, to obtain the changed values in the shear strength of the clay soil.

In the course of the experiment clay soil was contaminated with 2, 4 and 6 percent of sweet brut, heating oil and gasoline.

The decrease in the shear strength was compared to the initial shear strength with 0% contamination.

Table 5.2 shows the decrease of the shear strength in values (kPa) and in percentage compared to the initial shear strength. Full analysis of Table 5.2 is detailed in Chapter 4.

Table 5.2 Influence of oil contamination level on soil shear strength from triaxial tests

Contami-nation	Sweet Brut	Heating Oil	Gasoline
0%	23.5 kPa (initial shear strength) Percentage: 100%	23.5 kPa (initial shear strength) Percentage: 100%	23.5 kPa (initial shear strength) Percentage: 100%
2%	17.5 kPa Reduction: -6 kPa 23.5 - 6 = 17.5 kPa Reduction: - 25.53%	14.5 kPa Reduction: -9 kPa 23.5 - 9 = 14.5 kPa Reduction : - 38.30%	12.0 kPa Reduction: -11.5 kPa 23.5 - 11.5 = 12.0 kPa Reduction: - 46.80%
4%	15.0 kPa Reduction: -8.5 kPa 23.5 - 8.5 = 15.0 kPa Reduction : -36.17%	13 kPa Reduction: -10.5 kPa 23.5 - 10.5 = 13.0 kPa Reduction: -44.68 %	10.5 kPa Reduction: -13.0 kPa 23.5 - 13.0 = 10.5 kPa Reduction: -55.32%
6%	11,5 kPa Reduction: -12 kPa 23.5- 12.0 = 11.5 kPa Reduction : -51.6%	10.5 kPa Reduction: -13 kPa 23.5 - 13 = 10.5 kPa Reduction : -55.32	7.5 kPa Reduction : -16 kPa 23.5 - 16 = 7.5 kPa Reduction :- 68.08

5.4.2 Analysis of data from field investigation and tests

Let $X(t)$ represent the shear strength of the soil at an amount of contamination equal to t. To use the theory developed in previous chapters, it is needed to examine whether the experimental data could be fitted by $X(t)$, a Gaussian process, or not.

The data obtained by the experiment for Gaussianity need to be tested. To this end, both the Normal Probability Plot and the Darling-Anderson test for Gaussianity are used.

Figures 5.3 to 5.5 represent the Normal Probability Plot for Sweet Brut, Heating Oil, and Gasoline data. The normal probability plot is used to check whether the data are from normal distribution or not. The green line is the diagonal where the expected values equal the observed cumulative probabilities. The closer the red points are to the diagonal green line, the better are the results. If the red spots are on the straight line then the data meets the normality assumption.

The figures of straight lines give an indication whether these data follow the normal distribution. Moreover, the Darling-Anderson statistics for normality test are 0.191, 0.364 and 0.396 of P-values 0.732, 0.23 and 0.18, respectively. Since the P-values are all greater than 0.05, the Darling-Anderson test does not reject the Gaussianity of these data. Let $\widehat{X}$ denote the predicted value of the shear strength when the contamination of the soil is t. Table 5.3 shows the predicted value of the shear strength as well as the prediction error for the three soil types when $t = 8\%, 10\%$ and 11%. Table 5.5 shows $\hat{\mu}$, $\hat{\sigma}$ and $\hat{t}$, the estimated values

of the parameters μ, σ and τ, respectively. For the Gasoline case, the shear strength reaches the level zero before a contamination of 11%, as indicated in Table 5.3.
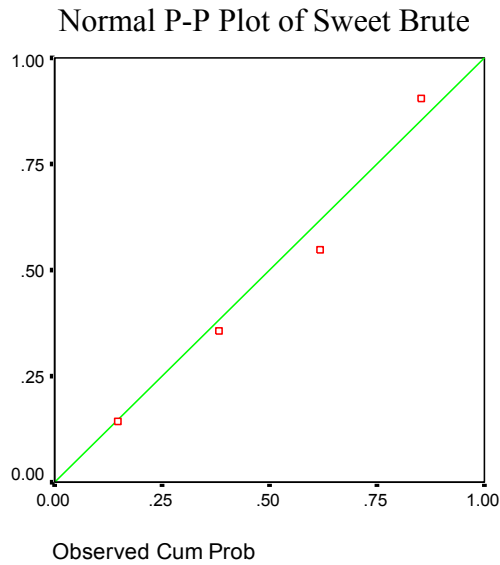
Figure 5.3 Normal probability plot for Shear strength: Sweet Brut data
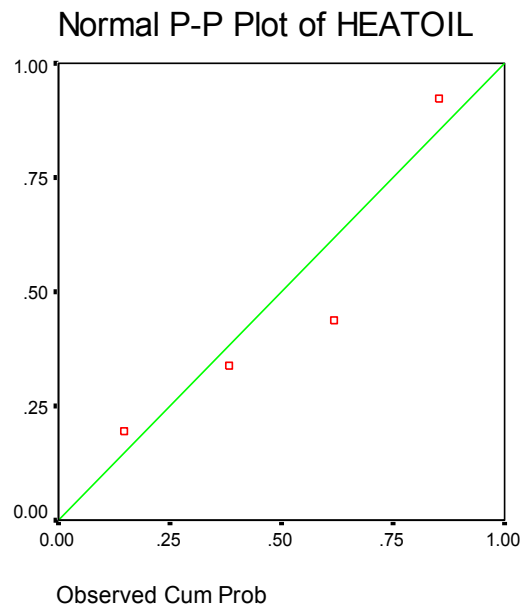
Figure 5.4 Normal probability plot for shear strength: Heating Oil data

Normal P-P Plot of GASOLINE
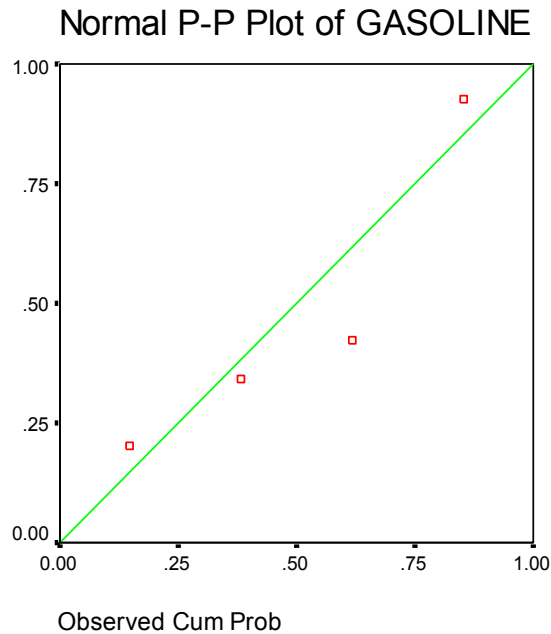
Figure 5.5 Normal probability plot for shear strength: Gasoline data

Table 5.3 Predicted shear strength (kPa) and its prediction error with input of experimental values at 0, 2, 4, 6 percent contamination.

Contami-nation	Sweet Brut		Heating Oil		Gasoline	
	$\hat{x}$	Error	$\hat{x}$	Error	$\hat{x}$	Error
8%	7.4186	0.2364	7.3526	0.2234	3.7852	0.4466
10%	3.2539	0.8798	4.0155	0.8221	0.3212	1.5302
11%	1.2931	1.3779	2.4211	1.2784	*	*

To check the sensitivity of the model, the prediction process was repeated by reducing the experimental data input to 0, 2, and 4 percent contamination of the clay for the three contaminants (sweet brut, heating oil, and gasoline). Thus, results are presented in Table 5.4. The prediction of the undrained shear

strength (first line of Table 5.4) vary from the corresponding experimental values (last line in Table 4.1) by 22%, 14%, and 40%, for the three contaminants, sweet brut, heating oil, and gasoline, respectively. Only one set of comparison could be made due to the limited number of contamination levels tested.   Further experimental tests on additional levels of contamination in future studies would give further insight into the sensitivity of the model to inputs of different number of experimental data points. Similarities can be noted in the results shown in tables 5.3 and 5.4. At 11% contamination, for example, it can be noted from the last lines of Tables 5.3 and 5.4, that the model predicts the shear strength to approach zero for both sets of experimental inputs. It is reasonable to expect that as the level of contamination is increased, the undrained shear strength of the clay will approach zero. The results from the model in Tables 5.3 and 5.4 show the shear strength to approach zero at 11% contamination, which is consistent with this expectation.

Table 5.4 Predicted shear strength (kPa) and its prediction error with input of experimental values at 0, 2, 4 percent contamination.

Contamination	Sweet Brut		Heating Oil		Gasoline	
	$\hat{X}$	Error	$\hat{X}$	Error	$\hat{X}$	Error
6%	8.9761	0.2123	9.0114	0.1976	4.4562	0.3496
8%	7.3984	0.3086	7.3461	0.2786	3.7852	0.4623
10%	3.5228	0.8016	3.9565	0.9012	0.3481	1.4911
11%	1.6534	1.2438	2.3012	1.2345		

It can be observed that contaminants, used in the present research, reduce the values of both experimental and predicted undrained shear strength to various degrees (Tables 4.2, 5.3). This observation is most obvious in the case of 6% gasoline contamination (Table 4.2), where the undrained shear strength dropped by 68.08% compared to the reference value of the uncontaminated clay. The reduction in the values of undrained shear strength produces less dramatic changes as the degree of contamination is reduced. With 6% heating oil contamination the undrained shear strength is reduced by 55.32%, while 6% of crude oil contamination results in a drop of 51.6% in the undrained shear strength of the clay. Similarly, the variation can be observed in the case of 8% contamination in Table 5.3, where the predicted undrained shear strength drops to 3.7852 kPa for gasoline, 7.3526 for heating oil, and to 7.4186 kPa for Sweet Brut.

The properties of these contaminants influence the friction angle of the soil to various degrees which is reflected in the undrained shear strength of the soil. Further research would be required to isolate the impact of constituent components of the contaminants on the reduction of the undrained shear strength of the clay.

Table 5.5 Predicted shear strength and its prediction error at different contamination values, contamination type vs. parameter

Contamination Type	Parameter Estimate		
	$\hat{\mu}$	$\hat{\sigma}$	$\hat{\tau}$
Sweet Brut	13.8354	3.6335	3.3941
Heating Soil	12.1740	2.15256	2.7272
Gasoline	9.5090	2.2675	2.3118

The model, developed in the present thesis, was tested by simulation. Results have proven that the model is functional and the predictions are reliable. Simulation is not the only way to test mathematical models. They can also be tested with a method called the calibration method. This, however, requires a much greater number of data than used in the present study, and it can be left to future researchers whose objective would be collecting sets of additional data that would be used in the calibration method.

5.4.3 Comments on results

Based on the above tables (5.2, 5.3, 5.4) the following comments can be made:

Comment 1. A dramatic decrease in the shear strength can be seen as the contamination level increases. Compared to the initial shear strength (clay soil with no contamination), the shear strength of the soil contaminated with 2% sweet brut decreased by 25.53%, while that contaminated by 4% and 6%

resulted respectively in a 36.17% and 51.60% decrease (Table 5.2, Figures 5.6, 5.7). When the same specimen were contaminated with 2, 4 and 6 percent heating oil the percent decrease in shear strengths were 38.30%, 44.68% and 55.32% respectively. Correspondingly for gasoline, the shear strength dropped by 46.80%, 55.32% and 68.08% under similar conditions of contamination.
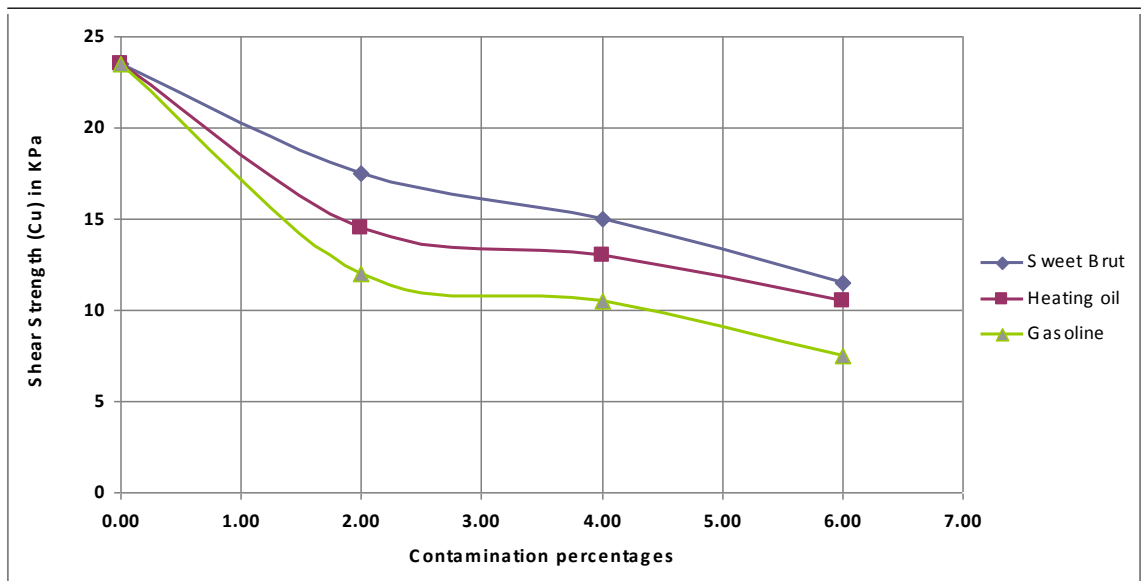
Figure 5.6 Effect of contamination percentages on the shear strength
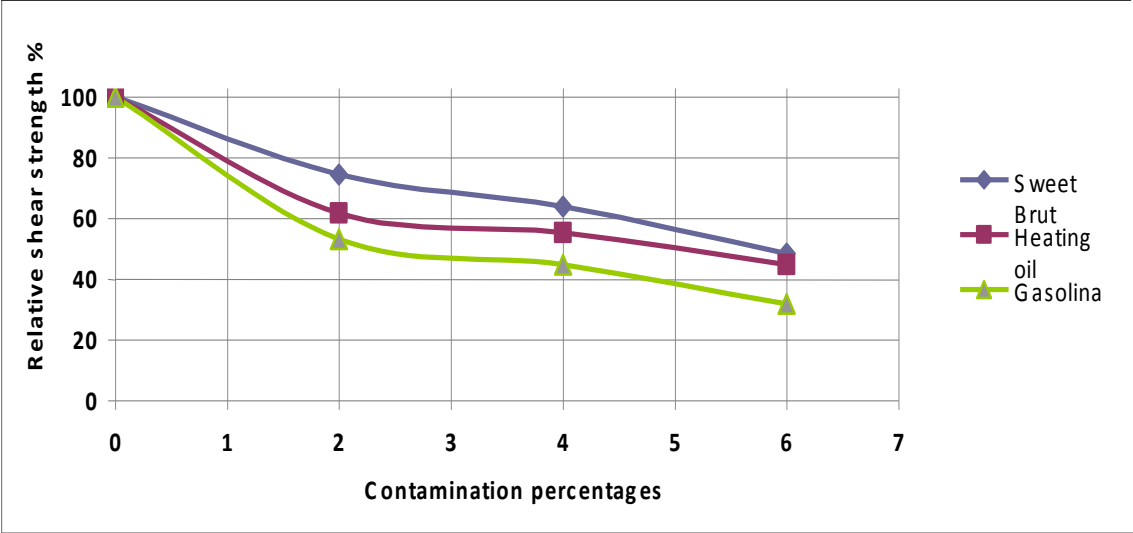
Figure 5.7 Effect of contamination percentages on the relative shear strength
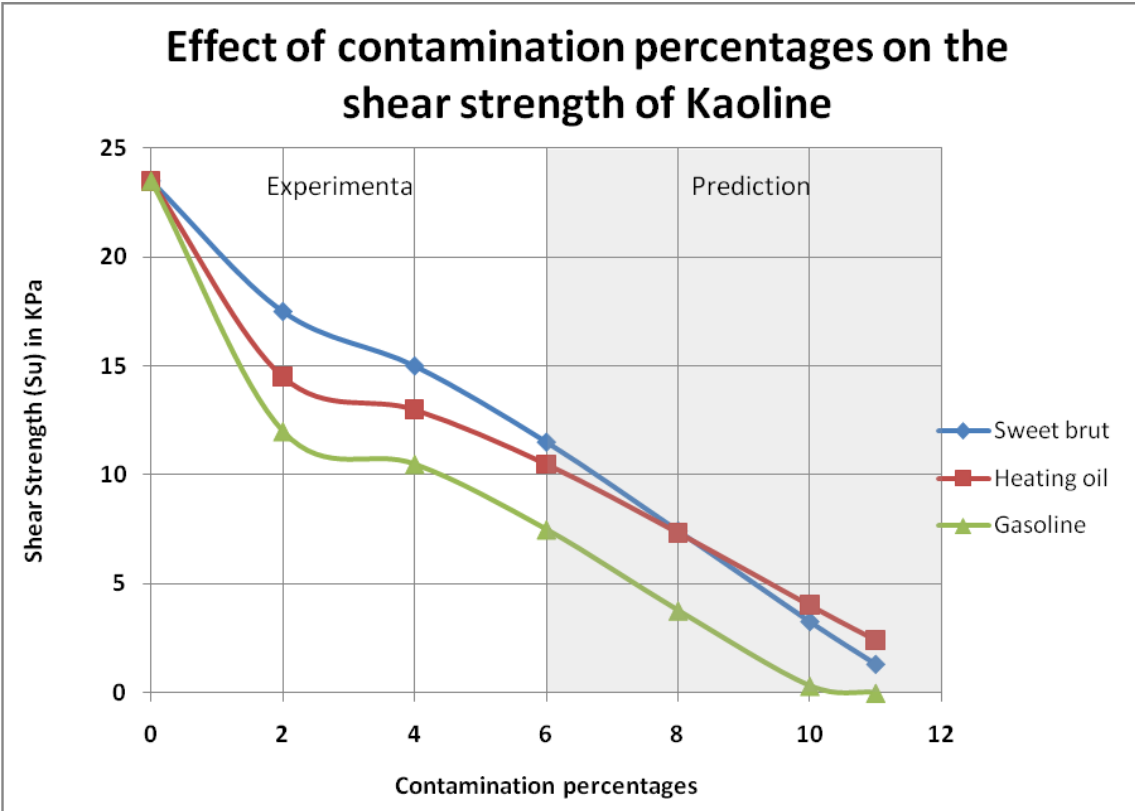
Figure 5.8 Effect of contamination percentages on the shear strength, experimental and prediction
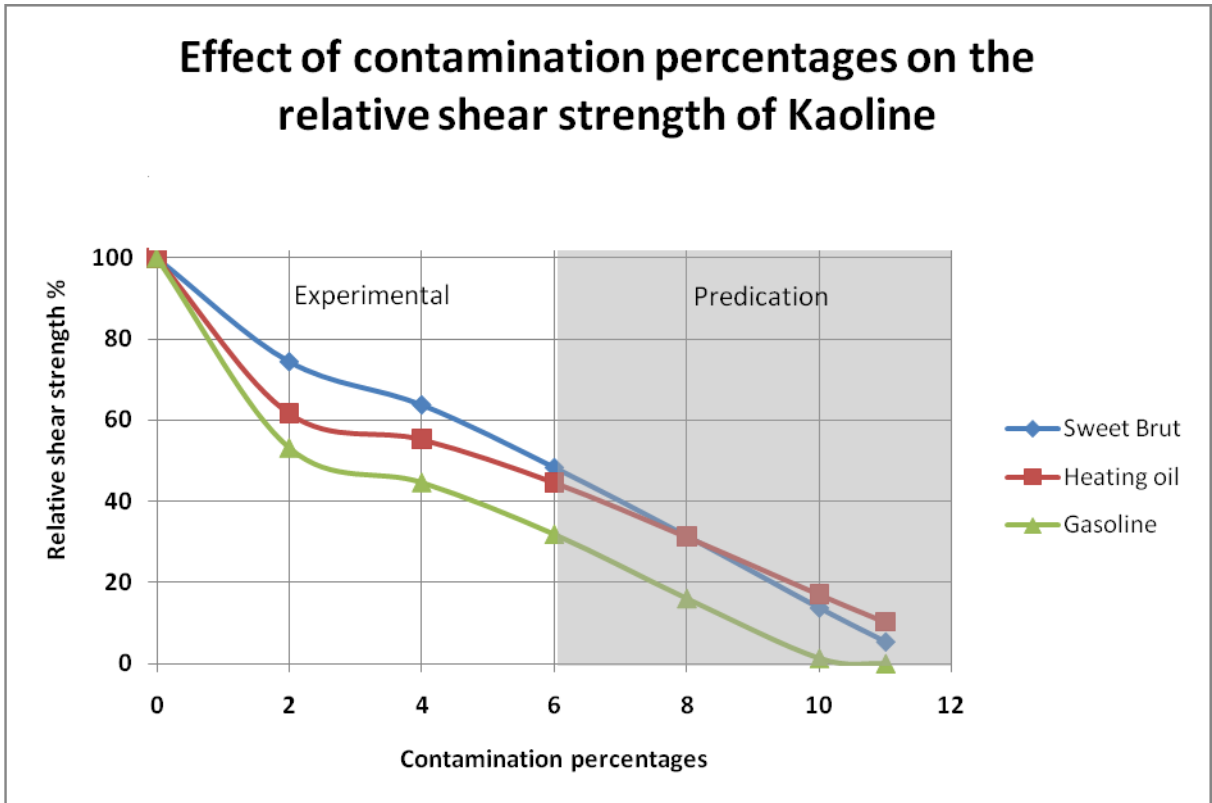
5.9 Effect of contamination percentages on the relative shear strength, experimental and prediction

Predicted values show (Table 5.3, Figures 5.8, 5.9) that the value of the undrained shear strength drops to zero between 10% and 11% contamination. The undrained shear strength reduction is explained via the Modified Cam-Clay model (Schofield et al, 1968, Devi et al., 2008) as shown in Figure 5.10. Specifically, the degree of contamination reduces the critical friction angle, φ'_{cs}, which implies a decrease in the critical state line (CSL) slope. One possible explanation, which needs further research, is that adsorbed oil tends to lubricate the surfaces of clay particles and reduce inter-particle friction thus decreasing the friction angle. This phenomenon is manifested by a reduction in the undrained shear strength.
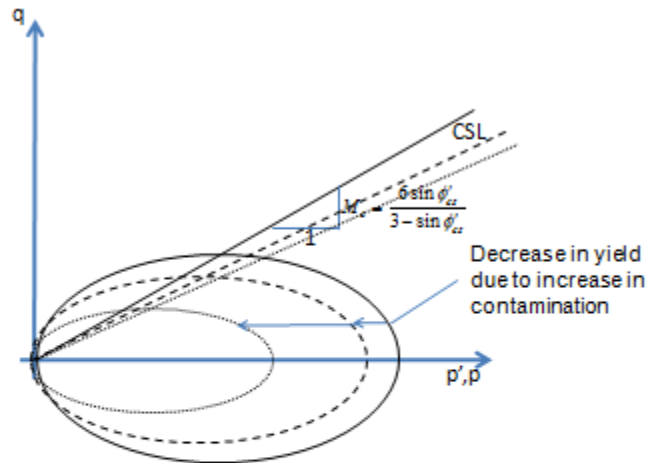
Figure 5.10   Degree of contamination vs. critical
friction angle, φ'_{cs}

Comment 2. The prediction error determined by the statistical model increases as the contamination increases.

Comment 3. Table 5.5 shows that the gasoline-contaminated soil has the smallest mean shear strength (9.509 kPa).

A thorough examination of the literature reveals that no study has been carried out on the undrained shear strength of contaminated clays. One experimental study which confirms the previous interpretation via the Cam-Clay Model was conducted by Hassan et al. (1995). Testing in that study included basic property tests, compaction and permeability tests, and triaxial and consolidation tests on clean and contaminated sand. Contaminated specimens were prepared by mixing the sand with oil in the amount of 6% by weight. The authors concluded

that oil contamination leads to a decrease in permeability and strength. The reduction in the angle of friction was 2° for specimens mixed with 6% of heavy crude oil. They also stated that contamination decreased soil modulus in the triaxial test. These results tend to parallel the present findings with regards to the friction angle of contaminated clays.

6. CONCLUSION

6.1 Observations drawn from the experimental investigation

A series of triaxial experiments was carried out in the frame work of this doctoral thesis to examine how petroleum, crude oil, and its derivatives (heating oil and gasoline contaminants) affect the undrained shear strength, S_u , of the clay soil.

The results of these triaxial experiments, as well as a random field model implemented in this thesis, confirm that a dramatic decrease in the undrained shear strength of clay soil occurs with petroleum contamination.

In the course of the triaxial experiments kaolin clay soil specimens were contaminated with 2, 4 and 6 percent Hibernia blend crude oil (sweet brut), heating oil and gasoline. These values of contaminants are typically encountered within sites that were occupied by oil refineries and commercial garages. In order to simulate short term field conditions undrained tests were conducted under a 100 kPa confining pressure in a triaxial cell.

These experiments indicated (Table 5.2, Figures 5.6 and 5.7) that when specimens were contaminated with two percent sweet brut, the resulting decrease in the undrained shear strength of the soil was 25.53%. Furthermore a four and six percent contamination respectively resulted in drops of 36.17% and 51.60% in the undrained shear strength of the soil compared to the specimen with zero percent contamination.

Likewise contamination with two, four and six percent heating oil (Table 5.2, Figures 5.6 and 5.7) resulted in a reduction of 38.30%, 44.58% and 55.32% in

the undrained shear strength of the clay compared to the initial undrained uncontaminated shear strength.

Similarly two and four percent gasoline contamination lessened the shear strength by 46.80%, 55.32%, while six percent of gasoline in the clay soil resulted in an enormous 68.08% (Table 5.2, Figures 5.6 and 5.7) drop in the undrained shear strength compared to the specimen with zero contamination.

Predicted values show (Table 5.3, Figures 5.8, and 5.9) that the value of the undrained shear strength drops to zero between 10% and 11%.

The theoretical study in this thesis confirms that the random field theory is very useful in determining the distribution of the undrained shear strength. Namely, this resulted in a successful prediction of the excursion set (Table 5.3), as well as some of its characteristics of a smooth and stationary Gaussian random field. The theoretically predicted undrained shear strength values given in Table 5.3 indicate the general trend observed in the lab tests. Specifically in the case of gasoline contamination, a complete failure is predicted at 11% contamination.

The validity and functionality of the model was proven when the prediction process was started from 4% of contamination of the clay instead of 6% for sweet brut and heating oil. Results in Table 5.4 are close to those obtained when prediction started from 6% (Table 5.3).

6.2. Contributions of the thesis

In this thesis we consider the limiting condition of a short term analysis, under the effect of contaminants, in order to satisfy the following two principles:

1. The foundation must not collapse or become unstable under any conceivable loading.

2. Settlement of the structure must be within tolerable limits.

A short term condition requires a total stress analysis (TSA). TSA is applicable to fine-grained soils (such as clays) and the shear strength parameter is the undrained shear strength S_u. This parameter is strongly affected by soil contamination. Consequently stability of the foundation and the integrity of the structure that rests on it are also strongly dependent on the soil contamination. The undrained shear strength is needed in order to verify point 1 above.

If the foundation is stable there is still a need to verify that settlements of the foundation are within tolerable limits (point 2). The parameters needed for calculation of the elastic settlement are the undrained initial tangent and secant moduli. These moduli are also strongly affected by contamination. This was observed in the lab tests via the deviatoric stress versus axial strain curves (Chapter 4).

.

6.3 Recommendation for further research

Based on the finding reported in this thesis, the following recommendations for future research are made:

Foundation analysis requires both a total stress analysis (TSA) for short term conditions and an effective stress analysis (ESA) for long term conditions.

1. It is recommended that researchers carry out further experiments in state-of-the-art triaxial laboratories in order to obtain effective stress parameters (ESA), such as φ_{cr}', the critical state friction angle for contaminated soils.

2. It is also recommended to obtain the drained elastic moduli.

3. The theoretical results obtained in this thesis should be used as a platform for further development in the field of random theories. moreover this theory should be extrapolated to other soil types.

4. Adequate time and financial support are essential in conducting very informative experiments for testing the validity of the developed random field theory in its entirety.

References

Adler, R. 1981. *The Geometry of Random Fields*. John Wiley and Sons, New York.

Al-Hattemleh, O. 1995. *Experimental Evaluation of the Subsurface Contamination by Kerosine on Soil Pile Interaction in Clayey Soil,* Ph.D. Thesis, Jordan University of Science and Technology, pp 29-30.

Alodat, M. 2006. *Size Distribution of One Connected Component of Elliptic Random Field,* Journal of The Korean Statistical Society, 36, pp. 479-489.

Aldous, D. 1989. Probability approximation via the Poisson clumping heuristic. Springer-Verlag, New York.

Alternative Fuels Data Center, U.S. Department of Energy, www.afdc.energy.gov/afdc/pdfs/fueltable.pdf

Annual Book of ASTM Standards, 2010, Volume 04.08, Section 4 Construction: Soil and Rock, ASTM International, West Conshohocken, PA, USA

Briaud, J-L, 2001. *Introduction to soil moduli,* Geotechnical News, BiTech Publishers, B.C., Canada

Budho M., 2007. *Soil Mechanics and Foundations,* John Wiley&Sons USA, pp 263-265.

Canada Mortgage and Housing Corporation, 1993. Soil Gases and Housing, pp. 3-4.

Cao, J., Worsley, K. 1999. The detection of local shape changes via the geometry of Hotelling's T fields, *Ann. Statist.*, 27(3), pp. 925-942.

Connor, J. 2000, *Positive Impact of ASTM Risk-Based Corrective Action Standard,* Standardization News, ASTM

Das B., 2005 *Laboratory Manual, Soil Mechanics,* 6th edition, Oxford University Press, New York, NY, USA, pp 129-133.

Devi, D., Singh, A., 2008, On Finite Element Implementation for Cam Clay Model, *International Association for Computer Methods and Advances in Geomechanics (IACMAG).*

Domask, 1984, Gasoline - Production, Import, Use and Disposal, www.atsdr.cdc.gov/ToxProfiles/tp72-c4.pdf, United States

Evgin, E. and Das, B. 1992. Mechanical behavior of oil contaminated sand, *Environmental and Geotechnical Proceedings of Mediterranean Conference*, Balkema Publisher, Rotterdam, The Netherlands, pp. 101-108

Hasofer, A. 1978. Upcrossings of random fields. *Suppl. Journal of Advances in Applied Probability,* No.10, School of Mathematics and Statistics, University of Sheffield, United Kingdom, pp 14-21

Hassan, A., Walid, K. and Nabi, F., 1995. Geotechnical Properties of Oil Contaminated Kuwaiti Sand*, Journal of Geotechnical Engineering*, vol. 121, No 5, ASCE

Hydro-Crude Oil Canada, (www.hydro.com/cgi-bin)

International Agency For Research On Cancer (IARC),1989, Crude Oil and Major Petroleum Fuels. Geneva Switzerland.VOL.: 45, p. 159

Kaolin Company, Sandersville, GA, USA

Katatbeh, Q., Alodat, M. and Kristof, J. 2007. Predicting the Excursion Set of Gaussian Random Field*, World Applied Sciences Journal*, 2, IDOSI, pp. 1-4 (2),

Lorincz, J., 1984. Effect of Infiltrating Hydrocarbons on the Soil Shear Strength*, Proceedings of Sixth Conference on soil mechanics and Foundation Engineering*, Budapest, Hungary.

Meegoda, N. and Ratnawecra, P., 1994. Compressibility of Contaminated Fine Grained Soil*, Geotechnical Testing Journal*. Vol.17/1, ASTM, Philadelphia, PA. pp 101-112.
Mallinckrodt Chemicals, 2008, MSDS, NJ, USA (www.vwrsp.com/msds/10)

Piterbarg, V. (1996). Asymptotic methods in the theory of Gaussian processes and fields. American Mathematical Society, Providence, RI, USA

Photos, Courtesy of Property Owner, 2004.

Schofield, A., Wroth, C. 1968. Critical State Soil Mechanics. McGraw-Hill, London.

Worsley, K. and Friston, K. 2000. A test for a conjunction. *Statistics and Probability Letters*, 47, Elsevier B.V., Amsterdam, The Netherlands, pp135-140.

Appendix

1. Output of the Agilent Vee Pro-Master Computer Program

2. Properties of Kaolin, Crude Oil used in the research

1. Output of the Agilent Vee Pro-Master Computer Program

0 % Contamination

Data Acquisition 34970-A
OUTPUTS: LVDT-I (mm)
Prepared By:-   Joseph W. Kristof
Dated:-   01-08-2008
Test Type   Static
Contamination: 0%

S. No.	Channel -I	With A	Time
	LVDT-I	Deviator Stress	
	Strain	s_1-s_3 (kPa)	
1	0.00%	0.000000	15:43:17
2	0.08%	4.463507294	15:43:21
3	0.15%	5.870017812	15:43:25
4	0.22%	7.274669035	15:43:28
5	0.30%	8.676772456	15:43:32
6	0.37%	10.40228799	15:43:36
7	0.45%	11.19586748	15:43:40
8	0.52%	12.4555036	15:43:44
9	0.59%	14.63653293	15:43:48
10	0.66%	14.85846869	15:43:52
11	0.74%	16.62169265	15:43:55
12	0.82%	18.08059032	15:43:59
13	0.89%	19.51502224	15:44:03
14	0.97%	20.86902177	15:44:07
15	1.04%	21.84483175	15:44:11
16	1.11%	22.92315098	15:44:15
17	1.19%	23.98486928	15:44:18

18	1.26%	25.02461176	15:44:22
19	1.34%	25.96056374	15:44:26
20	1.41%	26.9581121	15:44:30
21	1.49%	27.76906636	15:44:34
22	1.57%	28.56464009	15:44:38
23	1.65%	29.37009682	15:44:41
24	1.73%	30.03013588	15:44:45
25	1.81%	30.83849698	15:44:49
26	1.88%	31.39741069	15:44:53
27	1.97%	32.00559991	15:44:56
28	2.05%	32.59075289	15:45:00
29	2.13%	33.07970171	15:45:04
30	2.21%	33.67776181	15:45:08
31	2.30%	34.1589953	15:45:12
32	2.37%	34.62483022	15:45:16
33	2.44%	35.1449409	15:45:20
34	2.52%	35.56460379	15:45:23
35	2.60%	36.10844058	15:45:27
36	2.67%	36.45259239	15:45:31
37	2.75%	36.87061482	15:45:35
38	2.83%	37.21226864	15:45:39
39	2.91%	37.52138201	15:45:42
40	2.99%	38.00269207	15:45:46
41	3.07%	38.2905686	15:45:50
42	3.14%	38.5835178	15:45:54
43	3.22%	38.95297089	15:45:57
44	3.30%	39.2290055	15:46:01
45	3.37%	39.55732932	15:46:05
46	3.46%	39.85374062	15:46:09
47	3.54%	40.19010963	15:46:13
48	3.61%	40.45201639	15:46:17
49	3.69%	40.75677601	15:46:21
50	3.76%	40.95879093	15:46:25
51	3.84%	41.22593067	15:46:29

52	3.92%	41.47128852	15:46:32
53	4.00%	41.73991328	15:46:36
54	4.09%	41.9915111	15:46:40
55	4.16%	42.17476715	15:46:44
56	4.25%	42.34922066	15:46:48
57	4.32%	42.59698636	15:46:51
58	4.40%	42.77264671	15:46:55
59	4.48%	42.87876137	15:46:59
60	4.55%	43.07612057	15:47:03
61	4.63%	43.1993817	15:47:07
62	4.71%	43.47158297	15:47:11
63	4.78%	43.62144354	15:47:15
64	4.86%	43.83242698	15:47:18
65	4.95%	43.9300527	15:47:22
66	5.02%	44.06626556	15:47:26
67	5.10%	44.24092181	15:47:29
68	5.18%	44.39668351	15:47:33
69	5.25%	44.53197734	15:47:37
70	5.33%	44.69401498	15:47:41
71	5.40%	44.7899419	15:47:45
72	5.48%	44.98033332	15:47:48
73	5.56%	45.07700846	15:47:52
74	5.63%	45.20971022	15:47:56
75	5.71%	45.29997303	15:48:00
76	5.80%	45.48837894	15:48:04
77	5.88%	45.50193757	15:48:08
78	5.97%	45.64336009	15:48:11
79	6.03%	45.72674825	15:48:15
80	6.11%	45.83362839	15:48:19
81	6.19%	45.841347	15:48:23
82	6.27%	45.90150259	15:48:27
83	6.35%	46.01253539	15:48:31
84	6.42%	46.08735657	15:48:34
85	6.50%	46.23834707	15:48:38

86	6.58%	46.27979314	15:48:42
87	6.66%	46.34003969	15:48:46
88	6.74%	46.4113906	15:48:50
89	6.82%	46.4608026	15:48:54
90	6.90%	46.44138378	15:48:58
91	6.98%	46.60248244	15:49:01
92	7.06%	46.69327876	15:49:05
93	7.14%	46.71014673	15:49:09
94	7.22%	46.72279239	15:49:13
95	7.30%	46.71710217	15:49:17
96	7.39%	46.78911216	15:49:20
97	7.47%	46.82708883	15:49:24
98	7.56%	46.86741605	15:49:28
99	7.63%	46.9085772	15:49:32
100	7.72%	46.93643713	15:49:36
101	7.80%	46.91720331	15:49:40
102	7.88%	46.86304763	15:49:43
103	7.96%	46.95018902	15:49:48
104	8.04%	46.96110462	15:49:52
105	8.12%	47.00538607	15:49:55
106	8.19%	46.9420422	15:49:59
107	8.26%	46.9472149	15:50:03
108	8.35%	46.93451792	15:50:07
109	8.42%	46.91662767	15:50:11
110	8.51%	46.89864615	15:50:14
111	8.59%	46.75029786	15:50:18
112	8.66%	46.66466938	15:50:22
113	8.75%	46.63723333	15:50:26
114	8.83%	46.59742281	15:50:30
115	8.90%	46.46446201	15:50:33
116	8.98%	46.38355264	15:50:37
117	9.05%	46.29296214	15:50:41
118	9.13%	46.17436423	15:50:45
119	9.21%	46.09734814	15:50:49

120	9.29%	46.01448999	15:50:53
121	9.36%	45.82819424	15:50:56
122	9.44%	45.84769928	15:51:00
123	9.52%	45.74745224	15:51:04
124	9.60%	45.62974309	15:51:08
125	9.67%	45.52170786	15:51:12
126	9.75%	45.40034135	15:51:15
127	9.83%	45.35066109	15:51:19
128	9.91%	45.27133781	15:51:23
129	9.98%	45.15850175	15:51:27
130	10.06%	45.02841896	15:51:31
131	10.14%	44.93875619	15:51:35
132	10.22%	44.85054725	15:51:39
133	10.29%	44.75630986	15:51:42
134	10.37%	44.66015797	15:51:46
135	10.45%	44.56410542	15:51:50
136	10.52%	44.46815222	15:51:54
137	10.60%	44.37229836	15:51:58
138	10.68%	44.27654384	15:52:02
139	10.76%	44.18088866	15:52:05

2% Sweet Brut Contamination

Data Acquisition 34970-A
OUTPUTS: LVDT-I (mm)
Prepared By:-   Joseph W. Kristof
Dated:-   01-08-2008
Test Type   Static Compression Triaxial Test
Contamination: 2% Sweet Brut

S. No.	Channel -I	With A	Time
	LVDT-I	Deviator Stress	
	Strain	s1-s3 (kPa)	
1	0.01%	0.000000	15:46:48
2	0.08%	3.402320	15:46:51
3	0.15%	4.380315	15:46:55
4	0.22%	5.358309	15:46:59
5	0.30%	6.336304	15:47:03
6	0.37%	7.314299	15:47:07
7	0.45%	8.292293	15:47:11
8	0.52%	9.270288	15:47:15
9	0.59%	10.248283	15:47:18
10	0.66%	11.240453	15:47:22
11	0.74%	12.175921	15:47:26
12	0.82%	13.196442	15:47:29
13	0.89%	13.629005	15:47:33
14	0.97%	14.435090	15:47:37
15	1.04%	15.097582	15:47:41
16	1.11%	15.752417	15:47:45
17	1.19%	16.335949	15:47:48

18	1.26%	16.981113	15:47:52
19	1.34%	17.526666	15:47:56
20	1.41%	18.032418	15:48:00
21	1.49%	18.523276	15:48:04
22	1.57%	19.025079	15:48:08
23	1.65%	19.513509	15:48:11
24	1.73%	19.985684	15:48:15
25	1.81%	20.432391	15:48:19
26	1.88%	20.831260	15:48:23
27	1.97%	21.288899	15:48:27
28	2.05%	21.682033	15:48:31
29	2.13%	22.043780	15:48:34
30	2.21%	22.373306	15:48:38
31	2.30%	22.823514	15:48:42
32	2.37%	23.119715	15:48:46
33	2.44%	23.395314	15:48:50
34	2.52%	23.803169	15:48:54
35	2.60%	24.114841	15:48:58
36	2.67%	24.391163	15:49:01
37	2.75%	24.684919	15:49:05
38	2.83%	25.065672	15:49:09
39	2.91%	25.355504	15:49:13
40	2.99%	25.622836	15:49:17
41	3.07%	25.953654	15:49:20
42	3.14%	26.273614	15:49:24
43	3.22%	26.543085	15:49:28
44	3.30%	26.778028	15:49:32
45	3.37%	27.044348	15:49:36
46	3.46%	27.322399	15:49:40
47	3.54%	27.535755	15:49:43

48	3.61%	27.822159	15:49:48
49	3.69%	28.026666	15:49:52
50	3.76%	28.315471	15:49:55
51	3.84%	28.492843	15:49:59
52	3.92%	28.767063	15:50:03
53	4.00%	29.005816	15:50:07
54	4.09%	29.169232	15:50:11
55	4.16%	29.393507	15:50:14
56	4.25%	29.595591	15:50:18
57	4.32%	29.758108	15:50:22
58	4.40%	29.917464	15:50:26
59	4.48%	30.154667	15:50:30
60	4.55%	30.386910	15:50:33
61	4.63%	30.486950	15:50:37
62	4.71%	30.711020	15:50:41
63	4.78%	30.916786	15:50:45
64	4.86%	31.160543	15:50:49
65	4.95%	31.260071	15:50:53
66	5.02%	31.464506	15:50:56
67	5.10%	31.573249	15:51:00
68	5.18%	31.713415	15:51:04
69	5.25%	31.872980	15:51:08
70	5.33%	32.059685	15:51:12
71	5.40%	32.160100	15:51:15
72	5.48%	32.295969	15:51:19
73	5.56%	32.344554	15:51:23
74	5.63%	32.571053	15:51:27
75	5.71%	32.687210	15:51:31
76	5.80%	32.693680	15:51:35
77	5.88%	32.856039	15:51:39

78	5.97%	32.997345	15:51:42
79	6.03%	33.115941	15:51:46
80	6.11%	33.203445	15:51:50
81	6.19%	33.321605	15:51:54
82	6.27%	33.398384	15:51:58
83	6.35%	33.538640	15:52:02
84	6.42%	33.566574	15:52:05
85	6.50%	33.605091	15:52:09
86	6.58%	33.802204	15:52:14
87	6.66%	33.839822	15:52:17
88	6.74%	33.917236	15:52:21
89	6.82%	33.993137	15:52:25
90	6.90%	34.020205	15:52:29
91	6.98%	34.070176	15:52:33
92	7.06%	34.169922	15:52:36
93	7.14%	34.238796	15:52:40
94	7.22%	34.308939	15:52:44
95	7.30%	34.309833	15:52:48
96	7.39%	34.382362	15:52:52
97	7.47%	34.445588	15:52:56
98	7.56%	34.387339	15:53:00
99	7.63%	34.475075	15:53:04
100	7.72%	34.492399	15:53:08
101	7.80%	34.527493	15:53:12
102	7.88%	34.617986	15:53:15
103	7.96%	34.689900	15:53:19
104	8.04%	34.684699	15:53:23
105	8.12%	34.684795	15:53:27
106	8.19%	34.770014	15:53:30
107	8.26%	34.802602	15:53:34

108	8.35%	34.809687	15:53:38
109	8.42%	34.822892	15:53:42
110	8.51%	34.820557	15:53:46
111	8.59%	34.844349	15:53:49
112	8.66%	34.790266	15:53:53
113	8.75%	34.908412	15:53:57
114	8.83%	34.903207	15:54:01
115	8.90%	34.955280	15:54:05
116	8.98%	34.892237	15:54:09
117	9.05%	34.938427	15:54:13
118	9.13%	34.901334	15:54:17
119	9.21%	34.891654	15:54:21
120	9.29%	34.917899	15:54:25
121	9.36%	34.838055	15:54:28
122	9.44%	34.904583	15:54:32
123	9.52%	34.933982	15:54:36
124	9.60%	34.899639	15:54:40
125	9.67%	34.854688	15:54:44
126	9.75%	34.827023	15:54:48
127	9.83%	34.823688	15:54:51
128	9.91%	34.852692	15:54:55
129	9.98%	34.838008	15:54:59
130	10.06%	34.829311	15:55:03
131	10.14%	34.769562	15:55:07
132	10.22%	34.619902	15:55:10
133	10.29%	34.672671	15:55:14
134	10.37%	34.586119	15:55:18
135	10.45%	34.522080	15:55:22
136	10.52%	34.525346	15:55:25
137	10.60%	34.462865	15:55:29

138	10.68%	34.421324	15:55:33
139	10.76%	34.452833	15:55:37
140	10.83%	34.350217	15:55:41
141	10.91%	34.357828	15:55:45
142	10.99%	34.126063	15:55:49
143	11.07%	34.173841	15:55:53
144	11.14%	34.065685	15:55:57
145	11.22%	33.947291	15:56:01
146	11.30%	33.913479	15:56:05

4% Sweet Brut Contamination

Data Acquisition 34970-A
OUTPUTS: LVDT-I (mm)
Prepared By:-   Joseph W. Kristof
Dated:-   01-08-2008
Test Type   Static Compression Triaxial Test
Contamination: 4% Sweet Brut

S. No.	Channel -I	With A	Time
	LVDT-I Strain	Deviator Stress σ_1-σ_3 (kPa)	
1	0.00%	0	10:35:55
2	0.17%	6.951277755	10:35:59
3	0.23%	8.104851653	10:36:03
4	0.28%	9.347188099	10:36:07
5	0.36%	10.36947307	10:36:10
6	0.43%	11.43477579	10:36:14
7	0.51%	12.30207608	10:36:18
8	0.59%	13.1103365	10:36:22
9	0.66%	13.9123951	10:36:26
10	0.74%	14.68522665	10:36:30
11	0.82%	15.41243727	10:36:34
12	0.89%	16.010316	10:36:37
13	0.97%	16.76326016	10:36:41
14	1.05%	17.31482561	10:36:44
15	1.12%	17.82780754	10:36:48
16	1.20%	18.34324927	10:36:52
17	1.28%	18.74162942	10:36:55

18	1.35%	19.30786264	10:36:59
19	1.43%	19.76531806	10:37:03
20	1.50%	20.25798027	10:37:07
21	1.58%	20.70414545	10:37:10
22	1.66%	20.97835174	10:37:14
23	1.73%	21.3922492	10:37:18
24	1.81%	21.71755262	10:37:22
25	1.89%	22.05534057	10:37:25
26	1.96%	22.38281725	10:37:29
27	2.04%	22.59767287	10:37:33
28	2.12%	22.93552033	10:37:37
29	2.19%	23.22741344	10:37:41
30	2.27%	23.44424964	10:37:45
31	2.35%	23.71093143	10:37:49
32	2.42%	23.91891571	10:37:52
33	2.50%	24.16210936	10:37:56
34	2.57%	24.40490472	10:38:00
35	2.65%	24.69247522	10:38:04
36	2.73%	24.86182138	10:38:08
37	2.80%	25.05826563	10:38:11
38	2.88%	25.37999164	10:38:15
39	2.96%	25.52397145	10:38:19
40	3.03%	25.74863622	10:38:23
41	3.11%	25.94048344	10:38:27
42	3.19%	26.12667906	10:38:31
43	3.26%	26.31612776	10:38:35
44	3.34%	26.42125837	10:38:39
45	3.42%	26.64466723	10:38:42
46	3.50%	26.72318221	10:38:46
47	3.58%	26.87718346	10:38:50

48	3.65%	27.05084653	10:38:54
49	3.73%	27.14753131	10:38:58
50	3.81%	27.29901548	10:39:01
51	3.89%	27.37240755	10:39:05
52	3.97%	27.55376687	10:39:09
53	4.04%	27.65778862	10:39:13
54	4.12%	27.90143734	10:39:16
55	4.19%	27.9077444	10:39:20
56	4.28%	28.01244421	10:39:24
57	4.36%	28.07409252	10:39:28
58	4.44%	28.25032497	10:39:31
59	4.52%	28.30564013	10:39:35
60	4.60%	28.4445151	10:39:39
61	4.68%	28.52809053	10:39:43
62	4.77%	28.68680884	10:39:47
63	4.85%	28.67555727	10:39:51
64	4.92%	28.82000698	10:39:54
65	5.00%	28.85296637	10:39:58
66	5.08%	28.95740832	10:40:02
67	5.16%	29.00706432	10:40:06
68	5.24%	29.09488338	10:40:10
69	5.31%	29.16729435	10:40:14
70	5.38%	29.1943044	10:40:17
71	5.46%	29.2631751	10:40:21
72	5.55%	29.22065682	10:40:25
73	5.63%	29.3108513	10:40:29
74	5.71%	29.33557459	10:40:32
75	5.78%	29.38099974	10:40:36
76	5.86%	29.4904485	10:40:40
77	5.94%	29.49912893	10:40:43

78	6.03%	29.4855673	10:40:47
79	6.11%	29.52990449	10:40:51
80	6.19%	29.59101749	10:40:55
81	6.27%	29.56887659	10:40:58
82	6.35%	29.64219981	10:41:02
83	6.43%	29.58220345	10:41:06
84	6.51%	29.63561412	10:41:10
85	6.58%	29.63729934	10:41:13
86	6.67%	29.68428651	10:41:17
87	6.74%	29.71215336	10:41:21
88	6.82%	29.74843073	10:41:25
89	6.90%	29.71486291	10:41:29
90	6.98%	29.74372656	10:41:33
91	7.06%	29.7205573	10:41:37
92	7.15%	29.73465202	10:41:41
93	7.22%	29.73287573	10:41:44
94	7.29%	29.77335808	10:41:48
95	7.36%	29.75722846	10:41:52
96	7.44%	29.68953055	10:41:56
97	7.51%	29.7348795	10:41:59
98	7.59%	29.77382807	10:42:03
99	7.67%	29.71314226	10:42:07
100	7.75%	29.76741125	10:42:11
101	7.82%	29.74428165	10:42:15
102	7.90%	29.78165103	10:42:18
103	7.98%	29.75136704	10:42:22
104	8.05%	29.7311877	10:42:26
105	8.12%	29.67281119	10:42:30
106	8.20%	29.73468921	10:42:34
107	8.28%	29.70739803	10:42:38

108	8.35%	29.80146412	10:42:42
109	8.44%	29.75028693	10:42:45
110	8.51%	29.78674599	10:42:49
111	8.59%	29.75417535	10:42:53
112	8.67%	29.71597947	10:42:57
113	8.74%	29.68525307	10:43:01
114	8.82%	29.71283953	10:43:04
115	8.89%	29.67458979	10:43:08
116	8.96%	29.66926852	10:43:12
117	9.04%	29.6087062	10:43:16
118	9.12%	29.63597911	10:43:20
119	9.20%	29.56039022	10:43:24
120	9.27%	29.51246276	10:43:27
121	9.36%	29.49793172	10:43:31
122	9.44%	29.44940111	10:43:35
123	9.52%	29.4311404	10:43:39
124	9.60%	29.35360063	10:43:43
125	9.69%	29.41855949	10:43:47
126	9.77%	29.31472732	10:43:51
127	9.84%	29.28087175	10:43:54
128	9.92%	29.21154664	10:43:58
129	10.00%	29.20786956	10:44:02
130	10.08%	29.16171592	10:44:06
131	10.16%	29.08355526	10:44:10
132	10.23%	29.04748668	10:44:14
133	10.31%	28.9390951	10:44:18
134	10.40%	28.82368892	10:44:21
135	10.48%	28.73660191	10:44:25
136	10.56%	28.71948451	10:44:29
137	10.63%	28.56765042	10:44:33

138	10.71%	28.52734611	10:44:37
139	10.79%	28.45015819	10:44:41
140	10.87%	28.27813497	10:44:45
141	10.95%	28.13846589	10:44:49
142	11.03%	28.07362363	10:44:52
143	11.12%	27.95824115	10:44:56
144	11.19%	27.76258883	10:45:00
145	11.28%	27.62964621	10:45:02
146	11.36%	27.44093444	10:45:05

6% Sweet Brut Contamination

Data Acquisition 34970-A
OUTPUTS: LVDT-I (mm)
Prepared By:-   Joseph W. Kristof
Dated:-   01-08-2008
Test Type   Static Compression Triaxial Test
Contamination: 6% Sweet Brut

S. No.	Channel - I	With A	Time
	LVDT-I Strain	Deviator Stress σ_1-σ_3 (kPa)	
1	0.00%	0	09:16:43
2	0.06%	7.30942268	09:16:47
3	0.12%	8.204897683	09:16:50
4	0.17%	9.215280853	09:16:54
5	0.23%	9.961486616	09:16:58
6	0.28%	10.76972598	09:17:02
7	0.33%	11.46964	09:17:05
8	0.39%	12.0597595	09:17:09
9	0.46%	12.70030938	09:17:13
10	0.48%	13.2203626	09:17:16
11	0.54%	13.85571035	09:17:20
12	0.62%	14.36919606	09:17:24
13	0.70%	14.85496264	09:17:28
14	0.77%	15.23324541	09:17:32
15	0.84%	15.70915769	09:17:35
16	0.92%	16.07537957	09:17:39

17	1.00%	16.53387029	09:17:43
18	1.08%	16.79107834	09:17:46
19	1.15%	17.17066621	09:17:50
20	1.23%	17.50273806	09:17:54
21	1.30%	17.84809102	09:17:58
22	1.38%	18.12371712	09:18:02
23	1.46%	18.44623924	09:18:05
24	1.55%	18.62993695	09:18:09
25	1.63%	18.85466785	09:18:13
26	1.70%	19.16137731	09:18:17
27	1.78%	19.30836761	09:18:20
28	1.86%	19.48545416	09:18:24
29	1.94%	19.74337149	09:18:28
30	2.02%	19.84904269	09:18:32
31	2.10%	20.15335763	09:18:36
32	2.18%	20.34597309	09:18:39
33	2.26%	20.49561238	09:18:43
34	2.33%	20.57658992	09:18:47
35	2.41%	20.79630996	09:18:51
36	2.49%	20.94423392	09:18:54
37	2.57%	21.01509664	09:18:58
38	2.65%	21.17042989	09:19:02
39	2.73%	21.18930215	09:19:06
40	2.81%	21.42351962	09:19:10
41	2.88%	21.47124313	09:19:13
42	2.95%	21.55419144	09:19:17
43	3.02%	21.63743005	09:19:20
44	3.10%	21.70948705	09:19:24
45	3.18%	21.83922732	09:19:28
46	3.26%	21.87328781	09:19:32

47	3.34%	21.9504275	09:19:35
48	3.42%	21.97877496	09:19:39
49	3.50%	22.09852469	09:19:43
50	3.57%	22.11962829	09:19:47
51	3.65%	22.24233389	09:19:50
52	3.73%	22.35089448	09:19:54
53	3.81%	22.26531244	09:19:58
54	3.89%	22.37831129	09:20:01
55	3.97%	22.40677674	09:20:05
56	4.04%	22.4720739	09:20:09
57	4.12%	22.54757094	09:20:13
58	4.19%	22.72040266	09:20:17
59	4.28%	22.64422571	09:20:21
60	4.35%	22.69516761	09:20:24
61	4.43%	22.74940659	09:20:28
62	4.50%	22.78584049	09:20:32
63	4.57%	22.75861425	09:20:36
64	4.65%	22.73833007	09:20:39
65	4.73%	22.81502701	09:20:43
66	4.82%	22.81136613	09:20:47
67	4.89%	22.80993222	09:20:50
68	4.95%	22.83193761	09:20:54
69	5.02%	22.87158689	09:20:58
70	5.10%	22.8838241	09:21:02
71	5.18%	22.84911748	09:21:06
72	5.26%	22.89954381	09:21:09
73	5.34%	22.85708931	09:21:13
74	5.42%	22.7617793	09:21:17
75	5.50%	22.76867914	09:21:21
76	5.58%	22.80709474	09:21:25

77	5.65%	22.65929028	09:21:29
78	5.73%	22.6662119	09:21:32
79	5.80%	22.64522606	09:21:36
80	5.88%	22.63703593	09:21:40
81	5.96%	22.51025568	09:21:43
82	6.04%	22.53472033	09:21:47
83	6.12%	22.40993425	09:21:51
84	6.20%	22.38410149	09:21:55
85	6.28%	22.30869026	09:21:58
86	6.37%	22.26420581	09:22:02
87	6.45%	22.24513447	09:22:06
88	6.52%	22.15810696	09:22:09
89	6.60%	22.05188856	09:22:13
90	6.68%	22.11400413	09:22:17
91	6.75%	21.99758134	09:22:21
92	6.83%	21.88920516	09:22:25
93	6.91%	21.82629375	09:22:28
94	6.99%	21.64347012	09:22:32
95	7.07%	21.69595113	09:22:36
96	7.16%	21.59330931	09:22:40
97	7.23%	21.52408495	09:22:44
98	7.31%	21.46672869	09:22:47
99	7.38%	21.42442944	09:22:51
100	7.46%	21.2755029	09:22:55
101	7.54%	21.21481171	09:22:58
102	7.61%	21.21428113	09:23:02
103	7.69%	21.08837592	09:23:06
104	7.77%	20.97667966	09:23:09
105	7.85%	20.88427067	09:23:13
106	7.94%	20.79943493	09:23:17

107	8.00%	20.75380812	09:23:21
108	8.08%	20.65216141	09:23:25
109	8.16%	20.63299357	09:23:28
110	8.24%	20.52017142	09:23:32
111	8.31%	20.53396289	09:23:36
112	8.38%	20.37346116	09:23:40
113	8.46%	20.23429945	09:23:43
114	8.54%	20.21061889	09:23:47
115	8.62%	20.14371163	09:23:51
116	8.69%	19.99996102	09:23:55
117	8.77%	19.98321922	09:23:58
118	8.85%	19.89471389	09:24:02
119	8.92%	19.80146335	09:24:05
120	9.00%	19.70704974	09:24:09
121	9.08%	19.54187231	09:24:13
122	9.16%	19.45720708	09:24:16
123	9.23%	19.40442856	09:24:20
124	9.30%	19.36574	09:24:24
125	9.38%	19.26490965	09:24:28
126	9.45%	19.1396065	09:24:31
127	9.53%	19.09407603	09:24:35
128	9.60%	18.98530029	09:24:39
129	9.69%	18.89880836	09:24:42
130	9.77%	18.811593	09:24:46
131	9.84%	18.72263936	09:24:50
132	9.91%	18.61525966	09:24:53
133	9.99%	18.56412209	09:24:57
134	10.07%	18.45263808	09:25:01
135	10.15%	18.41657221	09:25:05
136	10.22%	18.33881156	09:25:08

137	10.30%	18.24435494	09:25:12
138	10.37%	18.09800748	09:25:16
139	10.46%	18.09602962	09:25:20
140	10.53%	17.99651222	09:25:24
141	10.61%	17.93436187	09:25:27
142	10.69%	17.83441053	09:25:31
143	10.76%	17.77131957	09:25:35
144	10.84%	17.73694212	09:25:38
145	10.91%	17.6271926	09:25:42
146	10.99%	17.4764601	09:25:46
147	11.06%	17.49701278	09:25:49
148	11.14%	17.37116027	09:25:53
149	11.21%	17.27745224	09:25:56
150	11.30%	17.29743183	09:26:00
151	11.38%	17.13060814	09:26:04
152	11.46%	17.02658721	09:26:08
153	11.53%	17.01800446	09:26:12
154	11.60%	16.98094968	09:26:15
155	11.68%	16.88271996	09:26:19
156	11.76%	16.86072582	09:26:23
157	11.85%	16.74538394	09:26:27
158	11.92%	16.67095204	09:26:31
159	12.00%	16.64875486	09:26:34
160	12.08%	16.60857241	09:26:38
161	12.16%	16.54544846	09:26:42
162	12.24%	16.50247095	09:26:45
163	12.32%	16.40176246	09:26:49
164	12.40%	16.33451547	09:26:53
165	12.48%	16.26323264	09:26:57
166	12.56%	16.17843333	09:27:01

167	12.64%	16.09677284	09:27:05
168	12.72%	16.03240879	09:27:09
169	12.79%	16.0485371	09:27:12
170	12.86%	15.91464897	09:27:16
171	12.94%	15.92358026	09:27:20
172	13.02%	15.79570358	09:27:24

2% Heating Oil Contamination

Data Acquisition 34970-A
OUTPUTS: LVDT-I (mm)
Prepared By:-   Joseph W. Kristof
Dated:-   01-08-2008
Test Type   Static Compression Triaxial Test
Contamination: 2% Heating Oil

S. No.	Channel - I	With A	Time
	LVDT-I Strain	Deviator Stress σ_1-σ_3 (kPa)	
1	0.00%	0	08:48:02
2	0.11%	2.257156669	08:48:05
3	0.19%	3.519989753	08:48:09
4	0.26%	4.78083007	08:48:13
5	0.34%	6.039677622	08:48:17
6	0.42%	7.296532408	08:48:21
7	0.50%	8.258534219	08:48:25
8	0.58%	10.19965265	08:48:28
9	0.66%	11.14217953	08:48:32
10	0.74%	12.11445577	08:48:36
11	0.81%	13.14704405	08:48:40
12	0.89%	13.85320783	08:48:44
13	0.97%	14.52538157	08:48:47
14	1.05%	15.19976184	08:48:51
15	1.13%	15.79434566	08:48:55
16	1.21%	16.38796439	08:48:59

17	1.29%	16.89058214	08:49:02
18	1.36%	17.42838747	08:49:06
19	1.44%	17.97666265	08:49:10
20	1.52%	18.30532957	08:49:14
21	1.60%	18.72902048	08:49:18
22	1.67%	19.15018003	08:49:21
23	1.75%	19.54384209	08:49:25
24	1.82%	19.94014863	08:49:29
25	1.89%	20.2761794	08:49:33
26	1.97%	20.63352059	08:49:37
27	2.05%	20.94965032	08:49:41
28	2.13%	21.24614487	08:49:44
29	2.21%	21.55483538	08:49:48
30	2.29%	21.72069138	08:49:52
31	2.37%	22.10390235	08:49:56
32	2.44%	22.40047219	08:49:59
33	2.52%	22.57137311	08:50:03
34	2.60%	22.83765444	08:50:07
35	2.67%	23.08953451	08:50:11
36	2.75%	23.25270209	08:50:14
37	2.82%	23.45850496	08:50:18
38	2.90%	23.66567924	08:50:22
39	2.98%	23.82227595	08:50:26
40	3.05%	24.10503888	08:50:29
41	3.12%	24.18773612	08:50:33
42	3.20%	24.4194107	08:50:37
43	3.28%	24.62139571	08:50:41
44	3.35%	24.80102005	08:50:44
45	3.43%	24.8744218	08:50:48
46	3.50%	25.05843895	08:50:52

47	3.58%	25.29010608	08:50:55
48	3.66%	25.40953197	08:50:59
49	3.73%	25.43473189	08:51:03
50	3.81%	25.6619387	08:51:06
51	3.89%	25.76140371	08:51:10
52	3.97%	25.89135995	08:51:14
53	4.04%	26.04045697	08:51:18
54	4.12%	26.17113297	08:51:22
55	4.19%	26.24031514	08:51:25
56	4.28%	26.39593527	08:51:29
57	4.35%	26.56184643	08:51:33
58	4.41%	26.67289918	08:51:37
59	4.49%	26.77287717	08:51:40
60	4.58%	26.90176619	08:51:44
61	4.66%	26.95765609	08:51:48
62	4.73%	27.07312031	08:51:52
63	4.82%	27.20579606	08:51:56
64	4.90%	27.32113277	08:51:59
65	4.98%	27.34259715	08:52:03
66	5.06%	27.46860491	08:52:07
67	5.13%	27.59928623	08:52:11
68	5.21%	27.6344512	08:52:15
69	5.28%	27.77314336	08:52:19
70	5.37%	27.72588337	08:52:22
71	5.45%	27.87149386	08:52:26
72	5.53%	27.88998429	08:52:30
73	5.61%	27.99289591	08:52:33
74	5.69%	28.08596552	08:52:37
75	5.77%	28.12395236	08:52:40
76	5.84%	28.26718845	08:52:44

77	5.92%	28.25188339	08:52:48
78	6.00%	28.29888241	08:52:51
79	6.08%	28.35006008	08:52:55
80	6.16%	28.36346983	08:52:59
81	6.23%	28.52786961	08:53:03
82	6.31%	28.51884237	08:53:07
83	6.38%	28.50198383	08:53:11
84	6.45%	28.57014487	08:53:15
85	6.52%	28.61105564	08:53:18
86	6.60%	28.66611317	08:53:22
87	6.67%	28.73382274	08:53:25
88	6.76%	28.67480182	08:53:29
89	6.82%	28.73019905	08:53:33
90	6.91%	28.71857781	08:53:37
91	6.99%	28.77958176	08:53:40
92	7.07%	28.83635446	08:53:44
93	7.15%	28.9195628	08:53:48
94	7.23%	28.83159841	08:53:51
95	7.29%	28.88638628	08:53:55
96	7.36%	28.80556965	08:53:59
97	7.43%	28.97439837	08:54:03
98	7.51%	28.94331765	08:54:06
99	7.59%	28.96062991	08:54:10
100	7.65%	28.98867636	08:54:14
101	7.73%	28.93254101	08:54:18
102	7.81%	28.93414862	08:54:22
103	7.89%	28.95411216	08:54:26
104	7.97%	28.94015731	08:54:30
105	8.03%	28.96971312	08:54:33
106	8.11%	28.92183358	08:54:37

107	8.19%	28.97885556	08:54:41
108	8.27%	28.91246332	08:54:45
109	8.35%	28.9835088	08:54:49
110	8.42%	28.89430148	08:54:52
111	8.50%	28.90544665	08:54:56
112	8.57%	28.85766302	08:55:00
113	8.66%	28.8165873	08:55:04
114	8.74%	28.85928622	08:54:49
115	8.82%	28.74043509	08:54:52
116	8.90%	28.77041955	08:54:56
117	8.98%	28.70167705	08:55:00
118	9.05%	28.69172527	08:55:04
119	9.13%	28.6427764	08:54:49
120	9.21%	28.60350013	08:54:52
121	9.29%	28.56579831	08:54:56
122	9.37%	28.5265195	08:55:00

4% Heating Oil Contamination

Data Acquisition 34970-A
OUTPUTS: LVDT-I (mm)
Prepared By:-   Joseph W. Kristof
Dated:-   01-08-2008

Test Type *Static   Compression   Triaxial Test*
Contamination: 4% Heating Oil

S. No.	Channel-I	With A	Time
	LVDT-I Strain	Deviator Stress σ_1-σ_3 (kPa)	
1	0.00%	0.000000	10:15:55
2	0.15%	7.569306	10:15:59
3	0.19%	8.862188	10:16:03
4	0.27%	10.234070	10:16:07
5	0.35%	11.359889	10:16:11
6	0.43%	12.477357	10:16:15
7	0.51%	13.485197	10:16:19
8	0.59%	14.387514	10:16:23
9	0.67%	15.308100	10:16:27
10	0.75%	15.919386	10:16:31
11	0.83%	16.710552	10:16:35
12	0.91%	17.393581	10:16:39
13	0.99%	18.072188	10:16:43
14	1.08%	18.705374	10:16:47
15	1.16%	19.268637	10:16:51

16	1.24%	19.731052	10:16:55
17	1.32%	20.249948	10:16:59
18	1.40%	20.651881	10:17:03
19	1.48%	21.118467	10:17:07
20	1.56%	21.561396	10:17:11
21	1.64%	21.967690	10:17:15
22	1.73%	22.368393	10:17:19
23	1.81%	22.708164	10:17:23
24	1.89%	23.079865	10:17:27
25	1.97%	23.460679	10:17:31
26	2.05%	23.736878	10:17:35
27	2.13%	23.954150	10:17:39
28	2.21%	24.226177	10:17:43
29	2.29%	24.518770	10:17:47
30	2.37%	24.750953	10:17:51
31	2.46%	24.887270	10:17:55
32	2.54%	25.151012	10:17:59
33	2.62%	25.336761	10:18:03
34	2.70%	25.459236	10:18:07
35	2.78%	25.620168	10:18:11
36	2.86%	25.756635	10:18:15
37	2.94%	25.796255	10:18:19
38	3.02%	25.853465	10:18:23
39	3.11%	25.852713	10:18:27
40	3.19%	25.781262	10:18:31
41	3.26%	25.672462	10:18:35
42	3.26%	25.657472	10:18:39
43	3.34%	25.514208	10:18:43
44	3.42%	25.443485	10:18:47
45	3.50%	25.354773	10:18:51

6% Heating Oil Contamination

Data Acquisition 34970-A
OUTPUTS: LVDT-I (mm)
Prepared By:-   Joseph W. Kristof
Dated:-   01-08-2008
Test Type   Static Compression Triaxial Test
Contamination: 6% Heating Oil

S. No.	Channel - I	With A	Time
	LVDT-I Strain	Deviator Stress σ_1-σ_3 (kPa)	
1	0.00%	0.000000	10:23:52
5	0.30%	2.808675357	10:24:06
6	0.37%	3.45282198	10:24:10
7	0.44%	4.072959	10:24:14
8	0.52%	4.860075843	10:24:17
9	0.59%	5.517724846	10:24:21
10	0.66%	6.208910994	10:24:24
11	0.74%	6.846505099	10:24:28
12	0.81%	7.59474873	10:24:32
13	0.89%	8.209034112	10:24:35
14	0.96%	8.766679605	10:24:39
15	1.03%	9.280910751	10:24:42
16	1.11%	9.825447823	10:24:46
17	1.18%	10.23509168	10:24:49
18	1.25%	10.73234018	10:24:53
19	1.33%	11.1651746	10:24:57

20	1.40%	11.54186833	10:25:00
21	1.47%	11.934287	10:25:04
22	1.55%	12.22185497	10:25:08
23	1.62%	12.59361117	10:25:11
24	1.69%	12.91113699	10:25:15
25	1.77%	13.18265352	10:25:18
26	1.84%	13.56094534	10:25:22
27	1.91%	13.87536128	10:25:26
28	1.99%	14.1909036	10:25:29
29	2.06%	14.48651521	10:25:33
30	2.13%	14.73470595	10:25:36
31	2.21%	15.01971941	10:25:40
32	2.28%	15.38846666	10:25:43
33	2.36%	15.50752591	10:25:47
34	2.43%	15.73480714	10:25:51
35	2.50%	16.01022409	10:25:54
36	2.58%	16.20549217	10:25:58
37	2.65%	16.5171693	10:26:01
38	2.72%	16.72645099	10:26:05
39	2.80%	16.95829492	10:26:09
40	2.87%	17.17994799	10:26:13
41	2.94%	17.4096657	10:26:17
42	3.01%	17.53072192	10:26:21
43	3.09%	17.69571975	10:26:25
44	3.16%	17.94094262	10:26:29
45	3.23%	18.04918889	10:26:32
46	3.31%	18.16145493	10:26:36
47	3.38%	18.39794839	10:26:40
48	3.46%	18.55517765	10:26:44
49	3.53%	18.66526005	10:26:48

50	3.61%	18.77225026	10:26:51
51	3.68%	19.03615324	10:26:55
52	3.76%	19.17524513	10:26:59
53	3.83%	19.28356112	10:27:02
54	3.91%	19.45299538	10:27:06
55	3.97%	19.59290421	10:27:10
56	4.05%	19.75674061	10:27:14
57	4.12%	19.88386354	10:27:18
58	4.19%	19.94754943	10:27:21
59	4.27%	20.05520216	10:27:25
60	4.35%	20.16107297	10:27:29
61	4.42%	20.27951508	10:27:33
62	4.49%	20.44120582	10:27:37
63	4.57%	20.55145467	10:27:40
64	4.65%	20.52903953	10:27:44
65	4.72%	20.66536918	10:27:48
66	4.80%	20.78910313	10:27:51
67	4.87%	20.85546535	10:27:55
68	4.95%	20.89726284	10:27:59
69	5.03%	20.90772072	10:28:03
70	5.10%	20.92385643	10:28:07
71	5.18%	20.89719705	10:28:10
72	5.26%	20.89438564	10:28:14
73	5.34%	20.91325338	10:28:18
74	5.41%	20.88006377	10:28:22
75	5.50%	20.91021776	10:28:25
76	5.58%	20.82192204	10:28:29
77	5.66%	20.78931178	10:28:33
78	5.74%	20.72008737	10:28:36
79	5.82%	20.65917261	10:28:40

80	5.90%	20.59937643	10:28:44
81	5.97%	20.53961391	10:28:47
82	6.06%	20.47970777	10:28:51
83	6.13%	20.41926538	10:28:55
84	6.21%	20.35953927	10:28:59
85	6.29%	20.30024063	10:29:03
86	6.37%	20.24040791	10:29:07
87	6.45%	20.18117924	10:29:11
88	6.52%	20.12064071	10:29:14
89	6.60%	20.06144945	10:29:18
90	6.68%	20.00042551	10:29:22
91	6.76%	19.94130936	10:29:26
92	6.84%	19.88054434	10:29:30
93	6.93%	19.81971729	10:29:33
94	7.01%	19.76141555	10:29:37
95	7.09%	19.70279862	10:29:41
96	7.18%	19.64487779	10:29:45
97	7.25%	19.58678144	10:29:49
98	7.33%	19.52864938	10:29:52
99	7.40%	19.47034436	10:29:56
100	7.48%	19.41003904	10:30:00
101	7.55%	19.35132728	10:30:04
102	7.63%	19.29220707	10:30:08
103	7.72%	19.23319526	10:30:12
104	7.80%	19.176686	10:30:16
105	7.88%	19.11737363	10:30:20
106	7.96%	19.0580013	10:30:24
107	8.03%	19.00013264	10:30:28
108	8.11%	18.94169056	10:30:32
109	8.20%	18.88406559	10:30:35

2% Gasoline Contamination

Data Acquisition 34970-A
OUTPUTS: LVDT-I (mm)
Prepared By:-   Joseph W. Kristof
Dated:-   01-08-2008
Test Type   Static Compression Triaxial Test
Contamination: 2% Gasoline

S. No.	Channel -I	With A	Time
	LVDT-I Strain	Deviator Stress $\sigma_1-\sigma_3$ (kPa)	
1	0.00%	0	11:56:10
2	0.29%	2.58339687	11:56:14
3	0.37%	2.961481924	11:56:17
4	0.44%	3.33899831	11:56:21
5	0.52%	3.715946026	11:56:25
6	0.59%	4.092325074	11:56:29
7	0.67%	4.468135452	11:56:32
8	0.74%	4.843377162	11:56:36
9	0.81%	5.218050202	11:56:40
10	0.89%	5.592154574	11:56:44
11	0.96%	5.965690276	11:56:47
12	1.04%	6.338657309	11:56:51
13	1.11%	6.711055673	11:56:55
14	1.19%	7.082885369	11:56:59
15	1.26%	7.454146395	11:57:03

16	1.34%	7.824838752	11:57:06
17	1.41%	8.19496244	11:57:10
18	1.49%	8.477940404	11:57:14
19	1.56%	8.812710039	11:57:18
20	1.63%	9.096396567	11:57:21
21	1.71%	9.423657007	11:57:25
22	1.78%	9.574500712	11:57:29
23	1.86%	9.861818121	11:57:32
24	1.93%	10.10803638	11:57:36
25	2.01%	10.39610689	11:57:40
26	2.08%	10.63827692	11:57:44
27	2.16%	10.77305364	11:57:48
28	2.23%	11.02560466	11:57:52
29	2.30%	11.24915759	11:57:55
30	2.37%	11.38190799	11:57:59
31	2.44%	11.56374027	11:58:03
32	2.49%	11.7386165	11:58:06
33	2.56%	11.95298961	11:58:10
34	2.64%	12.17814134	11:58:14
35	2.71%	12.33364229	11:58:18
36	2.78%	12.50160672	11:58:22
37	2.86%	12.68457332	11:58:25
38	2.94%	12.86483009	11:58:29
39	3.01%	12.99179026	11:58:33
40	3.08%	13.17211004	11:58:37
41	3.16%	13.30427222	11:58:40
42	3.23%	13.52824739	11:58:44
43	3.31%	13.65926122	11:58:48
44	3.39%	13.80266279	11:58:52
45	3.46%	13.97313646	11:58:55

46	3.54%	14.08820526	11:58:59
47	3.62%	14.21144671	11:59:02
48	3.69%	14.35207306	11:59:06
49	3.77%	14.53634878	11:59:10
50	3.85%	14.6285915	11:59:14
51	3.92%	14.71159825	11:59:17
52	3.99%	14.94418376	11:59:21
53	4.07%	15.03243315	11:59:24
54	4.15%	15.18116509	11:59:28
55	4.23%	15.31405893	11:59:32
56	4.31%	15.44901858	11:59:35
57	4.38%	15.53595512	11:59:39
58	4.45%	15.6312195	11:59:43
59	4.53%	15.76545865	11:59:47
60	4.60%	15.84625283	11:59:51
61	4.67%	15.97368836	11:59:55
62	4.75%	16.0836159	11:59:58
63	4.84%	16.23801646	12:00:02
64	4.91%	16.39443233	12:00:06
65	4.98%	16.42023492	12:00:10
66	5.05%	16.60097791	12:00:13
67	5.13%	16.68404861	12:00:17
68	5.20%	16.7622229	12:00:21
69	5.28%	16.90739705	12:00:24
70	5.35%	17.04498849	12:00:28
71	5.42%	17.10082165	12:00:32
72	5.50%	17.23600144	12:00:36
73	5.58%	17.33260637	12:00:40
74	5.66%	17.33982033	12:00:43
75	5.74%	17.56499824	12:00:47

76	5.82%	17.59488921	12:00:51
77	5.89%	17.66850028	12:00:55
78	5.96%	17.84679137	12:00:58
79	6.04%	17.90329949	12:01:02
80	6.11%	17.95753546	12:01:06
81	6.19%	18.06998443	12:01:10
82	6.27%	18.12378063	12:01:14
83	6.34%	18.21474474	12:01:17
84	6.42%	18.31352117	12:01:21
85	6.50%	18.42646994	12:01:25
86	6.57%	18.48435561	12:01:29
87	6.65%	18.62177136	12:01:33
88	6.72%	18.60786527	12:01:36
89	6.79%	18.72652572	12:01:40
90	6.87%	18.7846102	12:01:44
91	6.96%	18.81589888	12:01:47
92	7.04%	18.95682823	12:01:51
93	7.12%	19.07210903	12:01:55
94	7.20%	19.10878516	12:01:59
95	7.27%	19.16386721	12:02:02
96	7.35%	19.23059307	12:02:06
97	7.43%	19.32725078	12:02:10
98	7.50%	19.41685132	12:02:13
99	7.58%	19.47114227	12:02:17
100	7.65%	19.52060484	12:02:21
101	7.74%	19.53717431	12:02:25
102	7.81%	19.65625875	12:02:28
103	7.90%	19.74015612	12:02:32
104	7.98%	19.77264678	12:02:35
105	8.05%	19.77259897	12:02:39

106	8.13%	19.89116398	12:02:43
107	8.21%	19.91483308	12:02:46
108	8.28%	19.96057168	12:02:50
109	8.36%	20.09974002	12:02:53
110	8.43%	20.11755131	12:02:57
111	8.51%	20.20692479	12:03:00
112	8.58%	20.25587653	12:03:04
113	8.66%	20.2574882	12:03:07
114	8.73%	20.33189338	12:03:11
115	8.81%	20.38705455	12:03:15
116	8.89%	20.43139736	12:03:18
117	8.97%	20.45755947	12:03:22
118	9.05%	20.53348982	12:03:25
119	9.12%	20.48308621	12:03:29
120	9.20%	20.56380757	12:03:33
121	9.27%	20.6624635	12:03:37
122	9.35%	20.69270405	12:03:40
123	9.42%	20.73443781	12:03:44
124	9.49%	20.77390545	12:03:48
125	9.57%	20.86715338	12:03:51
126	9.64%	20.86960176	12:03:55
127	9.73%	20.92494589	12:03:58
128	9.80%	20.94020224	12:04:02
129	9.87%	20.94234602	12:04:06
130	9.95%	20.89949742	12:04:10
131	10.02%	21.03228115	12:04:13
132	10.10%	20.95710633	12:04:17
133	10.17%	21.09578932	12:04:21
134	10.25%	21.08259305	12:04:25
135	10.33%	21.11077357	12:04:28

136	10.41%	21.20108474	12:04:32
137	10.47%	21.13805873	12:04:36
138	10.55%	21.19893573	12:04:39
139	10.62%	21.21827241	12:04:43
140	10.70%	21.23173399	12:04:46
141	10.77%	21.2356764	12:04:50
142	10.84%	21.2755114	12:04:54
143	10.92%	21.24199322	12:04:58
144	11.00%	21.29476354	12:05:01
145	11.07%	21.25949033	12:05:05
146	11.14%	21.36413971	12:05:09
147	11.21%	21.32733248	12:05:12
148	11.29%	21.32952278	12:05:16
149	11.36%	21.43696447	12:05:20
150	11.44%	21.41148863	12:05:24
151	11.51%	21.39971236	12:05:28
152	11.59%	21.42343266	12:05:32
153	11.66%	21.3786243	12:05:35
154	11.74%	21.42341186	12:05:39
155	11.82%	21.44510314	12:05:43
156	11.89%	21.44570938	12:05:47
157	11.97%	21.36019552	12:05:50
158	12.05%	21.37233769	12:05:54
159	12.13%	21.40886581	12:05:58
160	12.20%	21.42562971	12:06:01
161	12.28%	21.39141318	12:06:05
162	12.35%	21.44108853	12:06:09
163	12.43%	21.36087703	12:06:12
164	12.51%	21.38341614	12:06:16
165	12.59%	21.38551541	12:06:20

166	12.66%	21.35957592	12:06:24
167	12.74%	21.45942713	12:06:27
168	12.82%	21.42978808	12:06:31
169	12.90%	21.36304342	12:06:35
170	12.97%	21.41216834	12:06:38
171	13.05%	21.36577271	12:06:42
172	13.13%	21.33546564	12:06:46
173	13.20%	21.32421963	12:06:50
174	13.28%	21.30690678	12:06:53
175	13.35%	21.34842181	12:06:57
176	13.42%	21.29203327	12:07:01
177	13.50%	21.34065889	12:07:05
178	13.57%	21.31738008	12:07:08
179	13.65%	21.3054843	12:07:12
180	13.73%	21.33585258	12:07:15
181	13.81%	21.29444303	12:07:19
182	13.88%	21.25760227	12:07:23
183	13.95%	21.22612757	12:07:27
184	14.03%	21.32002778	12:07:30
185	14.11%	21.25386908	12:07:34
186	14.19%	21.27581959	12:07:38
187	14.26%	21.2642625	12:07:42
188	14.34%	21.25083164	12:07:46
189	14.42%	21.23685034	12:07:50
190	14.48%	21.23790938	12:07:53
191	14.56%	21.20986419	12:07:57
192	14.64%	21.19687326	12:08:01
193	14.71%	21.19099512	12:08:05
194	14.78%	21.1429798	12:08:08
195	14.86%	21.18521115	12:08:12

196	14.93%	21.12831601	12:08:16
197	15.00%	21.0969903	12:08:19
198	15.08%	21.07974605	12:08:23
199	15.15%	21.1015533	12:08:27
200	15.22%	21.01990138	12:08:31
201	15.31%	21.07833614	12:08:35
202	15.38%	21.00722912	12:08:38
203	15.45%	21.02164997	12:08:41
204	15.53%	21.05381085	12:08:45
205	15.61%	21.01294934	12:08:49
206	15.68%	20.94205953	12:08:52
207	15.76%	20.95742332	12:08:56
208	15.84%	20.94218796	12:08:59
209	15.91%	20.85438444	12:09:03
210	15.99%	20.91836388	12:09:06
211	16.07%	20.8445614	12:09:10
212	16.15%	20.88635795	12:09:13
213	16.23%	20.79364861	12:09:17
214	16.30%	20.80231242	0.50649
215	16.37%	20.78351459	0.50654
216	16.44%	20.76733568	0.50657
217	16.52%	20.75362657	0.50662
218	16.60%	20.67771798	0.50666
219	16.68%	20.70464931	0.5067
220	16.77%	20.62474948	0.50675
221	16.84%	20.59648418	0.50678
222	16.93%	20.57605037	0.50683
223	17.00%	20.55517009	0.50686
224	17.09%	20.56899609	0.50691
225	17.16%	20.49900286	0.50696

226	17.23%	20.49955481	0.507
227	17.32%	20.43406836	0.50705
228	17.40%	20.43507014	0.50708
229	17.47%	20.38017948	0.50713
230	17.55%	20.39492521	0.50718
231	17.63%	20.33420006	0.50722
232	17.70%	20.31047504	0.50726
233	17.78%	20.30075965	0.5073
234	17.85%	20.26049567	0.50735
235	17.93%	20.3172461	0.5074
236	18.01%	20.22305448	0.50743
237	18.08%	20.2169992	0.50748
238	18.16%	20.22481577	0.50752
239	18.23%	20.17040588	0.50756
240	18.30%	20.10884315	0.5076
241	18.38%	20.16619798	0.50764
242	18.45%	20.04381118	0.50769
243	18.50%	20.02814516	0.50773
244	18.58%	19.9836642	0.50777
245	18.65%	20.00424459	0.50781
246	18.73%	19.91758771	0.50786
247	18.81%	19.88685319	0.50791
248	18.88%	19.89825472	0.50794
249	18.96%	19.85609092	0.50799
250	19.03%	19.83636869	0.50802
251	19.09%	19.82366061	0.50807
252	19.16%	19.78166921	0.50811
253	19.27%	19.7204513	0.50815
254	19.34%	19.66814704	0.50819
255	19.39%	19.66915359	0.50824

256	19.47%	19.65050272	0.50828
257	19.53%	19.64938382	0.50832
258	19.59%	19.57519576	0.50836
259	19.66%	19.52508175	0.5084
260	19.72%	19.56821167	0.50844
261	19.78%	19.47024678	0.50848
262	19.85%	19.49336766	0.50852
263	19.91%	19.40087597	0.50856
264	19.97%	19.3987488	0.5086
265	20.04%	19.32499814	0.50864
266	20.10%	19.35998225	0.50868
267	20.17%	19.3181068	0.50872

4% Gasoline Contamination

Data Acquisition 34970-A
OUTPUTS: LVDT-I (mm)
Prepared By:-   Joseph W. Kristof
Dated:-   01-08-2008
Test Type   Static Compression Triaxial Test
Contamination: 4% Gasoline

S. No.	Channel - I	With A	Time
	LVDT-I Strain	Deviator Stress σ_1-σ_3 (kPa)	
1	0.00%	0	13:19:56
2	0.08%	2.523132798	13:19:59
3	0.18%	3.22709125	13:20:03
4	0.19%	3.700824345	13:20:07
5	0.24%	4.245905862	13:20:11
6	0.31%	4.681230421	13:20:15
7	0.38%	5.009803649	13:20:18
8	0.44%	5.483872665	13:20:22
9	0.51%	5.825005558	13:20:26
10	0.58%	6.2641015	13:20:30
11	0.65%	6.709469955	13:20:34
12	0.73%	7.056670195	13:20:38
13	0.81%	7.388263506	13:20:41
14	0.88%	7.767199425	13:20:45
15	0.97%	8.023379424	13:20:49
16	1.04%	8.273372854	13:20:53

17	1.12%	8.606705095	13:20:57
18	1.19%	8.921303304	13:21:00
19	1.27%	9.248168803	13:21:04
20	1.34%	9.37880303	13:21:08
21	1.42%	9.760546153	13:21:12
22	1.50%	10.01777479	13:21:15
23	1.56%	10.18560009	13:21:19
24	1.64%	10.51521974	13:21:23
25	1.72%	10.70115753	13:21:26
26	1.79%	10.99946953	13:21:30
27	1.86%	11.1732532	13:21:34
28	1.94%	11.34549773	13:21:38
29	2.01%	11.58874071	13:21:41
30	2.09%	11.82326468	13:21:45
31	2.16%	12.00548617	13:21:49
32	2.24%	12.26851118	13:21:53
33	2.32%	12.46121932	13:21:57
34	2.39%	12.64012709	13:22:00
35	2.46%	12.84368755	13:22:04
36	2.54%	13.05691097	13:22:08
37	2.62%	13.28552544	13:22:11
38	2.69%	13.44284043	13:22:15
39	2.77%	13.60137928	13:22:19
40	2.85%	13.77400028	13:22:23
41	2.93%	14.02725189	13:22:27
42	3.01%	14.19274026	13:22:30
43	3.08%	14.39678229	13:22:34
44	3.16%	14.50713746	13:22:38
45	3.24%	14.71557822	13:22:42
46	3.32%	14.84096257	13:22:46

47	3.40%	15.0320041	13:22:50
48	3.48%	15.14585914	13:22:54
49	3.55%	15.35824914	13:22:57
50	3.64%	15.50009394	13:23:01
51	3.71%	15.69204896	13:23:05
52	3.80%	15.83346301	13:23:09
53	3.88%	15.96294203	13:23:13
54	3.96%	16.12380599	13:23:16
55	4.04%	16.25076558	13:23:20
56	4.11%	16.48326564	13:23:24
57	4.18%	16.54878668	13:23:28
58	4.27%	16.71763521	13:23:31
59	4.34%	16.78077797	13:23:35
60	4.42%	16.94538464	13:23:39
61	4.49%	17.0775465	13:23:42
62	4.58%	17.21182134	13:23:46
63	4.66%	17.27906683	13:23:50
64	4.73%	17.44353374	13:23:54
65	4.81%	17.5359224	13:23:57
66	4.88%	17.64815669	13:24:01
67	4.95%	17.72842609	13:24:04
68	5.03%	17.85079075	13:24:08
69	5.11%	17.92983252	13:24:12
70	5.18%	18.12546006	13:24:15
71	5.26%	18.18051882	13:24:19
72	5.33%	18.24631957	13:24:23
73	5.41%	18.38762591	13:24:27
74	5.49%	18.48645182	13:24:30
75	5.56%	18.59616288	13:24:34
76	5.63%	18.65693413	13:24:38

77	5.71%	18.76053453	13:24:41
78	5.78%	18.91274835	13:24:45
79	5.86%	18.97154049	13:24:49
80	5.93%	19.00352714	13:24:53
81	6.00%	19.17465477	13:24:56
82	6.08%	19.17450323	13:25:00
83	6.15%	19.30789754	13:25:04
84	6.22%	19.40769667	13:25:07
85	6.30%	19.52247464	13:25:11
86	6.38%	19.55291704	13:25:15
87	6.45%	19.5898372	13:25:19
88	6.53%	19.72150864	13:25:23
89	6.60%	19.81229235	13:25:26
90	6.68%	19.82584143	13:25:30
91	6.76%	19.90789102	13:25:34
92	6.83%	19.92415824	13:25:38
93	6.91%	20.00064741	13:25:41
94	6.99%	20.05907763	13:25:45
95	7.07%	20.13777071	13:25:49
96	7.16%	20.16322567	13:25:53
97	7.24%	20.2935819	13:25:56
98	7.31%	20.30414458	13:26:00
99	7.39%	20.3789713	13:26:04
100	7.47%	20.46693269	13:26:08
101	7.54%	20.47728529	13:26:12
102	7.61%	20.49486938	13:26:15
103	7.69%	20.60420491	13:26:19
104	7.77%	20.5661636	13:26:23
105	7.85%	20.70717699	13:26:27
106	7.94%	20.66964684	13:26:30

107	8.01%	20.73995237	13:26:34
108	8.09%	20.76655262	13:26:38
109	8.17%	20.76641536	13:26:42
110	8.25%	20.87151967	13:26:46
111	8.33%	20.85057254	13:26:50
112	8.41%	20.83443817	13:26:53
113	8.48%	20.93402915	13:26:57
114	8.56%	20.9798584	13:27:01
115	8.65%	20.96327909	13:27:05
116	8.72%	20.91062674	13:27:08
117	8.80%	20.92037578	13:27:12
118	8.88%	21.00484237	13:27:16
119	8.96%	20.95510163	13:27:20
120	9.04%	20.88878201	13:27:24
121	9.11%	20.90378721	13:27:27
122	9.19%	20.90409869	13:27:31
123	9.27%	20.89928533	13:27:35
124	9.35%	20.81343381	13:27:39
125	9.42%	20.8269394	13:27:42
126	9.50%	20.83930075	13:27:46
127	9.57%	20.82076284	13:27:50
128	9.66%	20.79978479	13:27:54
129	9.75%	20.73363781	13:27:58
130	9.81%	20.7774013	13:28:01
131	9.90%	20.69747438	13:28:05
132	9.98%	20.77781202	13:28:09
133	10.05%	20.66880027	13:28:13
134	10.13%	20.68708282	13:28:17
135	10.21%	20.61363772	13:28:20
136	10.28%	20.51211554	13:28:24

137	10.36%	20.64725799	13:28:28
138	10.44%	20.50440187	13:28:31
139	10.51%	20.56426715	13:28:35
140	10.59%	20.54232804	13:28:39
141	10.67%	20.5027053	13:28:43
142	10.75%	20.42530869	13:28:46
143	10.82%	20.3731471	13:28:50
144	10.90%	20.3668709	13:28:54
145	10.97%	20.24003525	13:28:58
146	11.05%	20.20109364	13:29:01
147	11.12%	20.07042993	13:29:05
148	11.20%	19.83728282	13:29:09
149	11.27%	19.77919648	13:29:13
150	11.35%	19.65719631	13:29:16
151	11.43%	19.58858148	13:29:20
152	11.51%	19.44496674	13:29:24
153	11.58%	19.34989754	13:29:28
154	11.66%	19.2531951	13:29:31

6% Gasoline Contamination

Data Acquisition 34970-A
OUTPUTS: LVDT-I (mm)
Prepared By:-   Joseph W. Kristof
Dated:-   01-08-2008
Test Type   Static Compression Triaxial Test
Contamination: 6% Gasoline

S. No.	Channel -I	With A	Time
	LVDT-I Strain	Deviator Stress σ_1-σ_3 (kPa)	
1	0.00%	0	13:56:52
2	0.26%	3.71090499	13:56:56
3	0.30%	3.884762272	13:57:00
4	0.33%	4.059084658	13:57:04
5	0.37%	4.232763895	13:57:07
6	0.45%	4.404618875	13:57:11
7	0.53%	4.576239721	13:57:14
8	0.60%	4.747811694	13:57:18
9	0.68%	4.918896792	13:57:22
10	0.75%	5.089967425	13:57:26
11	0.83%	5.260658769	13:57:30
12	0.90%	5.431246245	13:57:33
13	0.98%	5.601337324	13:57:37
14	1.05%	5.77157906	13:57:41
15	1.12%	5.941280312	13:57:45
16	1.20%	6.110475961	13:57:48

17	1.27%	6.279844308	13:57:52
18	1.35%	6.448436037	13:57:56
19	1.43%	6.604339577	13:58:00
20	1.51%	6.810302794	13:58:04
21	1.59%	6.939948285	13:58:08
22	1.67%	7.197417072	13:58:11
23	1.74%	7.33155192	13:58:15
24	1.81%	7.470995144	13:58:19
25	1.88%	7.658107939	13:58:23
26	1.96%	7.728269838	13:58:26
27	2.03%	7.835825312	13:58:30
28	2.10%	7.969956773	13:58:34
29	2.19%	8.082302362	13:58:38
30	2.26%	8.244032213	13:58:41
31	2.34%	8.344382029	13:58:45
32	2.42%	8.441903297	13:58:49
33	2.48%	8.59952605	13:58:52
34	2.56%	8.638579557	13:58:56
35	2.64%	8.660168042	13:59:00
36	2.71%	8.828260225	13:59:04
37	2.79%	8.944015343	13:59:07
38	2.87%	9.066015044	13:59:11
39	2.94%	9.16272262	13:59:15
40	3.01%	9.169709486	13:59:18
41	3.08%	9.347417553	13:59:22
42	3.16%	9.396164408	13:59:26
43	3.23%	9.519769282	13:59:30
44	3.31%	9.632577712	13:59:34
45	3.39%	9.732283676	13:59:38
46	3.47%	9.835606069	13:59:41

47	3.54%	9.837185364	13:59:45
48	3.62%	9.963835789	13:59:49
49	3.69%	10.07716577	13:59:53
50	3.77%	10.16161624	13:59:56
51	3.85%	10.20385328	14:00:00
52	3.93%	10.27135587	14:00:04
53	4.01%	10.34387422	14:00:07
54	4.08%	10.40992654	14:00:11
55	4.18%	10.54829427	14:00:15
56	4.26%	10.64336965	14:00:19
57	4.34%	10.71943159	14:00:23
58	4.41%	10.79157525	14:00:27
59	4.49%	10.87993416	14:00:31
60	4.57%	10.94996682	14:00:34
61	4.64%	11.05089024	14:00:38
62	4.72%	11.07087137	14:00:42
63	4.81%	11.21402445	14:00:46
64	4.88%	11.28190178	14:00:49
65	4.96%	11.35126731	14:00:53
66	5.04%	11.36332054	14:00:57
67	5.13%	11.45510065	14:01:00
68	5.21%	11.63386117	14:01:04
69	5.28%	11.61791131	14:01:08
70	5.36%	11.73148332	14:01:12
71	5.44%	11.74055821	14:01:15
72	5.52%	11.82053662	14:01:19
73	5.59%	11.97615359	14:01:22
74	5.66%	11.94636521	14:01:26
75	5.74%	12.01140846	14:01:30
76	5.81%	12.1096001	14:01:34

77	5.89%	12.18371839	14:01:37
78	5.97%	12.25914868	14:01:41
79	6.04%	12.30183684	14:01:45
80	6.11%	12.40545606	14:01:49
81	6.19%	12.38991225	14:01:52
82	6.26%	12.49189411	14:01:56
83	6.34%	12.47974916	14:02:00
84	6.42%	12.57625243	14:02:03
85	6.50%	12.53226406	14:02:07
86	6.57%	12.75921243	14:02:11
87	6.65%	12.79264808	14:02:14
88	6.73%	12.82613208	14:02:18
89	6.80%	12.8767293	14:02:22
90	6.87%	12.97434922	14:02:26
91	6.95%	13.01771673	14:02:30
92	7.02%	13.06376577	14:02:34
93	7.10%	13.13288579	14:02:37
94	7.18%	13.12563192	14:02:41
95	7.25%	13.27513076	14:02:45
96	7.32%	13.31692336	14:02:49
97	7.40%	13.30081183	14:02:52
98	7.48%	13.40160594	14:02:56
99	7.55%	13.44844649	14:02:59
100	7.63%	13.46134487	14:03:03
101	7.71%	13.50426399	14:03:07
102	7.78%	13.52552628	14:03:10
103	7.87%	13.65246091	14:03:14
104	7.94%	13.6754398	14:03:18
105	8.01%	13.73370144	14:03:22
106	8.07%	13.7469531	14:03:25

107	8.15%	13.7048788	14:03:29
108	8.22%	13.81981802	14:03:33
109	8.30%	13.85793085	14:03:37
110	8.37%	13.89781646	14:03:41
111	8.45%	13.88060251	14:03:44
112	8.53%	13.95807502	14:03:48
113	8.61%	13.99627343	14:03:52
114	8.69%	14.02794211	14:03:55
115	8.77%	14.0344225	14:03:59
116	8.83%	14.10564842	14:04:02
117	8.91%	14.16159762	14:04:05
118	9.00%	14.1781142	14:04:09
119	9.08%	14.24715255	14:04:13
120	9.16%	14.21216505	14:04:17
121	9.25%	14.28032947	14:04:21
122	9.33%	14.28055708	14:04:24
123	9.39%	14.36758181	14:04:28
124	9.46%	14.38683981	14:04:31
125	9.53%	14.39478127	14:04:35
126	9.61%	14.39417227	14:04:39
127	9.68%	14.41141648	14:04:42
128	9.77%	14.50705606	14:04:46
129	9.84%	14.50076186	14:04:50
130	9.92%	14.51544919	14:04:54
131	10.00%	14.57410655	14:04:58
132	10.08%	14.57806673	14:05:01
133	10.15%	14.54794874	14:05:05
134	10.22%	14.63077242	14:05:09
135	10.29%	14.55954281	14:05:12
136	10.37%	14.57594292	14:05:16

137	10.45%	14.62613427	14:05:20
138	10.53%	14.66071419	14:05:23
139	10.61%	14.70618381	14:05:27
140	10.68%	14.68848819	14:05:30
141	10.75%	14.73986174	14:05:34
142	10.83%	14.75276034	14:05:38
143	10.91%	14.77350313	14:05:42
144	10.98%	14.8008797	14:05:46
145	11.05%	14.74593679	14:05:50
146	11.13%	14.7358166	14:05:54
147	11.20%	14.79793095	14:05:57
148	11.28%	14.85173419	14:06:01
149	11.35%	14.81999963	14:06:05
150	11.43%	14.85516363	14:06:09
151	11.51%	14.84907262	14:06:13
152	11.58%	14.88860988	14:06:17
153	11.67%	14.8658672	14:06:21
154	11.75%	14.82434392	14:06:24

2. Properties of Kaolin and Crude Oil used in the research

MS

KAOLIN

SANDERSVILLE · GA
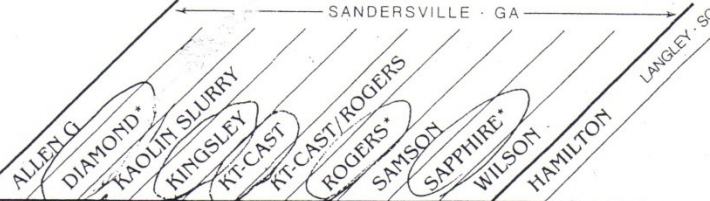
PHYSICAL PROPERTIES	ALLEN G.	DIAMOND*	KAOLIN SLURRY	KINGSLEY	KT-CAST	KT-CAST/ROGERS	ROGERS*	SAMSON	SAPPHIRE*	WILSON	HAMILTON
Dry M.O.R., psi	300	450	300	275	225	400	950	450	650	350	300
M.B.I., meq/100g	3.5	6.5±1.0	3.5	3.3	2.5	4.5	10.5	6.5	9.5±1.0	4.0	4.5
Surface Area, m²/g	13.5	18.0	13.0	12.5	12.0	13.5	24.0	18.0	22.0	15.0	24.0
pH	5.5	4.8	5.5	5.5	5.5	5.5	4.5	4.7	5.0	5.5	4.0
PARTICLE SIZE											
+325 Mesh, Max. % Retained	0.5	0.5	5.0	2.5	5.0	2.0	1.0	2.5	0.5	3.0	2.0
% Finer than 20μm	97	97	96	97	95	97	99	98	99	98	99
10μm	92	93	89	91	87	91	97	94	97	93	98
5μm	82	83	78	80	75	81	94	86	91	81	95
2μm	63	68	57	58	60	62	85	71	74	63	89
1μm	47	59	43	44	41	48	76	59	62	50	83
0.5μm	28	38	23	25	21	30	65	44	48	34	69
CHEMICAL ANALYSIS											
% SiO_2	45.0	45.6	45.3	44.8	45.1	45.1	46.5	46.7	46.3	46.1	44.0
Al_2O_3	38.5	37.9	38.2	38.4	38.8	38.1	37.5	38.1	38.2	38.1	38.8
Fe_2O_3	0.5	0.6	0.5	0.4	0.4	0.5	1.0	0.7	0.7	0.5	1.3
TiO_2	1.5	1.4	1.6	1.6	1.6	1.6	1.3	1.5	1.4	1.7	1.5
CaO	0.1	0.2	0.1	0.1	0.1	0.2	0.3	0.2	0.2	0.1	0.2
MgO	0.1	0.1	0.1	0.1	0.1	0.1	0.3	0.1	0.2	0.1	0.1
K_2O	0.2	0.2	0.2	0.1	0.1	0.2	0.3	0.2	0.2	0.2	0.2
Na_2O	0.1	0.1	0.1	0.1	0.1	0.1	0.1	0.1	0.1	0.1	0.2
L.O.I.	13.6	13.5	13.5	13.6	13.6	13.6	13.2	13.4	13.4	13.5	14.0
Carbon	0.04	0.06	0.05	0.03	0.03	0.05	0.10	0.07	0.08	0.04	0.03
Sulfur	0.04	0.07	0.05	0.04	0.03	0.06	0.13	0.09	0.10	0.04	0.08

*Extruded 50/50 Clay/Flint   Note: Kaolin Slurry shipped at 70% Solids

LANGLEY · SC
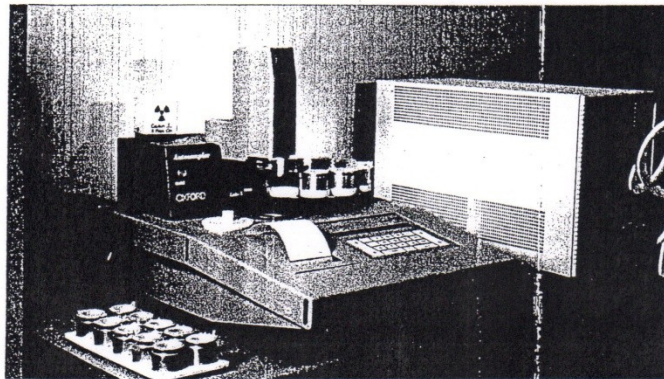
Quality from the ground up

WARNING: BALL CLAY, KAOLIN & FELDSPAR CO
OSHA Safety & Health Standards for crystalline s

Source: Hydro
.. /en/our_business/oil_energy/sales_distribution/products/crude_oil_canada.html

HYDRO

Crude oil Canada

Hibernia Blend

Load port	Whiffen Head, Newfoundland	
Operator	Hibernia Management Development Company	
Crude oil characteristics	API	35.6 deg
	Density	0.847 kg/l
	Sulphur	0.37 wt%
	Pour Point	12.8 deg C
	Viscosity	5.38 cSt at 20 deg C
	TAN	0.11 mg KOH/g
Comments	Typical blend data above. For 2003 blending of max 5% Avalon into Hibernia is expected	

Crude Oil Assay:

Canada, Hibernia, December 2002 (35 Kb)
Canada, Avalon, February 2001 (50 Kb)

Terra Nova

Load port	Whiffen Head, Newfoundland	
Operator	Petro-Canada	
Crude oil characteristics	API	32.1 deg
	Density	0.8649 kg/l
	Sulphur	0.58 wt%
	Pour Point	-3 deg C
	Viscosity	6.61 cSt at 20 deg C
	TAN	0.07 mg KOH/g
Comments		
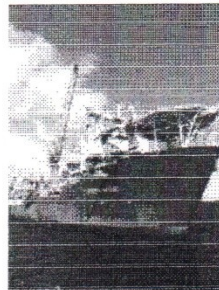
Crude Oil Assay:

Canada, Terra Nova, February 2003 (50 Kb)

→ Read more about our operations in Canada